To the Graduate Council:

I am submitting herewith a thesis written by Seth N. Bowman entitled "Lignin Composites with Phenol-Acrylates Cured by Electron Beam." I have examined the final electronic copy of this thesis for form and content and recommend that it be accepted in partial fulfillment of the requirements for the degree of Master of Science, with a major in Chemical Engineering.

Dr. Timothy G. Rials
Major Professor

We have read this thesis
and recommend its acceptance:

Dr. John Collier

Dr. Simioan Petrovan

Accepted for the Council:

Anne Mayhew
Vice Chancellor and
Dean of Graduate Studies

(Original signatures are on file with official student records)

Lignin Composites with Phenol-Acrylates Cured by Electron Beam

A Thesis

Presented for the

Masters of Science

Degree

The University of Tennessee, Knoxville

Seth Nathaniel Bowman

December 2006

Dedication

This thesis is dedicated to my father, Charles F. Bowman, for always believing in me (even when I didn't believe much in myself).

Acknowledgements

I would like to thank the following people for their assistance in completing this work: my advisor Dr. Timothy G. Rials for handing me an interesting project which had never before been done, Dr. John Collier and Simioan Petrovan for serving on my committee, the remainder of the staff of the department of Chemical Engineering at UT Knoxville for always holding me to the highest standards, Dr. Nikki Labbe and Dr. David Harper for advice and technical support.

Abstract

As the major by-product of the pulp and paper industry, determining a use for lignin represents a key priority to almost any bio-materials research organization. The purpose of this study is to investigate the interaction with and effects of lignin within phenol-acrylate composites cured by electron beam, characterizing changes to both physical and chemical properties. In order to more fully characterize the effects of lignin, results of pure lignin as well as cellulose samples subjected to electron beam radiation and tested by FT-IR are presented. For the composite material, results of both DMA and FT-IR spectroscopy will be presented. Results of these analyses are then be discussed and the impact of lignin on the chemical changes within the resulting composite identified.

Table of Contents

List of Figures

Nomenclature and Abbreviations

Nomenclature

R46	ethoxylated bisphenol-A dimethacrylate ether
R67	ethoxylated bisphenol-A diacrylate ether
T_g	glass transition temperature, $T(\tan E'/E'')_{max}$
E'	storage modulus
E	terminal storage modulus
E''	loss modulus
δ	storage modulus divided by loss modulus
R	universal gas constant
T*	temperature at the onset of rubbery plateau in DMA testing
E'*	terminal storage modulus in DMA testing
ρ	density
M_c	number average molecular weight between cross-links

Abbreviations

ORNL	Oak Ridge National Laboratory
FT-IR	Fourier Transform Infrared (spectroscopy)
DMA	Differential Mechanical Analysis
MOE	Modulus of Elasticity
SEM	Scanning Electron Microscope
ATR	Attenuated Total Reflectance
PCA	Component Analysis
PLS	Partial Least Squares (regression)
RMSEC	Root Mean Squared Error for Calibration
RMSEP	Root Mean Squared Error for Prediction

Chapter 1: Introduction

Lignin, a natural polymer found in wood, is the most abundant by-product of the paper industry[1]. The majority of lignin produced is used as fuel in that industry, though an expanding market exists for its commercial sale. New applications for lignin, whether as an inexpensive filler for existing products or as an enabler in the development of new products, possess great economic advantages due to low material cost[2]. In addition, as a renewable resource, lignin possesses a distinct environmental advantage over almost all of the materials it might , as these are nearly all petroleum products. There is even increasing evidence that incorporation of lignin increases the rate of degradation of composite materials when land filled as well, even if the other components are petroleum based or otherwise synthetic[3].

New developments in electron-beam (e-beam) treatment of resin systems offer a significant cost savings over traditional heat-cured resins. E-beam treatment is shown to be productive in creating reactive sites on wood fibers, while cellulosic fibers are being used as reinforcement for a variety of thermoplastics[4]. If electron beam-curable resins could be combined with lignin, the resulting composites would possess dramatic economic advantages in both the cost of the materials and the cost of production. In addition, the environmental advantages are increased by use of an e-beam curable resin system because competing materials are most often cured by process heat[5]. It is therefore the purpose of this study to investigate the potential application of lignin in electron-beam cured resin systems.

Current research at the Oak Ridge National Laboratory (ORNL) is directed towards the development of rapid, low temperature e-beam-cured resin-wood systems for use as structural panels and engineered wood products[5]. Such development would significantly

lower production costs, since traditional resins require both longer cure times and large amounts of process heat to cure. To simplify this investigation, the author chose resins already characterized by this research in their pure forms. They are ethoxylated bisphenol-A dimethacrylate ether (R46) and ethoxylated bisphenol-A diacrylate ether (R67). To examine the interaction of these resins with lignin, pure lignin is first irradiated at different dosages and then examined by Fourier Transform-Infrared Spectroscopy (FT-IR) to determine the chemical changes taking place under treatment by e-beam. To further the overall goals of current research (coupling e-beam resins with wood), the author also has examined pure cellulose and hemi-cellulose samples irradiated by e-beam as well. Composite materials are then made by the addition of several different concentrations of lignin to the two separate resins (5, 10, 20, 30 and 40 wt% lignin). These are cured at different dosages of electron beam radiation (0, 5, 10, 20, 40, 80, 120 and 180 kGy, or kilo-gray). The author then tests the resulting composite materials for changes to the chemical composition by FT-IR. Imagery will be taken using both scanning electron microscopy and IR imagery in order to determine any observable structures present. In addition, the author presents results of Dynamic Mechanical Analysis (DMA) testing for each composite in order to fully characterize their mechanical and thermal properties. The changes to mechanical properties with varying dosages and concentrations are then correlated to the changing chemical properties of the composite materials produced. The expected behavior of both physical and chemical properties for all composites is that increasing dosage of e-beam radiation will increase the overall cure of the material, whereas increasing concentrations of lignin will retard the overall cure.

Chapter 2: Literature Review

2.1 Lignin

Lignin comprises 28% of the mass of wood-like plants. Lignin binds cellulosic fibers together, giving wood its structure. It has a dark brown color, which significantly degrades the whiteness of paper[1]. In paper production, it is therefore bleached out through a series of chemical treatments, most often by the Kraft Process. Lignin is formed when water is irreversibly lost from sugars to form aromatic (ring) containing polymers. In wood, lignin consists of a family of phenyl-propane type polymers in a variety of structural units. Various carbon-carbon and ether bonds link these units together[6]. In addition, lignin has a complex chemical functionality of carboxyl groups and alcohols, among other things[2]. Naturally, the structure of lignin varies from plant to plant. Figure 1 is a representative compound for lignin. Note the large number and type of functional groups present within the molecule.

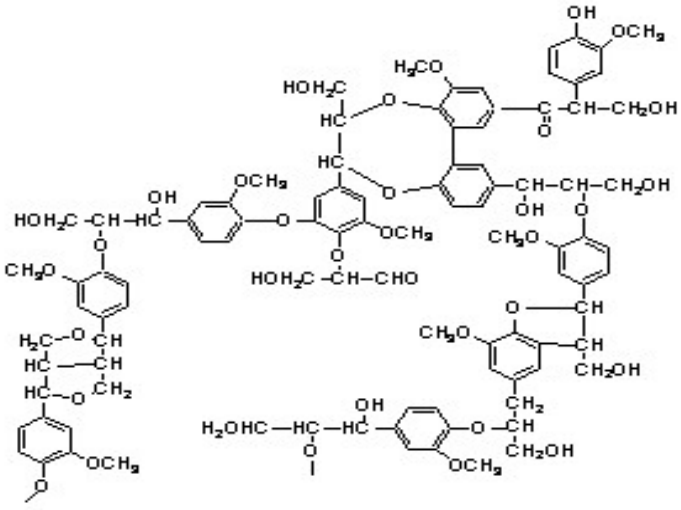

Figure 1: Representative structure of a lignin compound[1]

Lignin has been examined in several studies in the formation of biodegradable thermoplastic composites. The requisite quality of any polymer additive, including lignin, to compatibilize in any matrix or resin is its ability to interact at the molecular level, or at the very least associate[7]. That being said, total miscibility is nearly unachievable, though phase compatibility has been observed at the nano level for many systems. In most cases, the presence of even small amounts of lignin is found to significantly affect the physical properties of the material, most often showing an increased modulus at room temperature. It is likely that this is due to an increase in the crystallinity of the material due to the presence of lignin[7].

Research at IBM has focused on the incorporation of lignin into laminate composites for printed wiring boards. In the study, lignin is combined with diglycidyl ether of phenol A (DGEBA) at concentrations up to 67% lignin. This research was initiated due to the pervasive use of such boards in cellular phones, personal computers and audio and video equipment and potential end-of-life and disposal issues for such equipment and concerns about the materials used[3]. While recycling is a realistic option for plastic components such as housings, it is less so for intricate electronic parts. It is highly improbable that printed wiring boards might be recycled due to their fiberglass laminate backbone and complex embedded wiring. As a result, the majorities are incinerated for their precious metal content or landfilled[3]. The use of lignin in such laminates is shown to be beneficial in increasing the rate of biodegradation of the board once land filled. Because of its phenolic-based structure, lignin is an ideal candidate to usurp components of resins used in wiring boards. Epoxies with lignin concentrations of up to 25-67 wt% lignin produce promising material properties including glass transition temperature (up to 180 deg C) and dielectric constant. However, these properties tend to degrade after higher than 60 wt% lignin[3].

2.2 Wood Composites Treatment by Electron Beam

Under treatment from an electron-beam, lignin compounds are known to undergo several radical initiated reactions such as aryl hydroxylation, fragmentation and cleavage[6]. Aryl hydroxylation refers to the removal of an alcohol group from an aromatic ring. Fragmentation refers to the degradation of the molecule or breaking of a non-ether bond. Cleavage refers to the breaking of the β-aryl bond[1]. These reactions leave the compound open to interaction with a number of different resin systems, changing both the mechanical properties and biodegradability of the resulting composite, rather than merely acting as filler.

In her research at Gr. T. Popa University in Romania, Mihaela Pascu has combined argon plasma exposure and electron beam treatment to blends of polypropylene with epoxy-modified lignin and methacrylate-grafted polypropylene. Both treatment types allow the creation of polar groups on the exposed film. These groups are then responsible for increases in surface polarity, observable by measuring free surface energy[8]. The study concludes that the main effects of an electron beam treatment for this system were: chain scission, oxidation and increase of unsaturation, and these effects are highly dependant on dosage of radiation and oxygen content in the exposure environment[8]. These changes are responsible for increased fractionalization of the surface.

In another study, reactive additive was added to wood fiber-reinforced polypropylene in a reactive extrusion process in order to make the synthetic and natural components more compatible. The extrusion process is followed by treatment by an electron beam to create active sites on both the matrix and reinforcement. The resulting composite has both a high MOE and higher flex and tensile strength. Additionally, the composite possesses increased thermal tolerance over non-electron beam treated blends and the original polypropylene[4]. The study further determines that an electron beam is productive in creating reactive sites on wood fibers, though the e-beam creates reactive centers on components of wood in different ways: by creating chemical bonds between components,

by creating cross linking bridges and side chains through reactive additives and by chain reactions randomly initiated at reactive centers through e-beam[4].

Several international producers of rayon as well as the manufacturers of particle accelerators are working together to add an electron beam process to the manufacturing of rayon. In the production of rayon, cellulose from wood is converted into fiber, filament, cord, film and packaging materials. The industry is suffering greatly from high production costs and increasing environmental regulation. Production costs can be lowered through the use of electron beam treated pulp while providing significant environmental benefits[11]. In addition, electron beam treatment causes chain cleavage in cellulose and formation of a variety of different products. Cleavage produced this way is highly reproducible and can lead to superior process control by subverting the aging step in the production of rayon[11].

In starch films, lignin in concentrations up to 30 wt% and e-beam treatment of 400 kGy were incorporated to increase the water resistance at the surface of the film. This benefit is generally attributed to an increase in intermolecular covalent bonding at the surface due to e-beam exposure, often between the starch and lignin[6]. In a starch matrix, irradiation generates radicals on both the starch and lignin molecules. This allows for the grafting of lignin molecules onto the matrix, or the creation of lignin cross-links between the starches. It is most likely that the hydroxyl groups on the lignin molecule serve as the initiators of such reactions[6]. Because lignin is hydrophobic, these reactions increase the water resistance of the film. In addition, unlike more traditional systems containing polyolefins, lignin systems combined with irradiation by e-beam preserves the biodegradability of the film. This is shown by the kinetics of CO_2 release from film samples immersed in soil during incubation[6].

2.3 Electron Beam Treatment of R46 and R67

Both resins R46 and R67 are ethoxylated bisphenol A diacrylate ethers, with the difference between the two being a methyl group attached to the terminal acrylates on R46. The difference is significant: methyl groups at terminal acrylates for many oligomers often serve as cross-linking points during cure[10].

As previously mentioned, research currently underway at ORNL and Tennessee Forest Products Center is directed towards the curing of these two resins by e-beam treatment at low temperatures. The goal of said research is the production of wood composites for structural panels and engineered wood products. Small resin samples are compiled and cured by e-beam at dosages of 5, 10, 20, 30, 40, 60 and 80 kGy. FT-IR spectroscopy is employed to determine chemical changes to the cured samples, and DMA is performed to determine degree of cure by consequent changes to physical properties[11]. Figure 2 is ethoxylated bisphenol A diacrylate, or R67. Figure 3 is ethoxylated bisphenol A dimethacrylate, or R46.

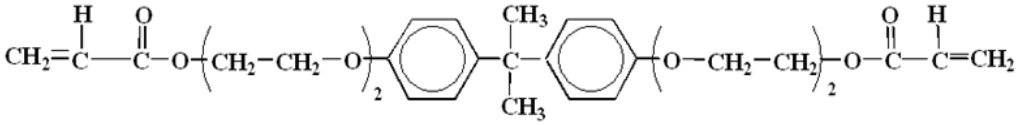

Figure 2: R67 Courtesy of www.sartomer.com

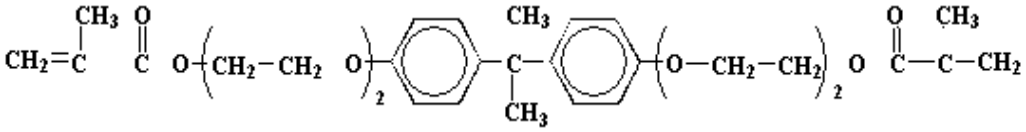

Figure 3: R46 Courtesy of www.sartomer.com. R46 possesses a single methyl group attached to the acrylate while R67 does not.

Glass transition temperature (T_g) is commonly used as a means to measure the degree of cure for resin systems. In general, the higher the T_g, the more complete the cure. T_g increases at an exponential rate during e-beam treatment. Both R46 and R67 show a slight anomaly in this respect, with a max T_g at 90 kGy and a slight decrease before flattening thereafter. Figure 4 is the T_g for R46 and R67 plotted versus dosage when cured by e-beam. This data is obtained by testing with DMA. Multiple samples go into the creation of the below data, with particular attention paid to the 90 kGy dosage. While this behavior may be an anomaly among other e-beam cured resins[11], it does not appear to be such for R46 and R67. Because lignin produces hydroxyl radicals in large numbers during cure, it is likely that composite materials produced from these resins and lignin have curves with a longer exponential section and shorter linear section over the same range of dosage and hence a greater cure dosage for the same T_g. This is due to the electron-scavenging nature of hydroxyl radicals. Therefore rather than stopping at the apparent optimal dosage for T_g, the author chooses to cure the composite materials for this study up to 180 kGy.

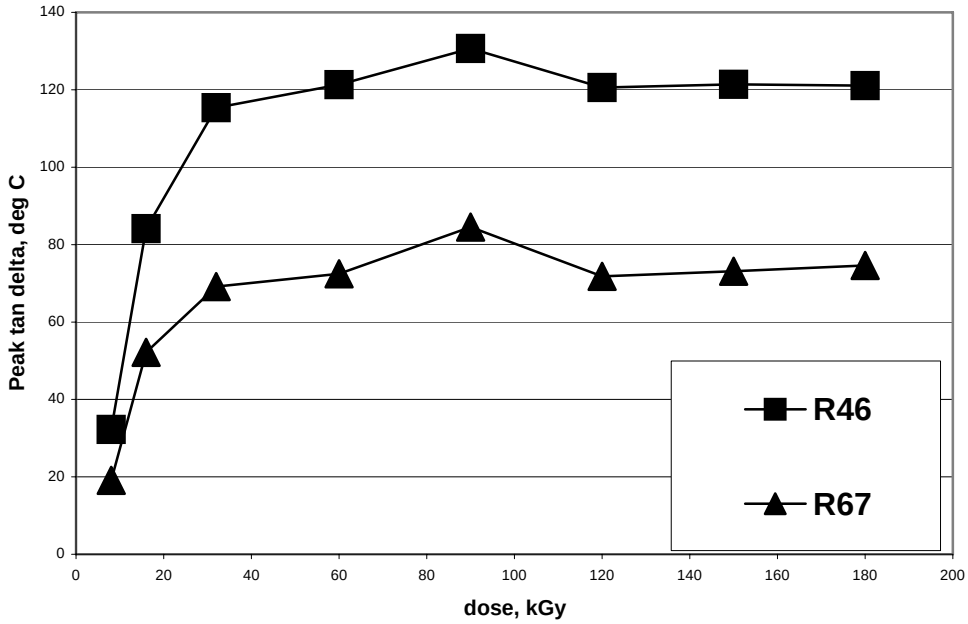

Figure 4: T_g for R46 and R67.[11]

Spectra of R38, a polyether-based acrylate, obtained by Griffith et al using FT-IR show the highest peak at 1720 cm^{-1}. This corresponds to the carbonyl functionality and remains unchanged with increasing dose.[11] The peak at 810cm^{-1} reduces rapidly in the region between 0 and 20 kGy while the peak found at 1160 cm^{-1} increases over the same region. The corresponding DMA data suggests that this is due to the increase in conversion of the monomer taking place in the same region: At the molecular level, this is due to the fact that 810cm^{-1} corresponds to the acrylic functionality, or -C=C-, and the decline represents the saturation of these bonds. The increase at 1160 cm^{-1} represents the formation of the -CH2-CH2- bond as the monomers combine forming polymeric chains. Very little change is observed after 20 kGy, either in T_g or spectra, and this suggests that for a polyether-based acrylate very high conversions can be obtained with only a 20 kGy dose. Resins such as R46, of meth-acrylic functionality, will likely show different behavior[11]. Determining that behavior is therefore one of the intermediate goals of this study. In addition, as previously mentioned, due to the electron-scavenging nature of hydroxyl radicals formed from lignin under e-beam treatment, composite materials made from similar resins and lignin will likely show different behavior as well.

Chapter 3: Experimental Methods

3.1 Sample Preparation

Quantities of R46 and R67 resins were heated at 45 deg C for 20 minutes to bring down their viscosities. The resins were then each mixed with Organosolv lignin at quantities by desired mass fraction. The purpose of mixing is to spread the lignin as evenly as possible within the resin till no visible lignin clusters remain. For samples with concentrations up to 10% lignin, this can be accomplished by hand. For samples at 20, 30 and 40% lignin, a high-speed shear mixer is required. Samples at these concentrations were mixed for one minute at 400 rpm. All samples for a shown resin and concentration were prepared at the same time. The un-cured composite material was then drawn into one-milliliter syringes. For the three higher concentrations, this had to be performed in an oven set to 45 deg C, since the increased concentrations of lignin raised the viscosity of the mixture significantly. The syringes were then labeled and samples selected randomly into equal groups for shipment to SteriGenics, after each group was assigned a required dosage of e-beam radiation. Each unique sample (resin used, concentration of lignin, dosage received) has eight replicants. The resulting composites, once removed from the syringes, have a cylindrical shape roughly half a centimeter in diameter and four centimeters in length (more or less, based upon shrinkage during cure). They range in physical properties from a brittle, crystalline solid to a gel to a liquid, depending upon dosage of e-beam radiation and concentration of lignin used.

3.2 Dynamic Mechanical Analysis (DMA)

DMA is a mechanical test to examine the physical properties of the material. For this case, researchers employ a Perkin Elmer Pyris Diamond DMA with liquid nitrogen cooling attachment. The DMA uses a three point bend test which applies a force on the sample in sinusoidal oscillation at a frequency of 1 Hz. For this research a range of temperatures from –50 to 150 deg C was used at a rate of 3 deg C per minute

Output from the machine shows the elastic (storage) modulus or E', also the viscous (loss) modulus or E", both with respect to temperature. The storage modulus is a measure of the energy stored by the composite during a bending cycle. The loss modulus is a measure of the energy lost by the cycle. Values for both of these moduli are shown at each temperature. A further output is the tan δ curve, since this is merely the ratio of E'/E".

$$\tan\delta = E'/E'' \qquad (1)$$

One commonly used method to measure the glass transition temperature is to read it from the peak of the tan δ curve, and this method is used throughout this investigation when referring to DMA data.

Another useful product of DMA data is the terminal storage modulus, which describes the elastic behavior of the polymer at the rubbery plateau, at temperatures well above the glass transition. This can be related to the number-average molecular weight between cross-links (M_c) by the equation below:

$$Mc = \frac{3\rho RT^*}{E'^*} \qquad (2)$$

Here ρ is the density of the material, measured by assuming a cylinder shape and manually measuring volume and weight; R is the gas constant; T* is the absolute temperature at onset of the plateau, and E'* is the terminal storage modulus. Cross-link

density is related to the degree of cure. However, the value of M_c is relative: it only has meaning when the fully-cured (M_{cmin}) value has already been found for comparison and a percentage value of the sample M_c and the lowest value of M_c from the entire sample set (M_{cmin}) obtained. Once this has been done, a direct relationship between cross-link density and degree of cure can be made. Consequently, in treating the following DMA data, the value of M_{cmin}/ M_c expressed as a percentage will be referred to as the 'degree of cure'. (Burts, 2000, pg 1)

3.3 Fourier Transform-Infrared Spectroscopy

To characterize more fully the chemical changes taking place during cure, a Perkin-Elmer Spotlight® Fourier-transform infrared spectrometer (FT-IR) with an attenuated total reflectance (ATR) attachment was used. Sixteen scans per replicant were taken at a resolution of 4 cm^{-1}. The range used was mid-IR, 650 to 4000 cm^{-1}.

A data analysis software package (the Unscrambler® by Camo) was used to treat the resulting data. First, the data were transformed from reflectance to absorbance. The data were then normalized and a component analysis (PCA) was performed. The PCA creates a covariance matrix from the data. It then takes the eigenvalues of the matrix forming a matrix of eigenvectors (components). Each component accounts for one portion of the covariance matrix, and a certain percentage of the total variance. The component with the highest percentage is the component of the variation in the data. The primary product of PCA is each sample's two different components graphed against one another, normally the two accounting for the greatest amount of explained variance, PC1 graphed versus PC2 for each sample. This is referred to as a graph of PCA 'scores'. A second product of PCA is the 'loadings' graph. This is a graph of the significance of each x variable (here wavenumbers) to the analysis as a 'loading' graphed versus that wavenumber. For the purposes of this research, PCA loadings generally will indicate which wavenumbers (and thereby functional groups) are significant to any particular analysis. Naturally components that account for a high percentage of the total variance

are of more interest than others. PCA is useful for identifying outliers within a data set, identifying similarities and general trends (though it is not intended a regression analysis). 'Good' data from a PCA analysis show scores of all replicants for a particular sample in distinct groups with little or no overlap with replicants of a different sample group.

Within the Unscrambler®, a regression analysis known as partial-least squares (PLS) is also performed. The important products of PLS are a graph of the predicted (calculated) values charted versus the measured (observed) values, as well as a graph of the number of regression coefficients per x variables (again, wavenumbers). Similar to the loadings for PCA, regression coefficients determine which wavenumbers and thereby functional groups are significant in developing the model. In modeling the large quantities of spectral data available in this investigation, PLS regression is applied in two different ways for different sample sets. The first is a PLS model with a single variable by which the behavior of the spectral data is predicted. This is applied to the pure lignin and cellulose samples irradiated by e-beam to determine the chemical effects of the treatment on them by the changes to the statistical characteristics of the spectral data. The second application of PLS regression is actually two regressions: a calibration and prediction. In this case the data set to be analyzed is randomly divided by thirds, with two-thirds being used by the calibration and the remainder by the prediction. First a PLS is performed on the two-thirds of the sample producing the 'calibration' for the model. Then a prediction is performed, feeding new samples (the remaining one-third of the data) into the calibration in order to obtain predicted values. The prediction is sometimes called the validation of the model. This type of PLS regression is performed on the individual composites (resin and concentration of lignin specific) to determine the chemical effects of e-beam radiation with increasing dosage during the cure.

Chapter 4: Results and Discussion

4.1 FT-IR Testing of Pure Lignin and Cellulose

4.1.1 Lignin

Lignin is a complex molecule with multiple functional groups. As previously mentioned, lignin is known to experience several radical-initiated reactions under treatment by e-beam, including aryl hydroxylation, fragmentation and cleavage. Two or more of these processes will likely be taking place at the same dosage of radiation, and this likelihood makes determining the chemical dose-response of lignin during treatment very difficult. Figure 5 is the spectra for Aspen Organosolve lignin samples treated by e-beam. Eight samples at each dosage were collected by FT-IR, and the resulting spectra were normalized and averaged for presentation in Figure 5. Figure 6 is a chart of PCA scores from Aspen Organosolve lignin spectra treated by e-beam at various dosages of radiation. Here PC1 accounts for 45% of explained variance while PC2 accounts for 27%. No grouping is apparent, excepting with 80 kGy. This indicates that spectra of samples treated at that dosage are different from other samples in a statistically significant way.

Figure 7 is a graph of loadings of PC1 for the same analysis. The band at 1130 cm^{-1} (corresponding to stretching of the C-H bond in alkanes) indicates that this functional group is statistically significant in the analysis. The band at 3200 cm^{-1} (corresponding to the stretching of O-H bonds in the alcohol) indicates that this functional group is also significant in the analysis. For the purposes of this investigation, the absence of bands at 1160 cm^{-1} and 810 cm^{-1} (corresponding to bands in the -CH2-CH2- bonding and C=C acrylate bonds, respectively) is more significant, since these are the two functional groups which relate directly to polymerization of both R46 and R67 resins.

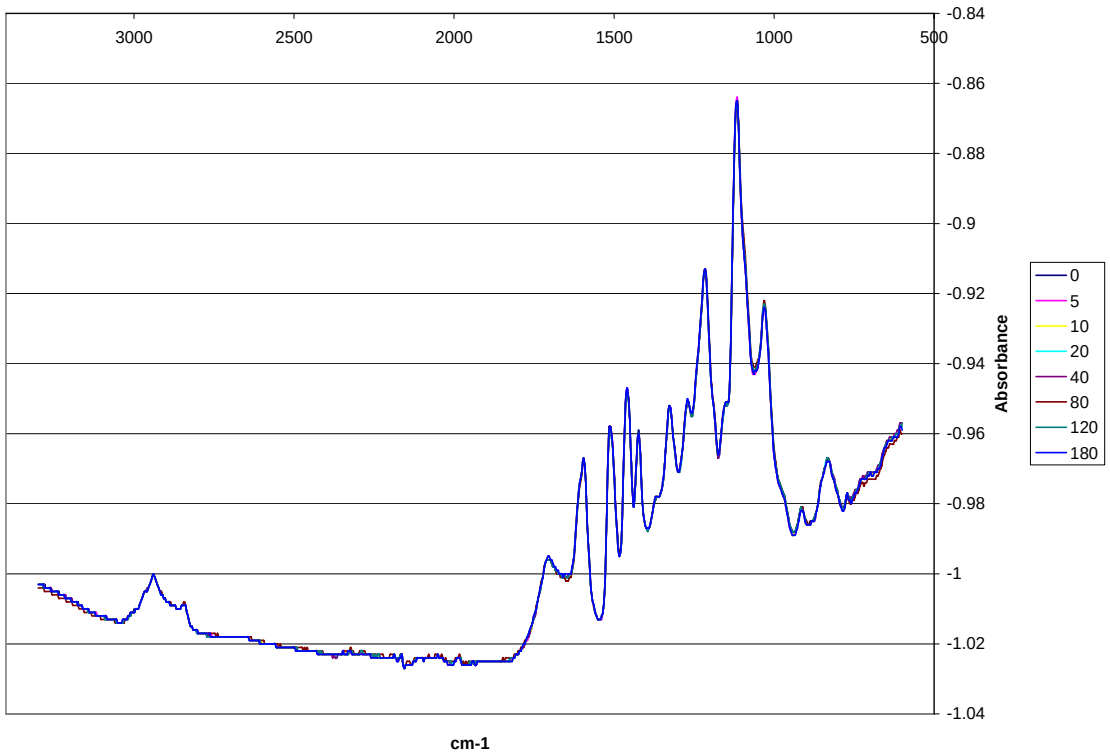

Figure 5: Spectra of Aspen Organosolve lignin treated by e-beam

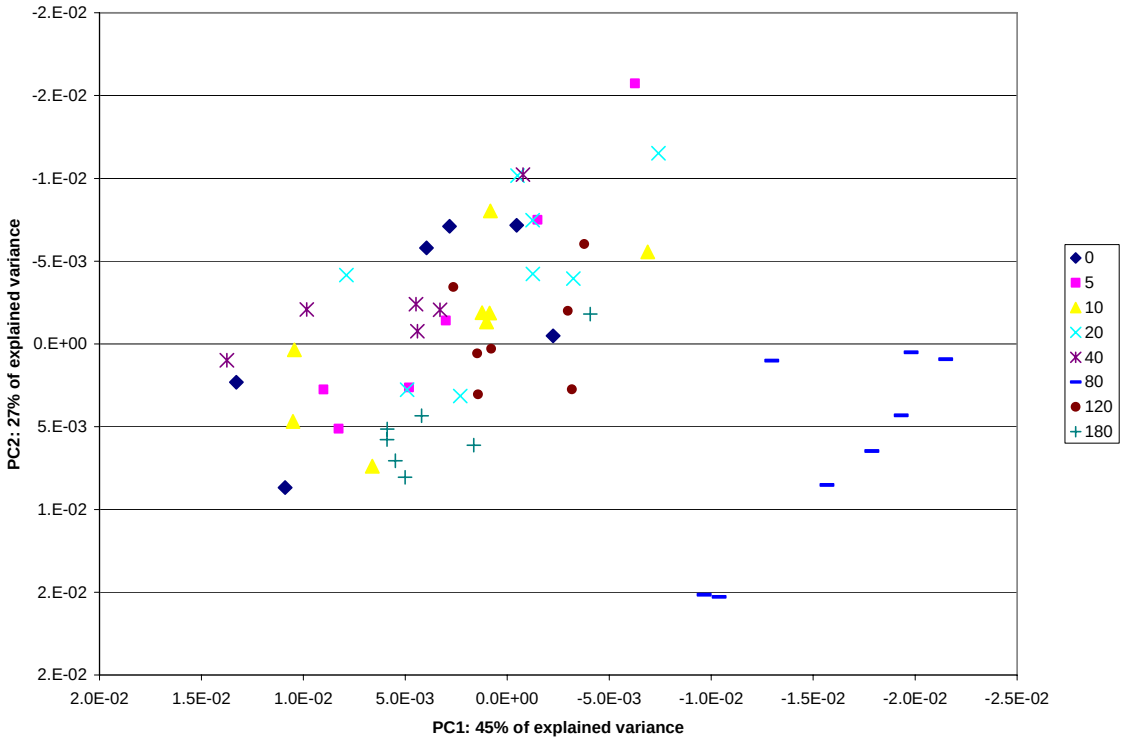

Figure 6: PCA scores of spectra of lignin treated by e-beam at various dosages

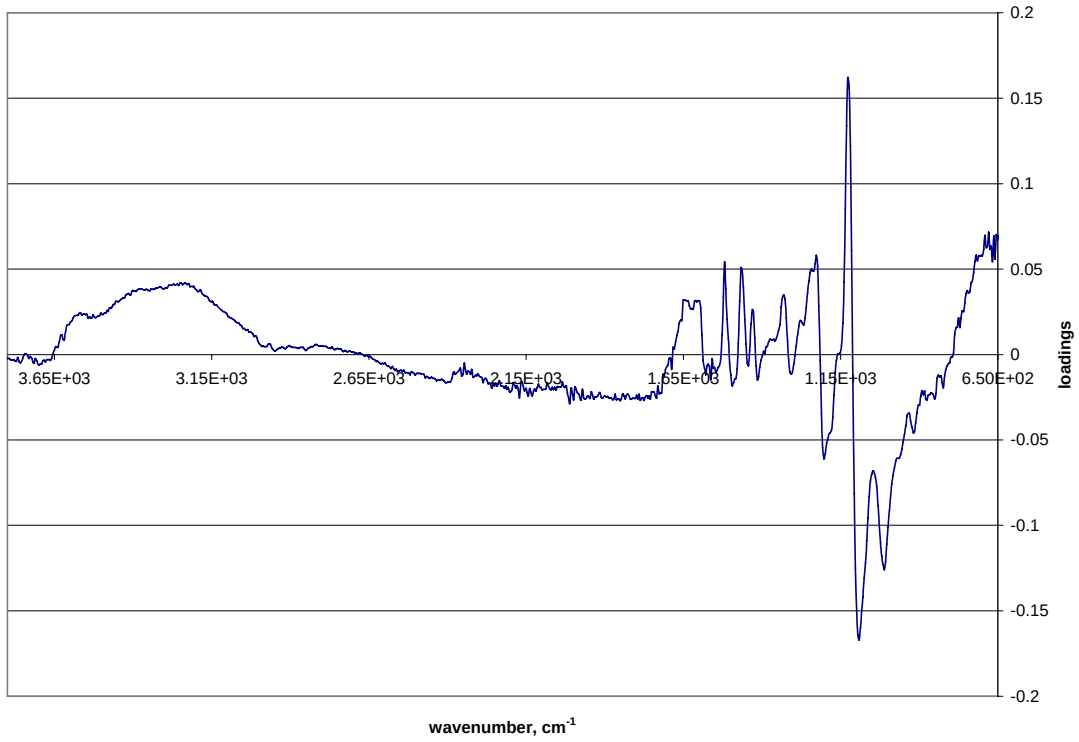

Figure 7: PCA loadings FT-IR spectra collected from Aspen Organosolve lignin samples treated by e-beam

PLS used in this case is attempting to predict the behavior of the spectra data with respect to changing e-beam dosages. Figure 8 gives measured values of dosage of e-beam versus predicted values for lignin samples. The correlation coefficient for this regression (R) is very good at 0.97 with a root-mean squared error (RMSEC) of 16. Since the dosage varies between 0 and 180 kGy with a minimum interval of 5 kGy, this amount of error is poor. By a graph of regression coefficients versus wavenumber (Figure 9) we see that the band about 1650 cm^{-1} is of importance in building a model for the changes with increasing dosage of e-beam radiation. This peak corresponds to a number of different ketones and aldehydes[13]. Of these, the complex and oxygen rich lignin molecule presents several candidates (Figure 1).

4.1.2 Cellulose

Cellulose samples DP670 and Foley were prepared and treated by e-beam radiation at dosages of 0, 5, 10, 20, 40, 80, 120 and 180 kGy. The spectra were then normalized and averaged for presentation in Figures 10 and 11. The spectra are nearly identical. Peaks of note include: a tall peak at 1050 cm^{-1}, which corresponds to the C-O-C bond stretch in the ether. A second peak is seen at 3300 cm^{-1}, which corresponds to the O-H stretch in the alcohol functional groups[13].

To determine any statistical differences within the spectra due to dosage of e-beam, PCA was performed for both cellulose sample sets. The analysis was very similar for both sets of cellulose samples. The following is a discussion of the results of such analysis for the DP670 cellulose samples.

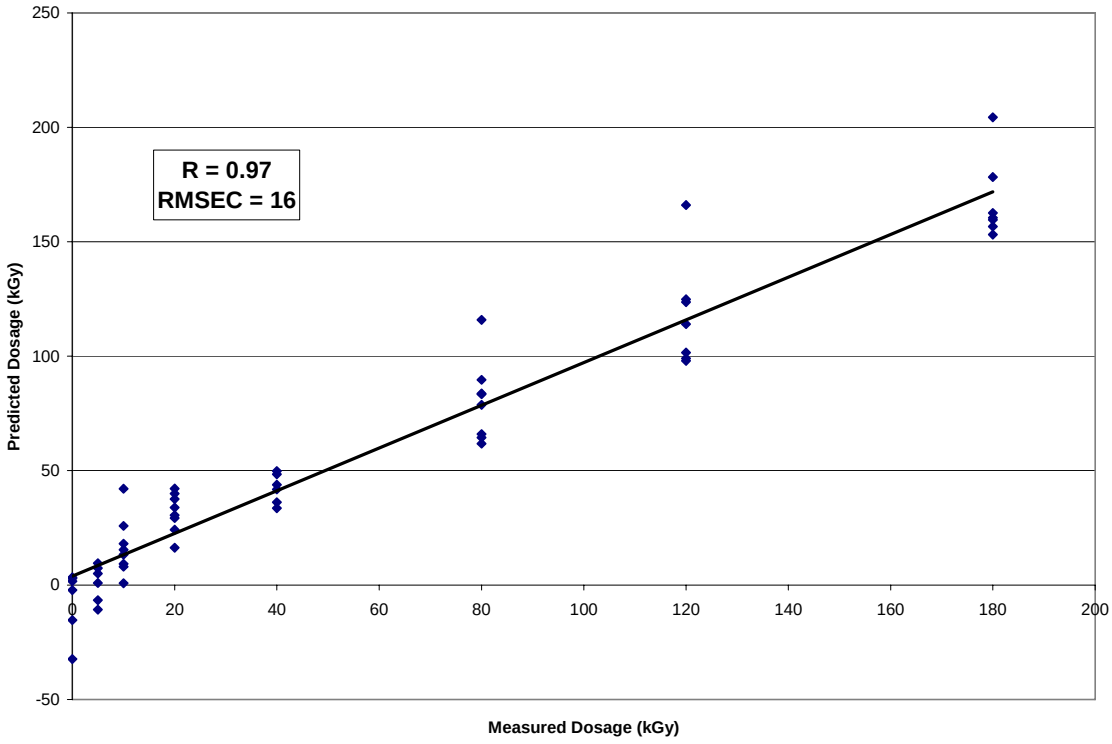

Figure 8: PLS of lignin spectra measured dosage versus predicted dosage

Figure 9: PLS regression coefficients by dosage of e-beam for irradiated lignin samples.

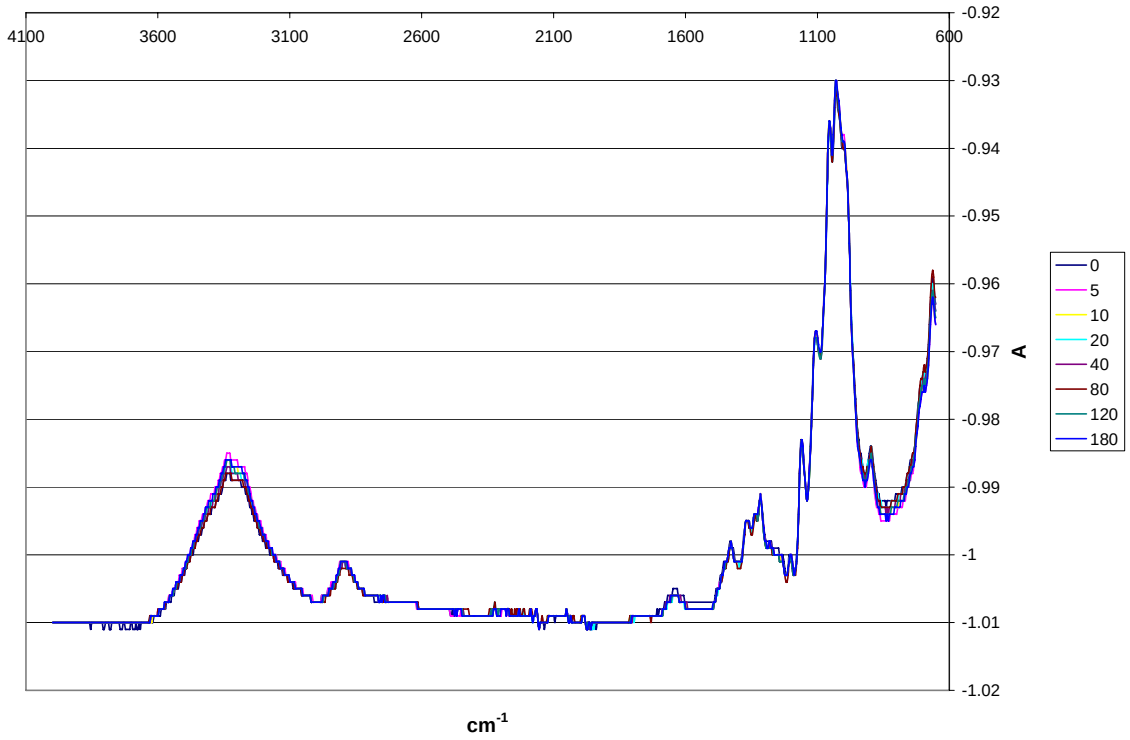

Figure 10: Mid-IR spectra for cellulose sample DP670

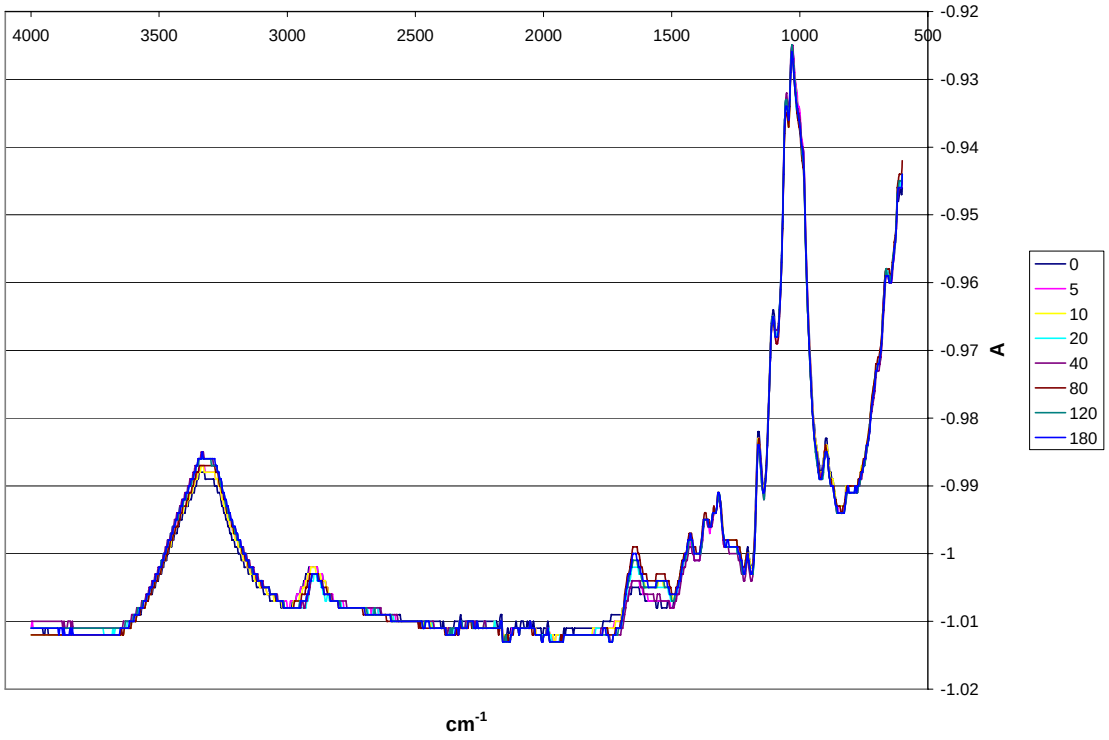

Figure 11: Mid-IR spectra for Foley cellulose samples.

For DP670, a graph of scores for PC1 (43% explained variance) and PC2 (34% explained variance) shows grouping for 0-20 and 180 kGy (Figure 12). This indicates that changes are taking place from 0-20 kGy, characterized by PC1, but very little is taking place over the range of 40-120 kGy. Loadings for PC1 of the same analysis (Figure 13) indicate changes at the 3200 cm^{-1} band which corresponds to stretching of the O-H bond in the alcohol, as well as a band at 1640 cm^{-1}.

The presence of a band at 1640 might indicate the presence of a C=O bond[13] such as in the aldehyde group of cellulose acetate. This would indicate chain scission is occurring as the cellulose molecule is subjected to increasing dosages of e-beam radiation. Note that this band also plays a part in the development of the PLS molecule below.

To determine an effective model predicting the behavior of spectra of cellulose samples irradiated by e-beam, PLS regression was performed for both sample sets. The following is a discussion of the results of the model for the Foley samples.

A graph of predicted versus measured dosage of e-beam graph (Figure 14) gives a strong correlation coefficient (R) of 0.95 at 4 PC's with a rather high error (RMSEC) of 18. A graph of regression coefficients (Figure 15) shows a strong band at 2920 cm^{-1}. This corresponds to the stretching of the C-H bond in alkanes. A second large band is seen at 3300 cm^{-1}, which corresonds to the O-H stretch in the alcohol functional groups. A third strong band is seen at about 1050. This band corresponds to the C-O-C bond in the ether. Though less significant to the model than to the PLS analysis (Figure 13), the band at 1640 cm^{-1} is again present.

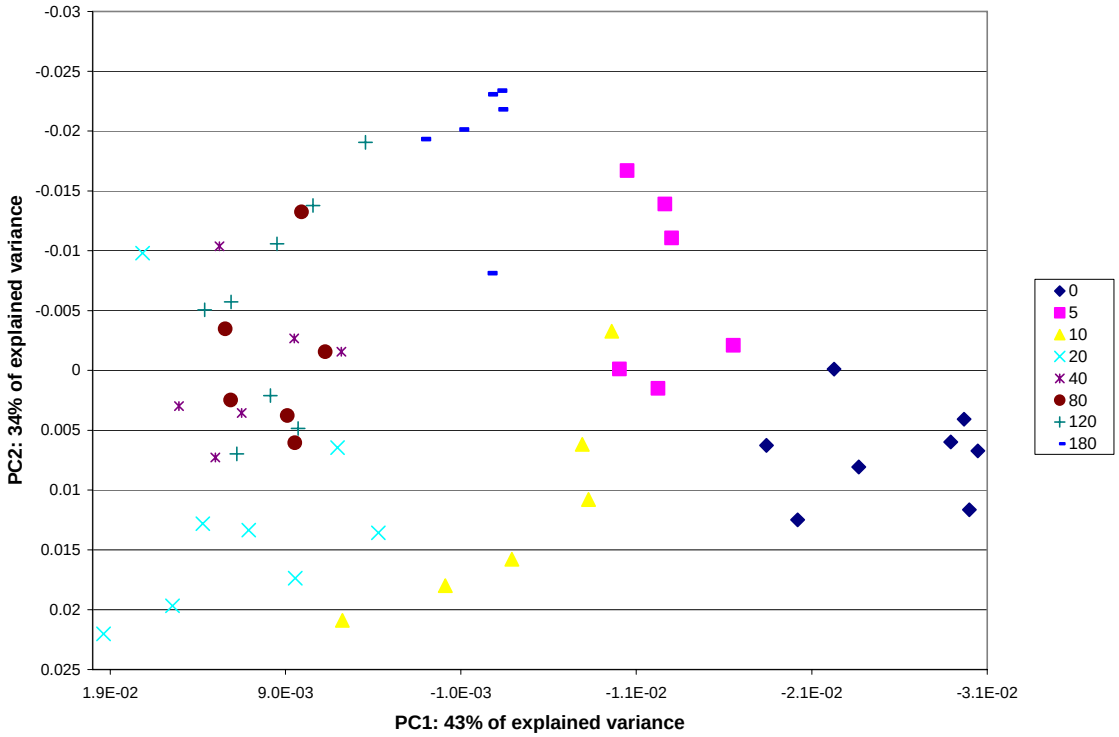

Figure 12: PCA scores of spectra collected from DP670 cellulose samples irradiated by e-beam.

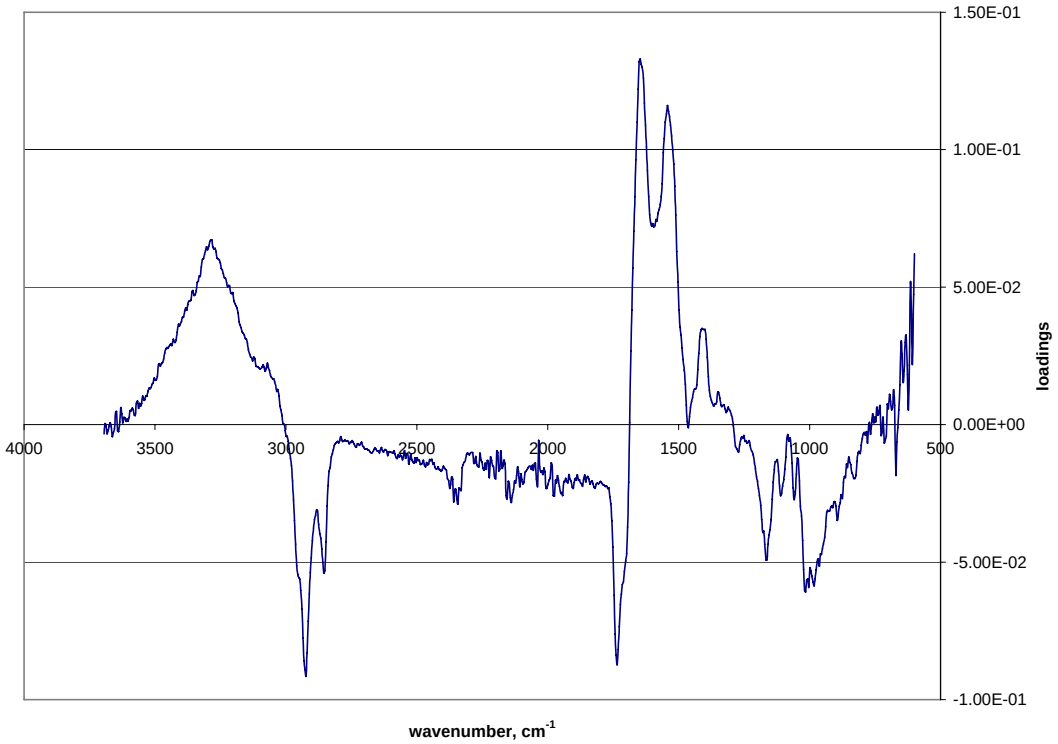

Figure 13: PCA loadings of PC1 for spectra collected from DP 670 samples irradiated by e-beam.

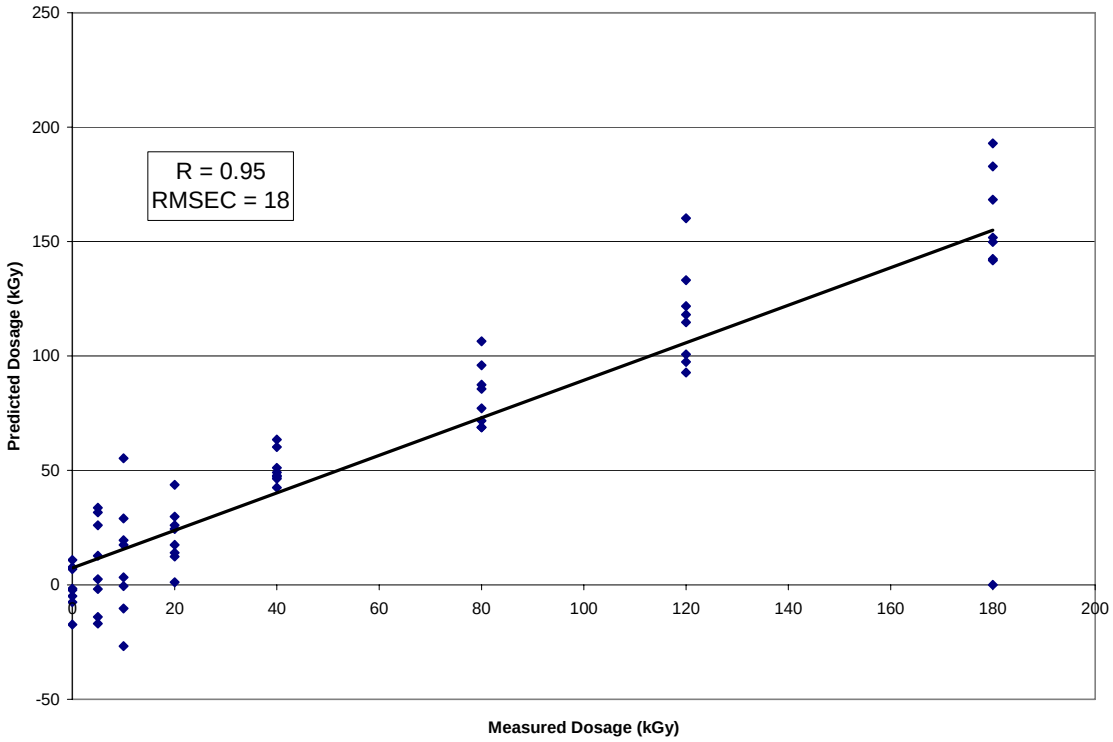

Figure 14: PLS regression predicted versus measured dosage for spectra collected from Foley cellulose samples irradiated by e-beam.

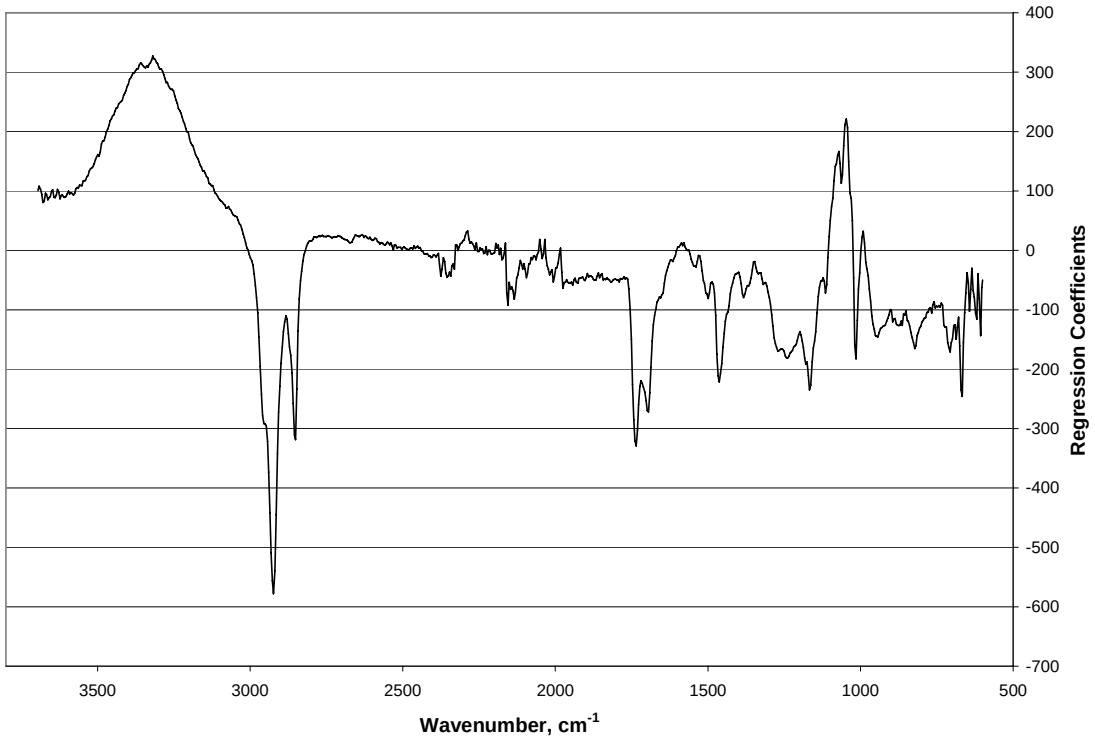

Figure 15: PLS regression coefficients for spectra collected from Foley cellulose samples irradiated by e-beam.

4.2 Imagery of R46 and R67 Composites

4.2.1 Scanning Electron Microscope (SEM)

SEM imagery was taken at ORNL's Oak Ridge facility. Below are Figures 16 and 17, which are micrographs taken of cross-sections of samples at 24 and 31 times magnification, respectively. Of note in these images is the concentric layer surrounding the sample. This is likely a phase boundary created by either shear stress at the wall during the sample making process or temperature variations during sample preparation or shipping. Undoubtedly, this skin-core effect will prove useful in eventual product development phases. In further physical and analytical testing, the 'skin' phase will also prove more significant for both, since ATR is a contact measurement based on reflected spectra (surface), and in DMA because of the nature of the bending process, the outside is more significant in mechanical effects. FT-IR imagery was ineffective in determining the concentration of this phase.

The DMA data presented in section 4.3 confirms the presence of a second phase in several samples by a second peak in the tan δ curve. Another example of the source of this second phase is presented in the SEM images in Figures 18-21. In this case the structures are small spherical shapes appearing within the sample in very small numbers. These spheres likely are the product of nucleation during the cooling process as the material goes from its temperature at mixing (45 deg C) to room temperature. This is a common occurrence for all polymer blends, since miscibility is both a function of concentration and temperature. On a blend's phase diagram, normally nucleation and growth takes place at constant concentration with lowering temperatures between the spinoidal and binoidal curves.

Beyond possible phase-related structures, the appearance of the surface of the composite shifts from very laminar to chalky with the smallest addition of lignin (Figures 22 and 23).

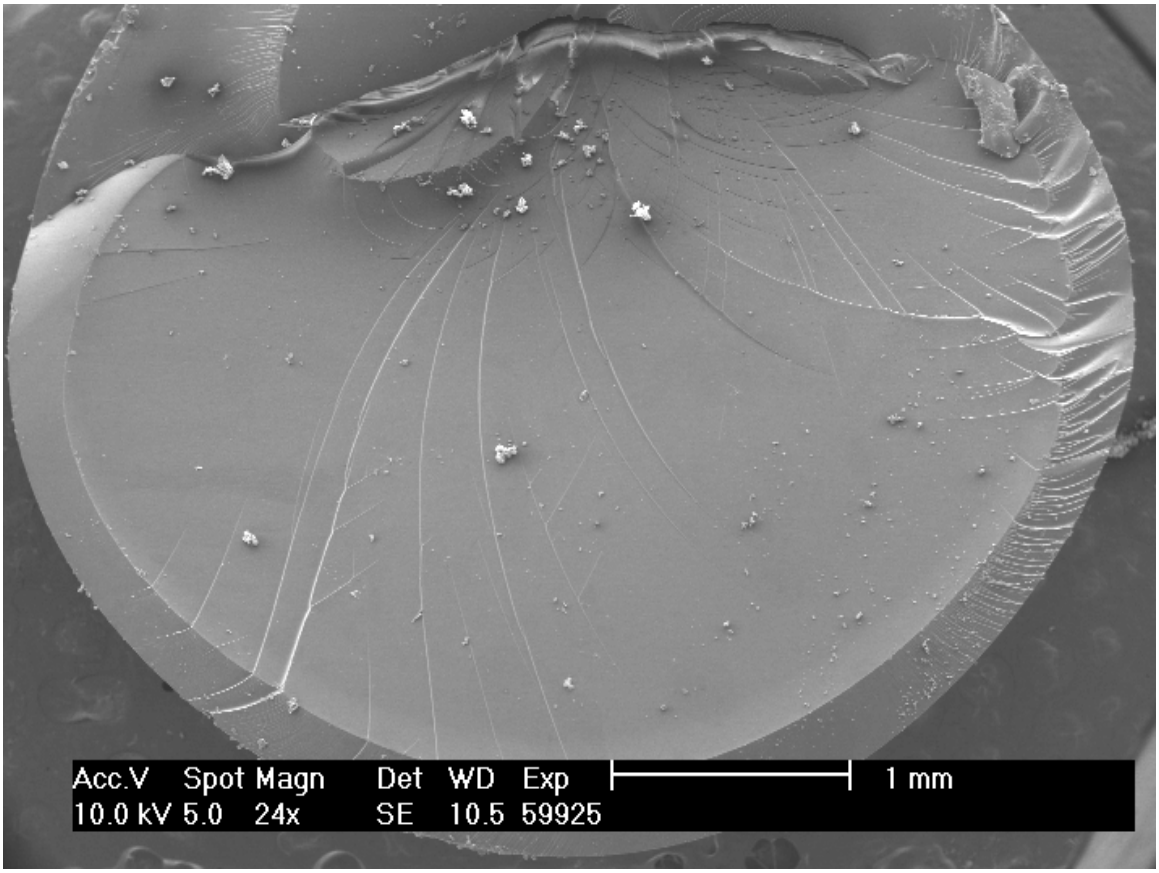

Figure 16: Micrograph of cross-section of R46, 10% lignin sample 80 kGy

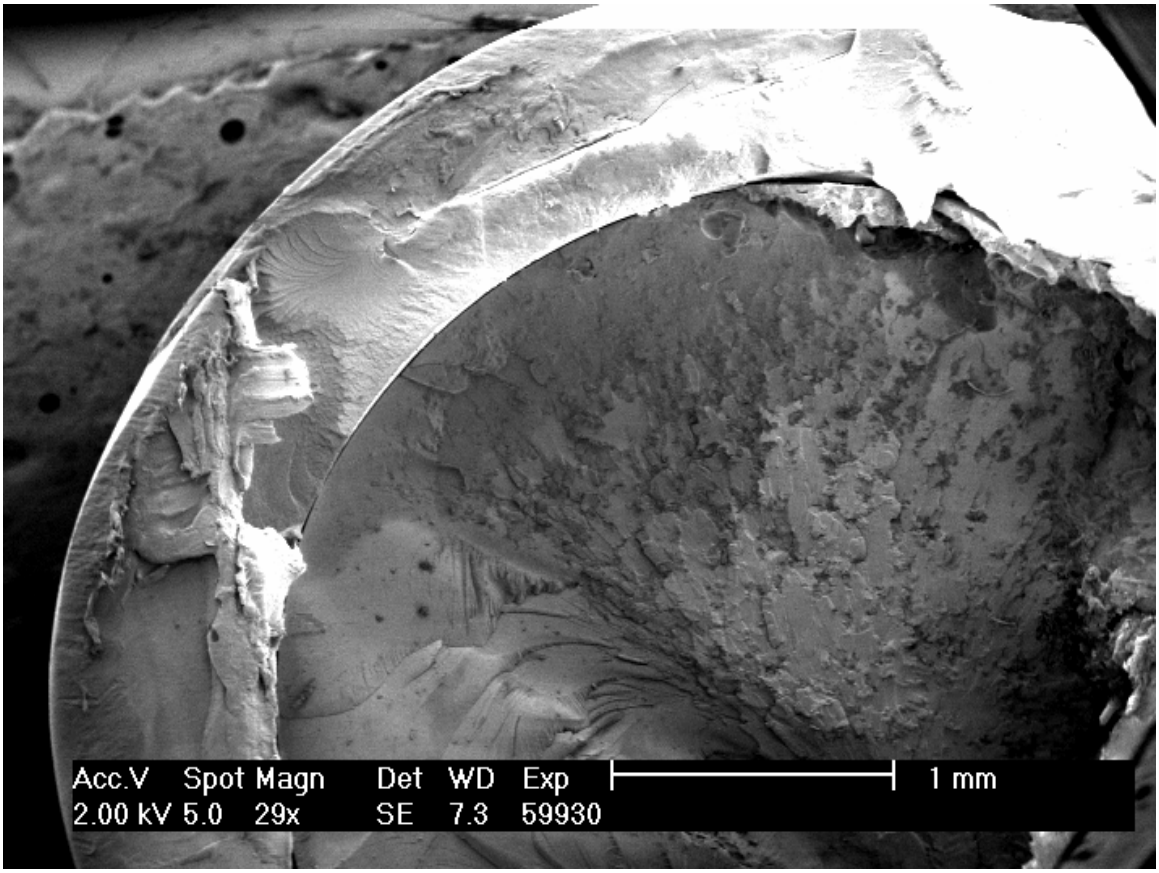

Figure 17: Micrograph of cross-section of R67 sample, 30% lignin cured at 120 kGy

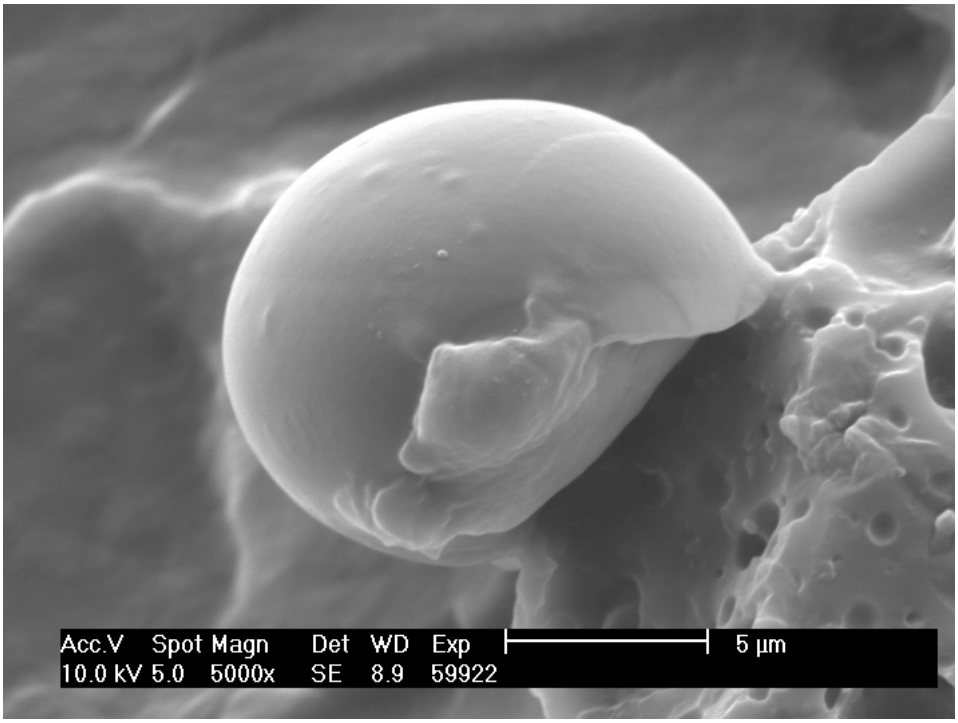

Figure 18: SEM imagery of R46, 30% lignin cured at 80 kGy 5k times magnification

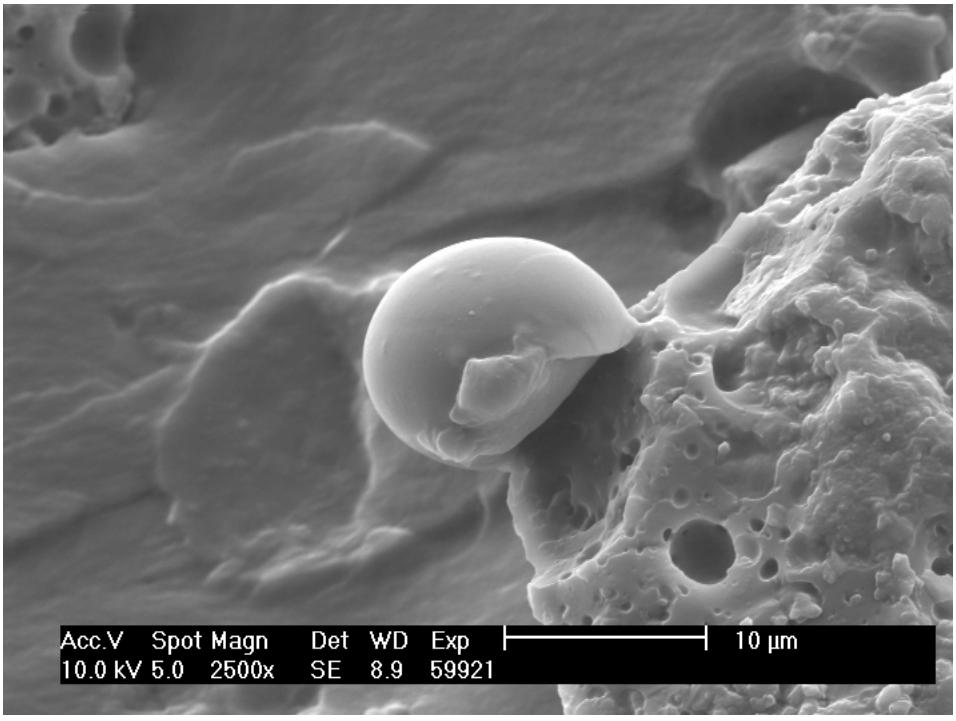

Figure 19: Same image as 20, zoomed out to 2.5k times magnification

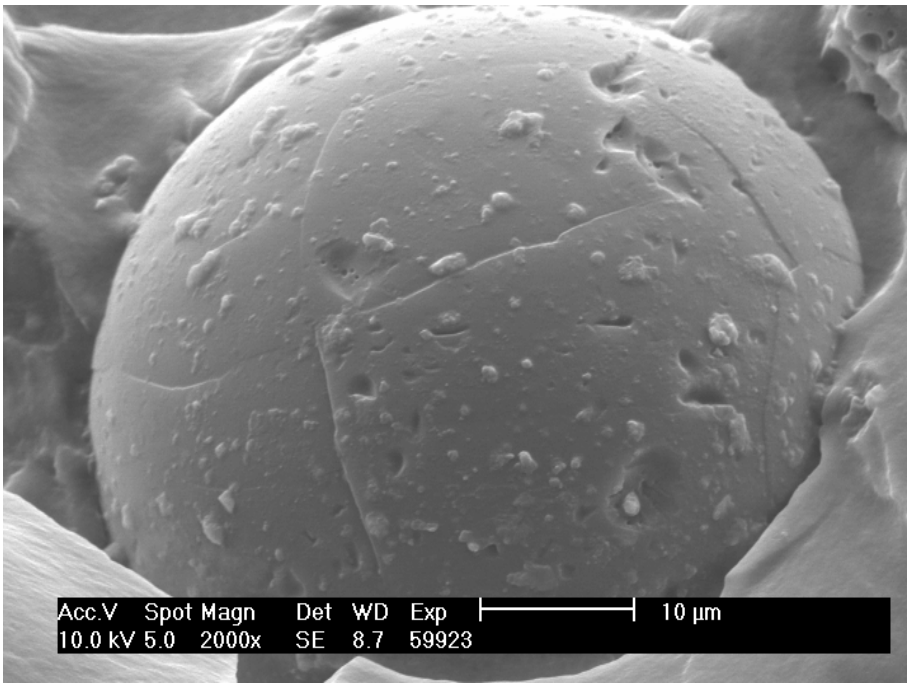

Figure 20: SEM imagery of R46, 30% lignin 80 kGy 2k times magnification

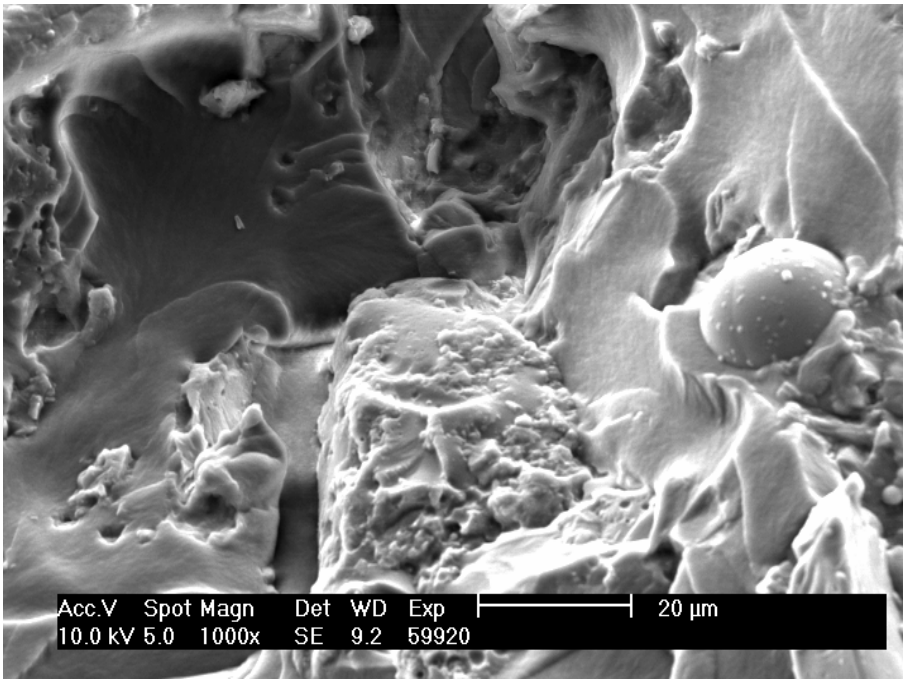

Figure 21: Same image as Figure 22, zoomed out to 1k times magnification

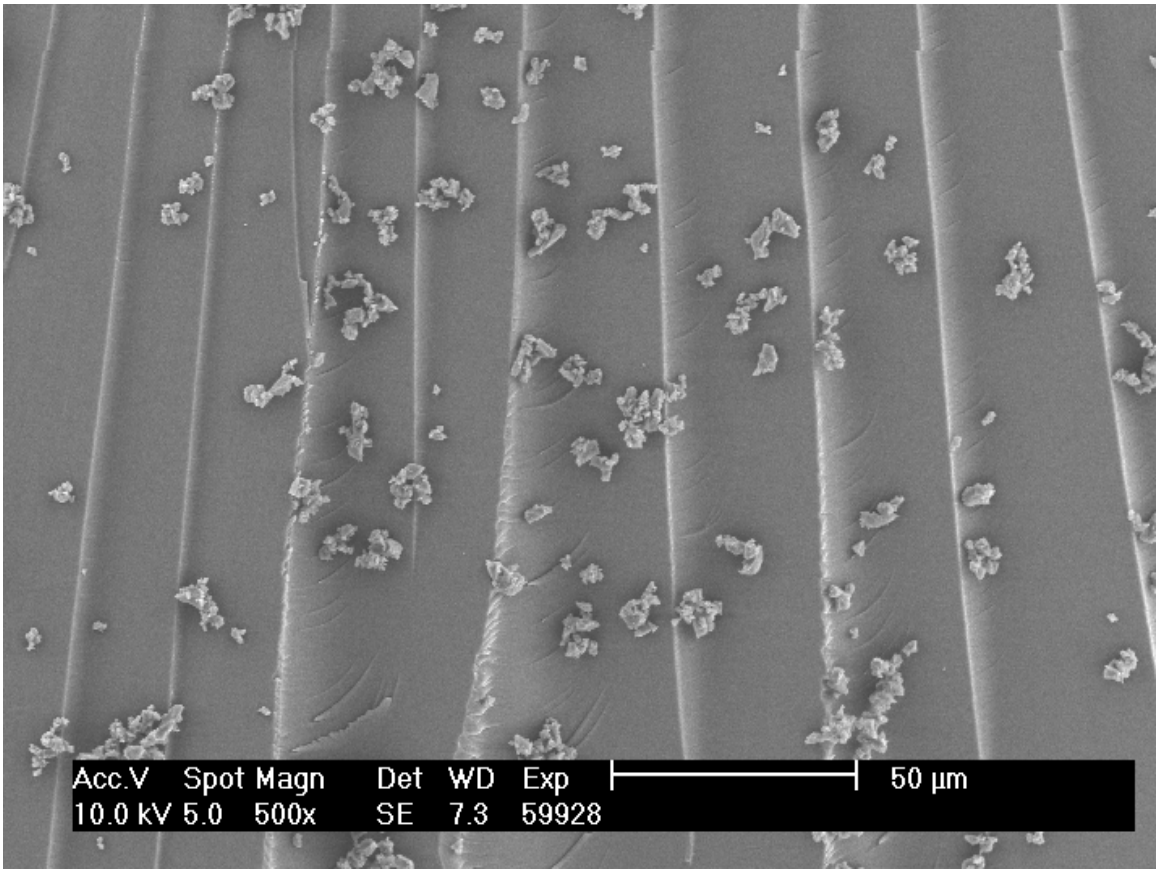

Figure 22: SEM imagery of R67, 0% lignin cured at 120 kGy and shown at 500 times magnification. The structure appears very laminar.

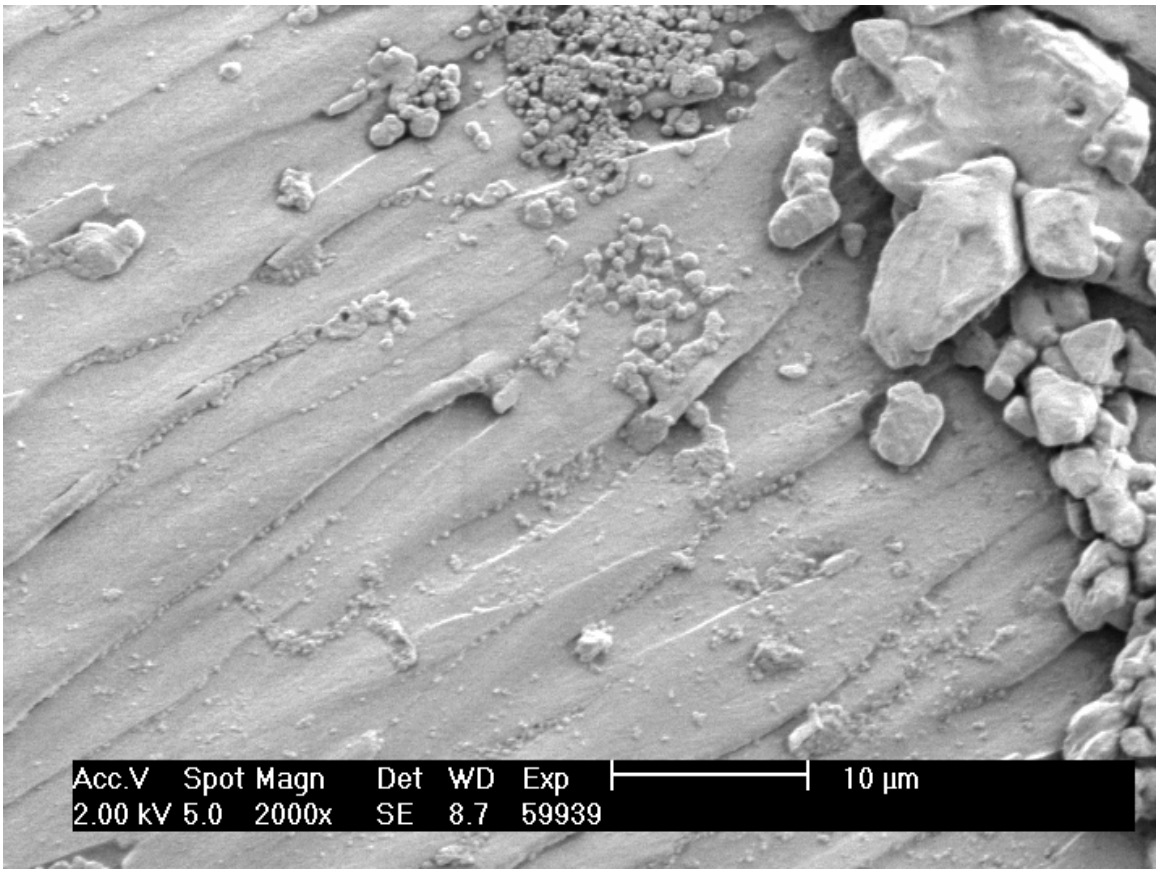

Figure 23: SEM imagery of R67, 5% lignin cured at 120 kGy and shown at 2k times magnification. The material appears to have a ‘chalky’ texture.

4.3 Physical Testing of R46 and R67 Composites

The following sections show results of DMA testing of all composite samples. Again, note that because of the mechanical method used for testing, the outside or 'skin' phase will be more significant in the analysis.

4.3.1 Glass Transition Temperature

Tan δ curves from DMA testing of composite samples gave peaks at certain temperatures which represent the glass transition temperature of those samples. The results show an exponentially increasing curve with increasing dosage of e-beam concentration for both resins, as well as a decreasing response with increasing concentrations of lignin. Figure 24 and 25 show the results for R46 and R67 respectively for different concentrations of lignin and with increasing dosage of e-beam radiation.

There is data missing from both of these graphs. This is due to the material being in a liquid (uncured) state after processing and so being unfit for physical testing. It should be noted that the curves are behaving in a manner consistent with both expected behavior and previous work: increasing dosages of e-beam radiation lead to a 'more cured' composite and so a higher T_g; increasing concentrations of lignin have the opposite result, leading to a lower T_g at the same dosage of radiation; last, there is an anomalous peak about 80 kGy, similar to that from previous work found for pure resin samples at 90 kGy in Figure 4. The exceptions to this are the 20% lignin and higher samples. These only increase after 80 kGy, the first point at which the samples were solid enough to be measured. The peak may be explained by decay of the molecule after cure is complete for the 0-10% lignin samples.

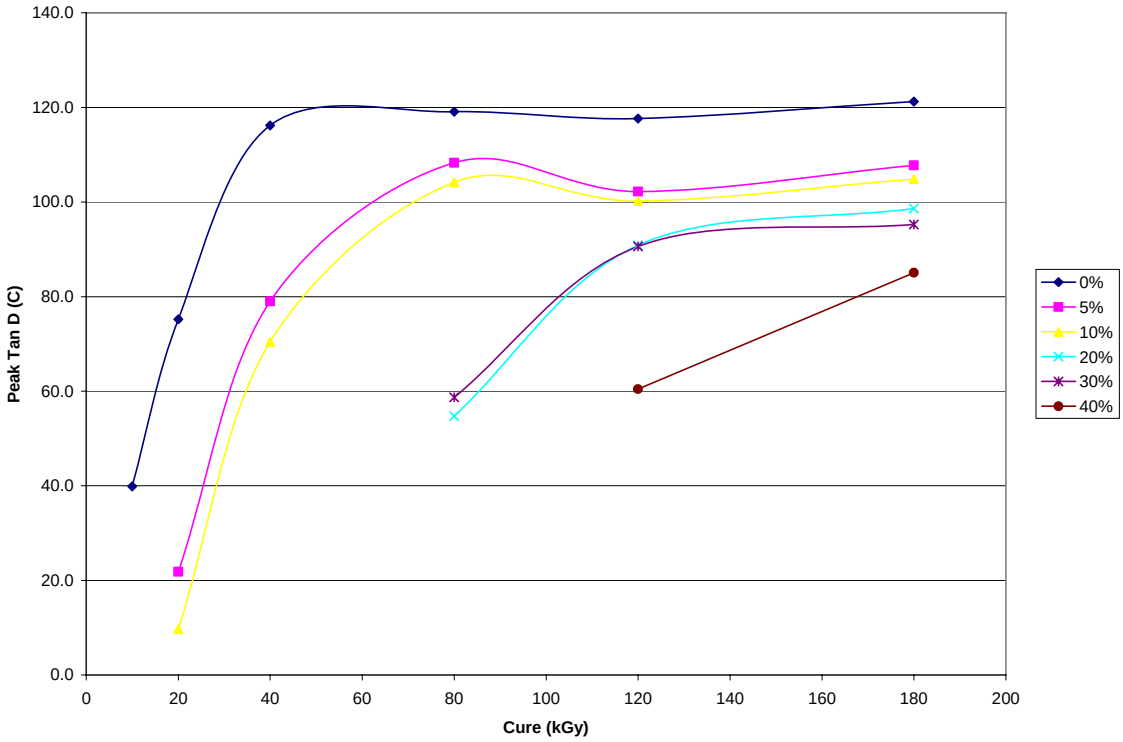

Figure 24: Glass transition temperature for R46 at various concentrations of lignin with increasing cure.

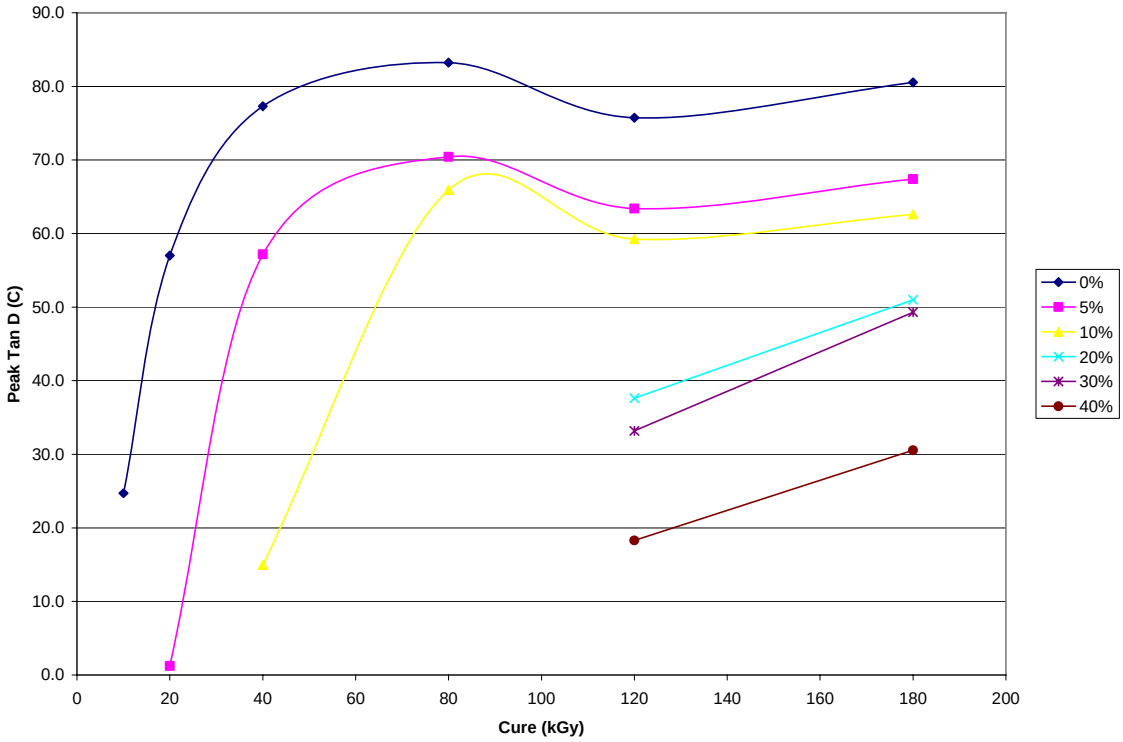

Figure 25: Glass transition temperature for R67 at various concentrations of lignin with increasing cure.

It should also be noted that by comparing the graphs we see R46 at a higher T_g for the same concentration and dosage. This is likely due to the methyl group attached to the acrylate group on R46, which allows is a reactive center for cross-linking. A more cross-linked polymer region will also have a higher T_g.

In addition, for both Figure 24 and 25 it is clear that samples with higher lignin contents (40% for R46, 20, 30 and 40% for R67) are still in the initial (exponential) stages of cure even at 180 kGy. Without their final (linear) stage data, the cure cannot be fully characterized.

A more in-depth way of analyzing the glass transition temperature would be to view the individual tan δ curves. Figures 26-31 show the tan δ curves for R46, each for a single concentration of lignin. As mentioned previously, a tan δ curve with more than one peak indicates more than one transition meaning more than one phase or material present.

Again we see for each concentration of R46 and lignin that increasing dosages of e-beam radiation force the tan δ peaks to the right when graphed versus temperature (increasing the glass transition temperature). The exception being 80 kGy, which is the dosage with the highest T_g at lower concentrations of lignin and lowest at increasing concentrations. As previously mentioned, this is likely because the lower concentrations of lignin cure at much lower dosages of radiation: at the point when their molecular structure begins to break down under increased dosages, the higher concentrations are just beginning to start their cure.

Six of the curves (out of 24 shown) have multiple peaks or shoulders. It is likely then that this is due to the skin-core effect seen in the micrographs in Figures 16 and 17. None of the pure R46 samples show multiple peaks (Figure 25), further supporting this assertion. In addition, higher concentrations of lignin appear more apt to have this problem.

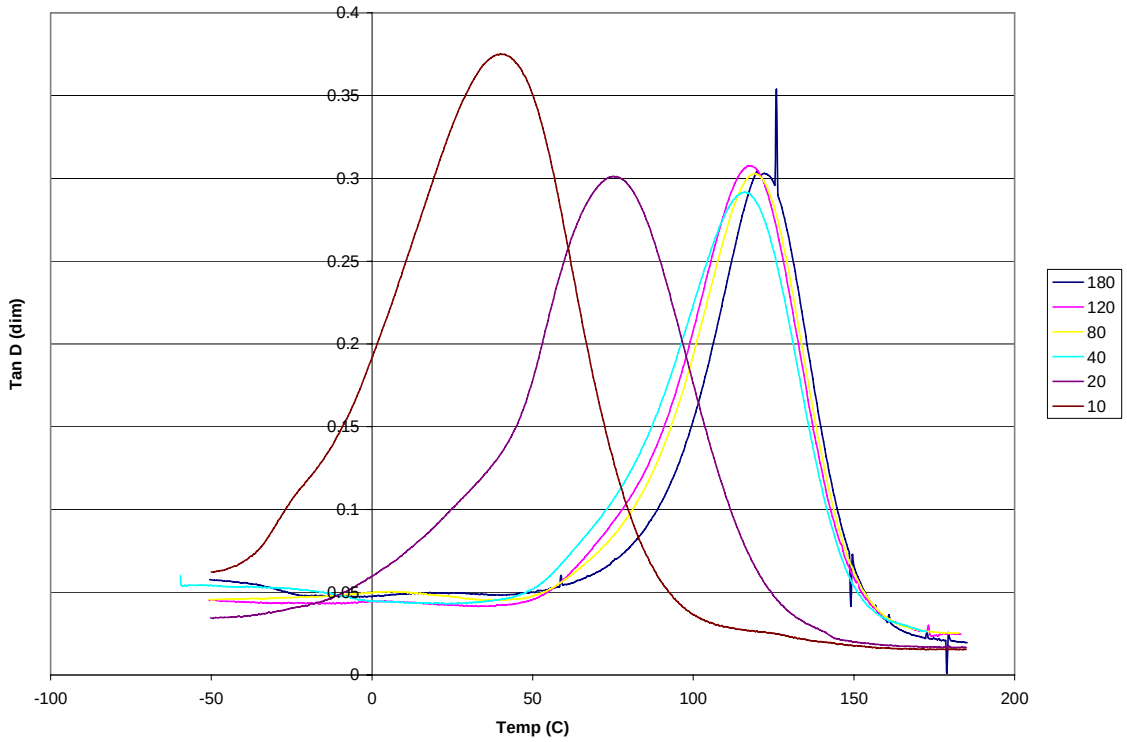

Figure 26: Pure R46 samples at 0% lignin for various dosages of e-beam radiation. The disruption at 180 kGy is likely noise.

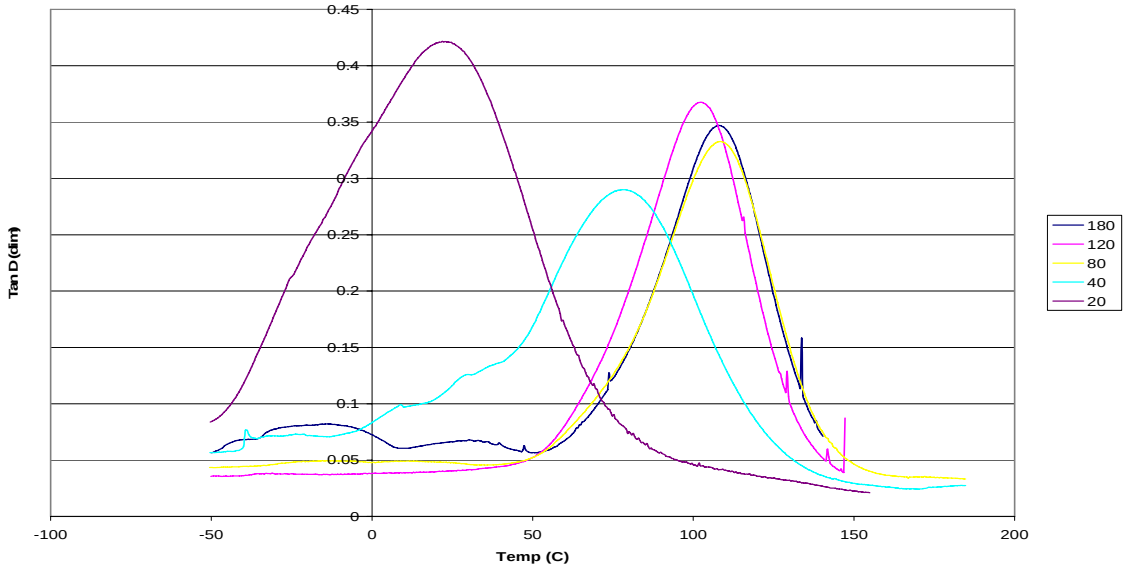

Figure 27: R46 samples at 5% lignin for various dosages of e-beam radiation.

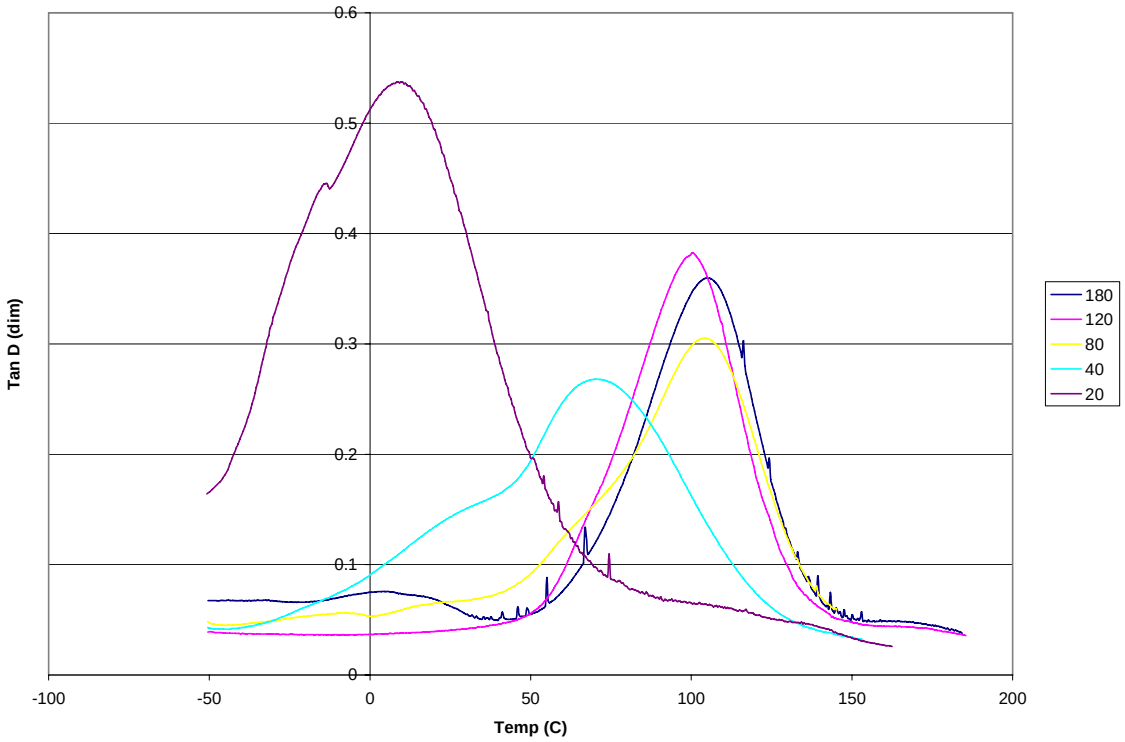

Figure 28: R46 samples at 10% lignin for various dosages of e-beam radiation

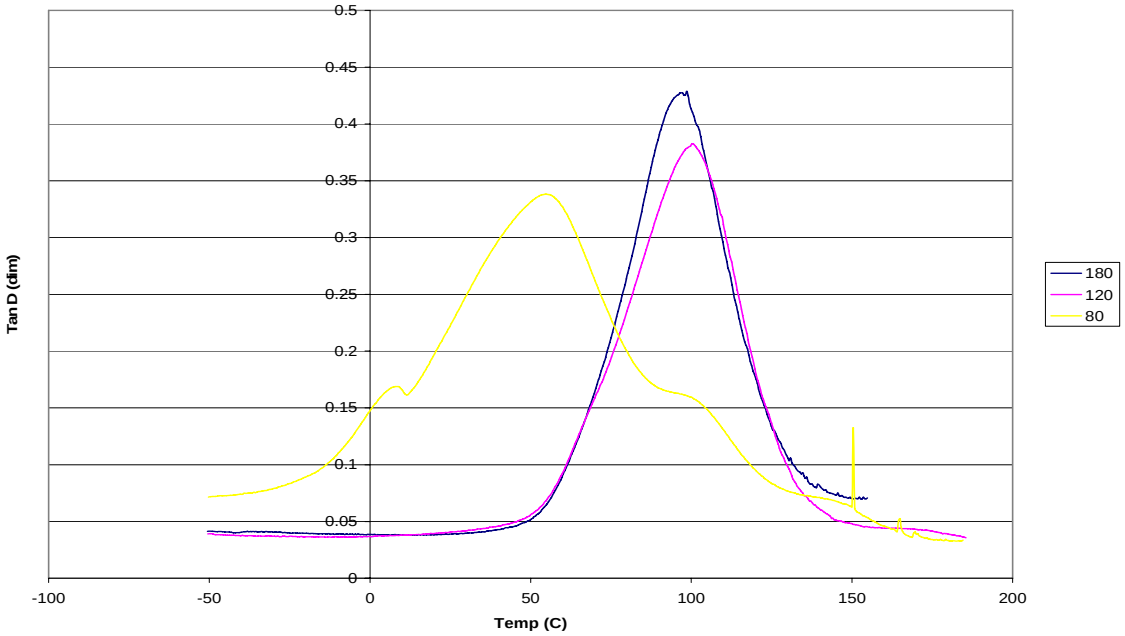

Figure 29: R46 samples at 20% lignin for various dosages of e-beam radiation

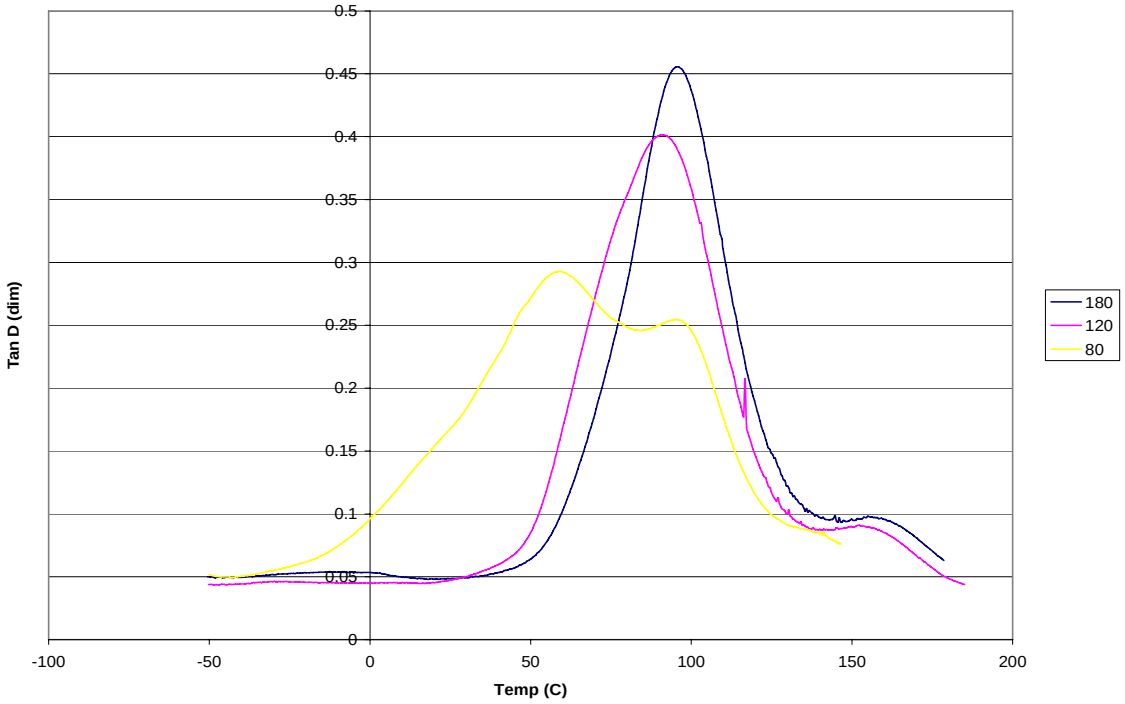

Figure 30: R46 samples at 30% lignin for various dosages of e-beam radiation

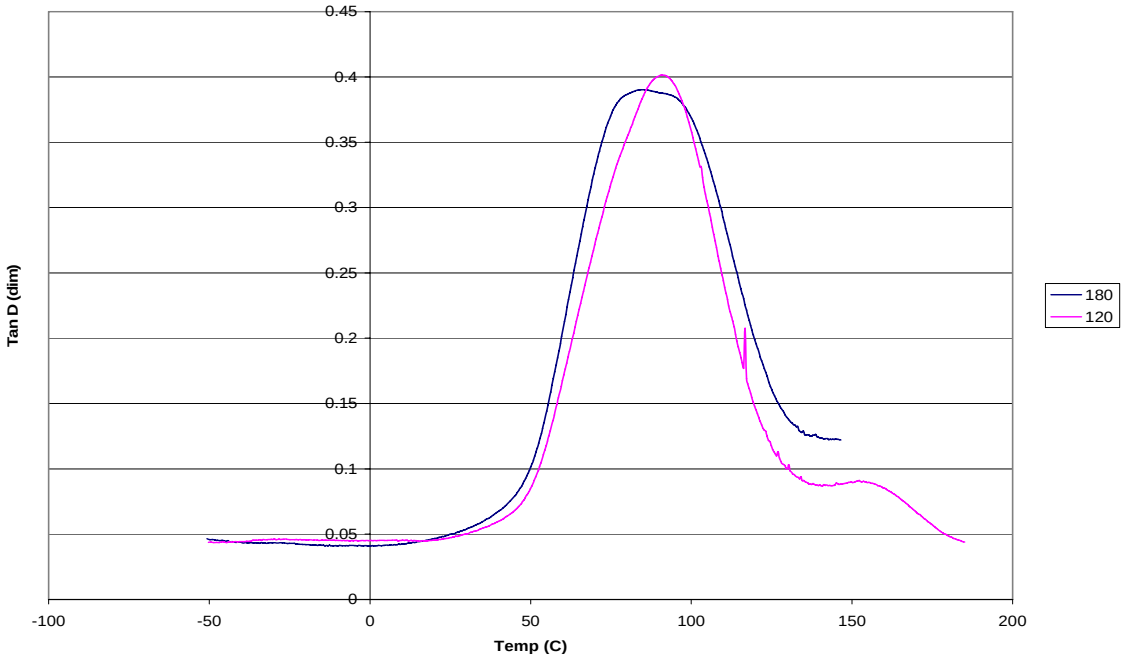

Figure 31: R46 samples at 40% lignin for various dosages of e-beam radiation

The following charts, Figures 32-37 show the same data for R67. Again several samples are missing due to their low cure leaving them in a liquid state rather than the solid state necessary for DMA testing by three-point bend. This is unfortunate since the key dosage (80 kGy) could not be tested for 20-40% lignin samples. However, in all lower concentrations, 80 kGy shows the peak farthest to the right (highest transition temperature). Several samples show two peaks, likely again indicating a lignin rich phase or skin-core effect. This shows another indication of possible issues with sample preparation or handling.

4.3.2 Storage Modulus (E') and Number Average Molecular Weight Between Cross-Links (M_c)

Results of the storage modulus curve which are of interest include E' at room temperature (E'_{25}) and the terminal storage modulus (E) from which the number average molecular weight between cross-links (M_c) can be derived. This value, considered as a fraction of the minimum value, is a measure of the degree of cure of the sample. Below in Figure 38 is E'_{25} for R46. Figure 39 which follows is the same for R67.

For both resins, low concentrations (less than 20% lignin) experience change in E'_{25} rapidly in the range of 0-80 kGy. This is consistent with T_g data presented previously. One notable exception is in Figure 38, where for R46, 30% lignin samples are at every dosage exhibiting a higher E'_{25} than the 20% samples. However, the difference is not very great; this might represent simply an anomaly within the data set.

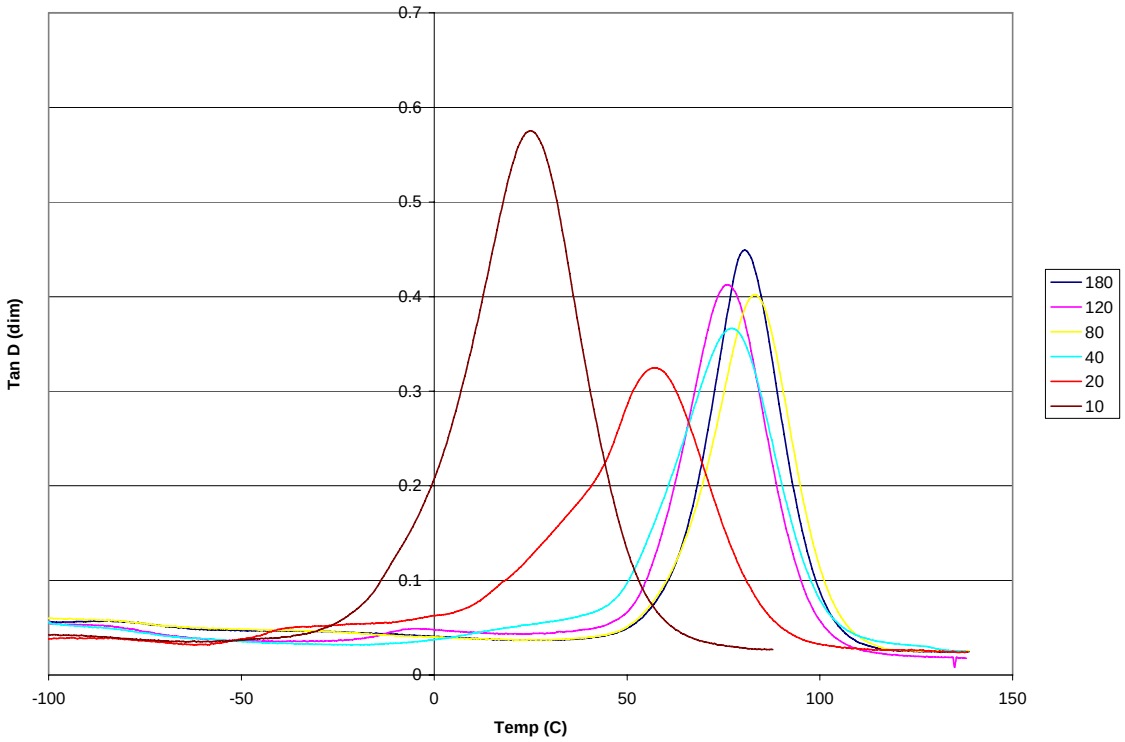

Figure 32: R67 samples at 0% lignin for various dosages of e-beam radiation.

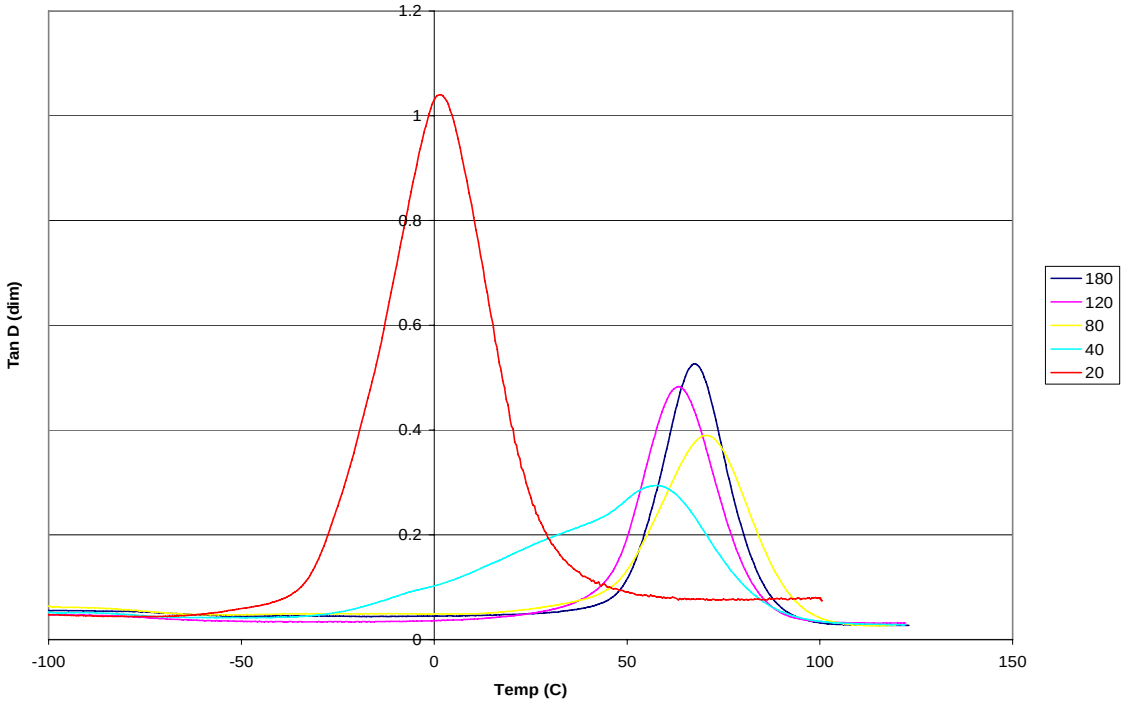

Figure 33: R67 samples at 5% lignin for various dosages of e-beam radiation.

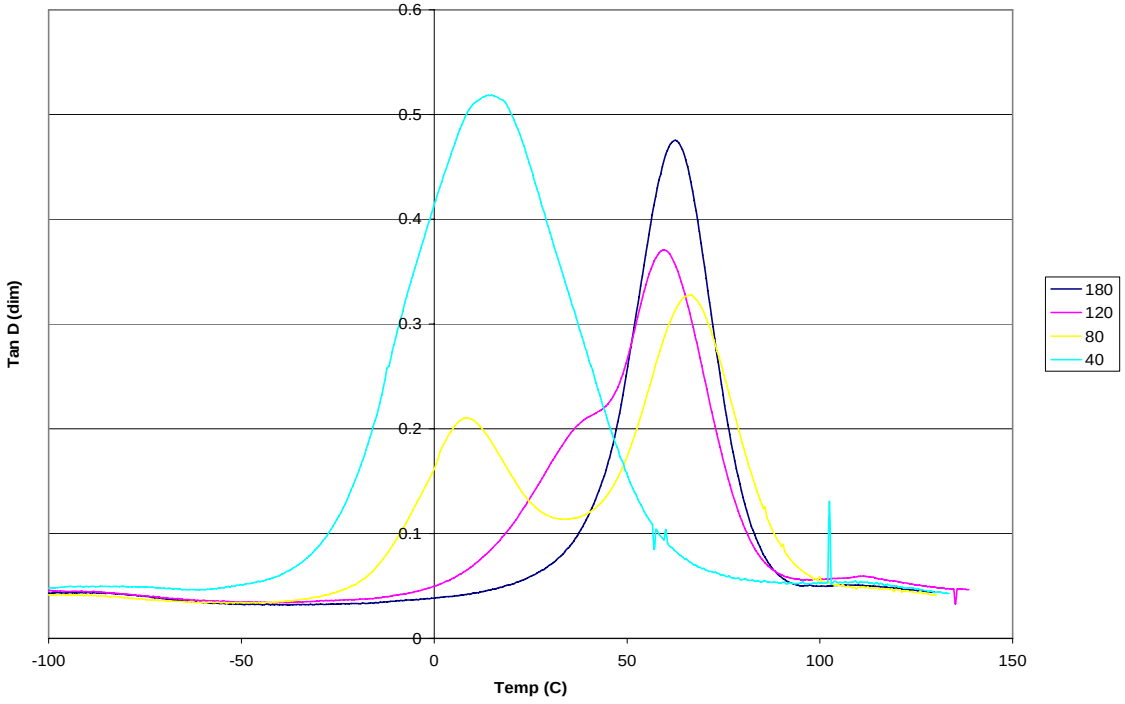

Figure 34: R67 samples at 10% lignin for various dosages of e-beam radiation.

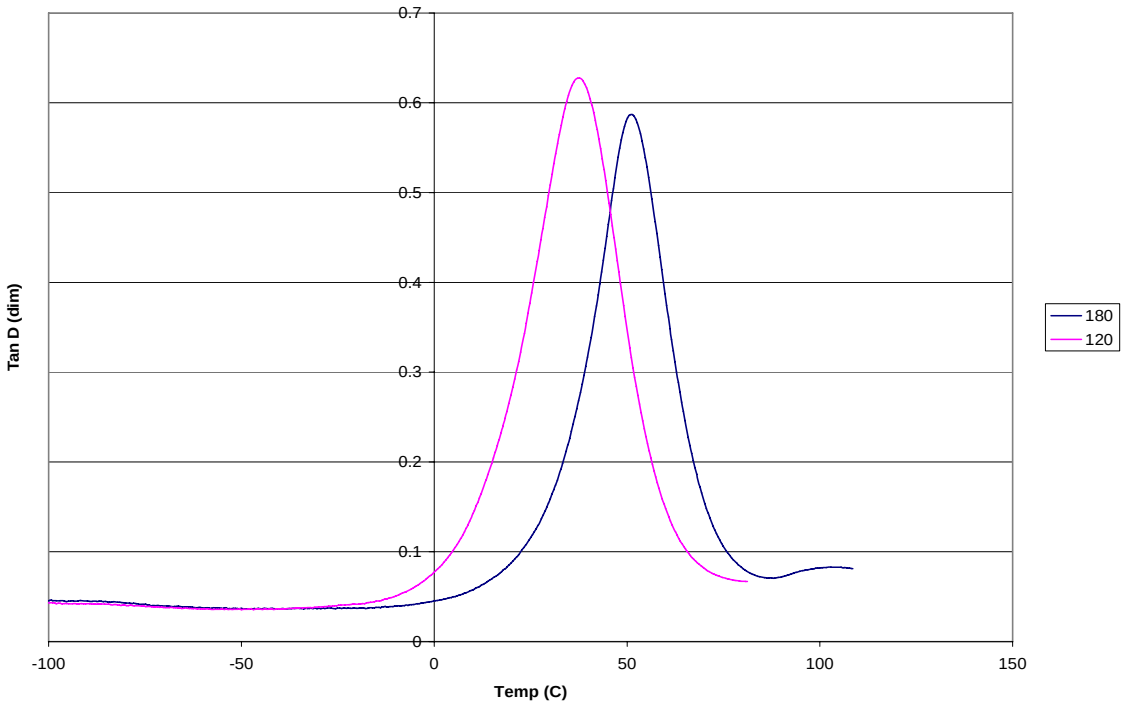

Figure 35: R67 samples at 20% lignin for various dosages of e-beam radiation.

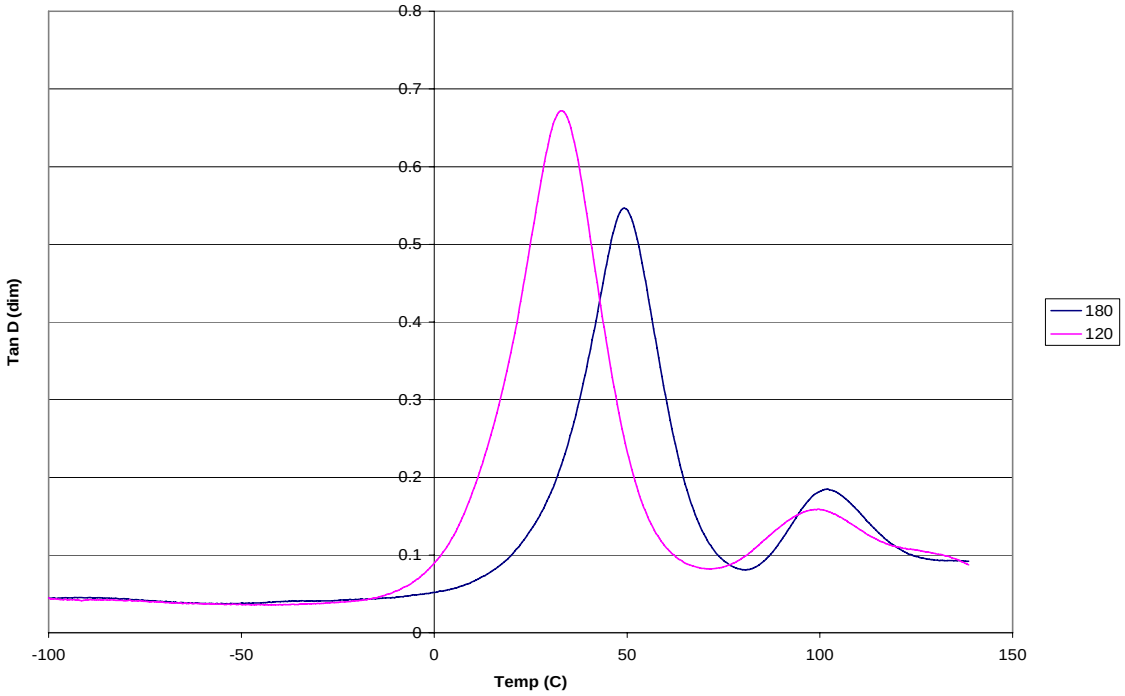

Figure 36: R67 samples at 30% lignin for various dosages of e-beam radiation.

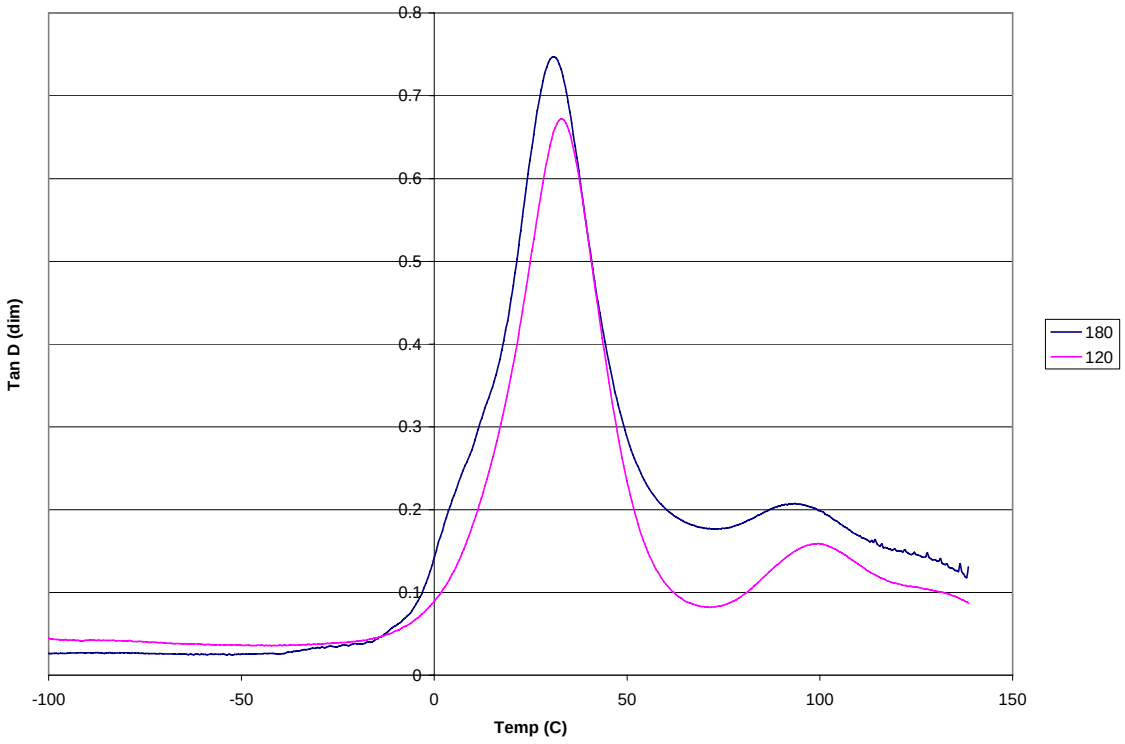

Figure 37: R67 samples at 40% lignin for various dosages of e-beam radiation.

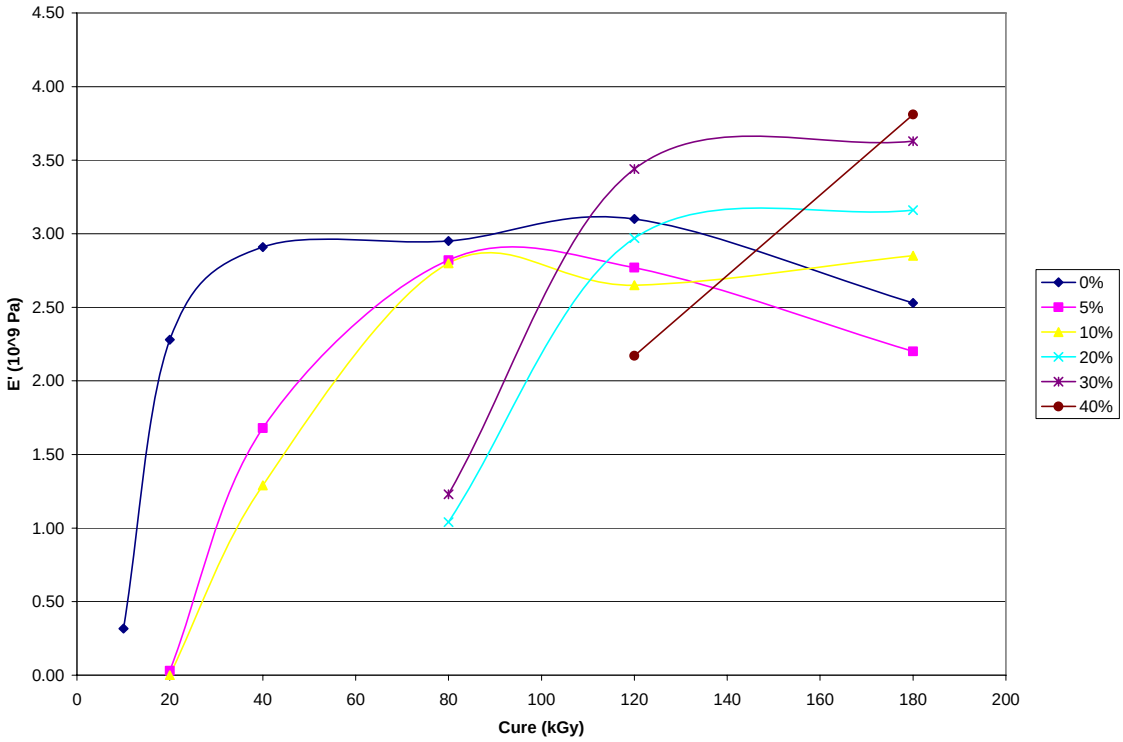

Figure 38: Changes in E' at 25C for R46 with increasing dosage of e-beam radiation for various concentrations of lignin

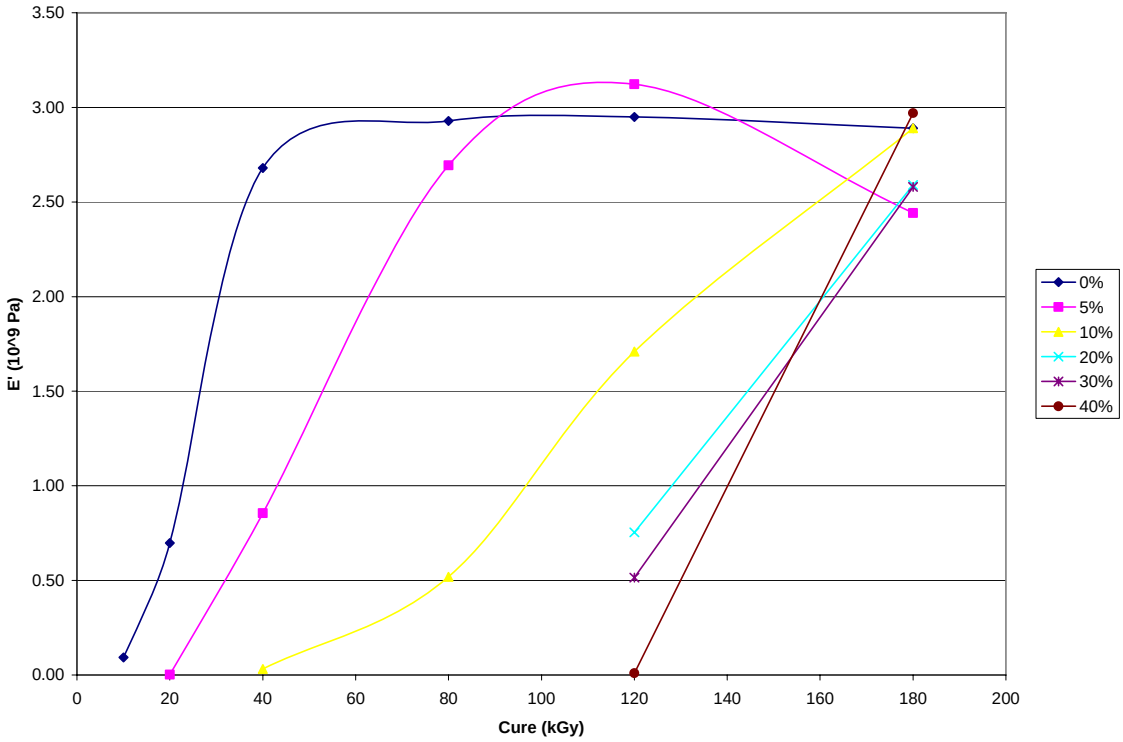

Figure 39: Changes in E' at 25C for R67 with increasing dosage of e-beam radiation for various concentrations of lignin

As previously mentioned, M_c only has relevance when expressed as a percentage of M_{cmin}, though this percentage can be referred to as the degree of cure. The value of M_c is based on the material's density and terminal storage modulus, which is closely related to the modulus of elasticity. Because lignin tends to add a very brittle element to most composite materials, it is somewhat questionable as to whether samples with higher concentrations of lignin (30, 40%) are showing in their values of M_c the properties due to crosslink density or properties due to the physical properties of lignin. The degree of cure for each resin at a shown percentage of lignin is shown below in Figures 40 and 41. The pattern of the above figures for degree of cure closely follows that of Figures 24 and 25 for T_g: increasing dosage of e-beam radiation increases the degree of cure, while increasing concentrations of lignin show lower degree of cure at the same dosage. For both resins, the minimum value of M_c (and hence the 'fully cured' state) comes at 0% lignin and 80 kGy.

For the higher concentrations of lignin (20, 30 and 40%) it should be noted that for the purposes of this or any other physical testing which would require bending, the cure in effect begins at 120 kGy.

It is interesting to note that unlike T_g the degree of cure does not go down after 80 kGy for resins of lower concentrations of lignin. This may be because this analysis comes at degree of cure from cross-link density. Perhaps it is the case that while the cure as measured by T_g has reached its peak at 80 kGy the cross-linking mechanism as determined from terminal E' has not. Another point of note is that R67 samples in Figure 40 show a much greater rate of cross-linking (with respect to dosage)at the ends of their curves. It may be the case that because of the methyl group at each end of the R46 monomer which acts as a cross-linking node, much less radiation is required to saturate the cross-linking capabilities of this resin compared to R67, which likely must rely on interaction from its phenolic groups with those of the lignin within the sample to form cross-links (this is only of interest for 0, 5 and 10% samples as the others are still in the exponential stage of curing).

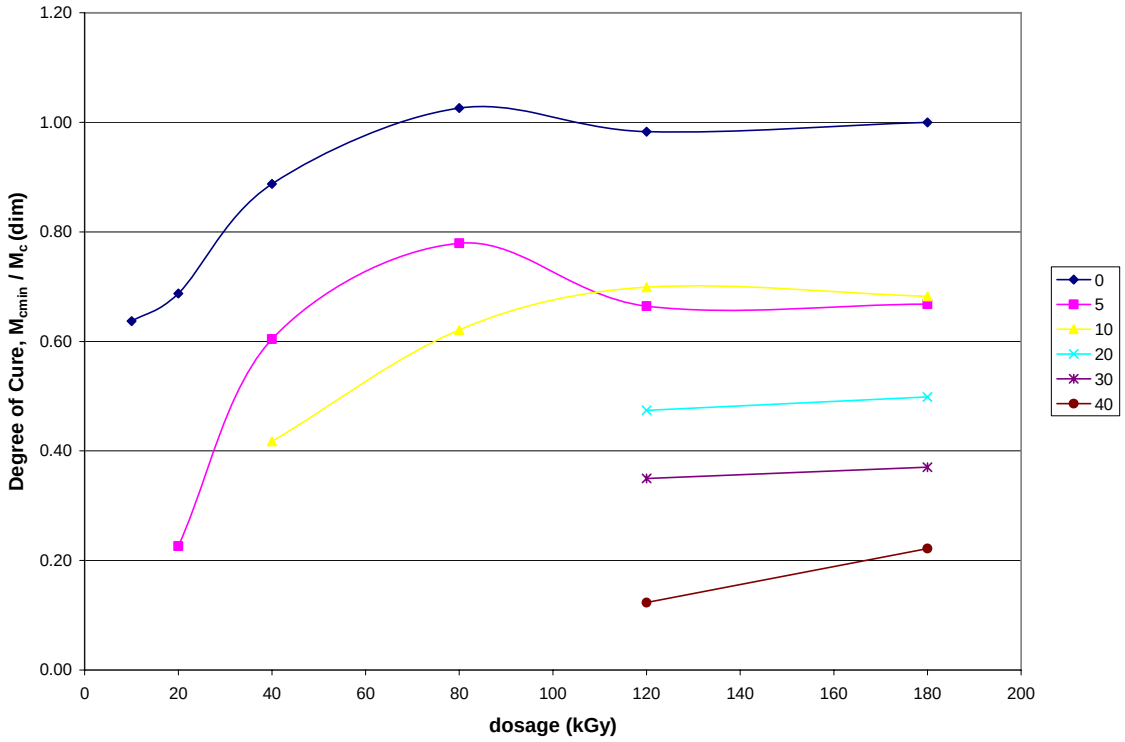

Figure 40: Degree of cure for R46 samples at various concentrations of lignin by cure dosage.

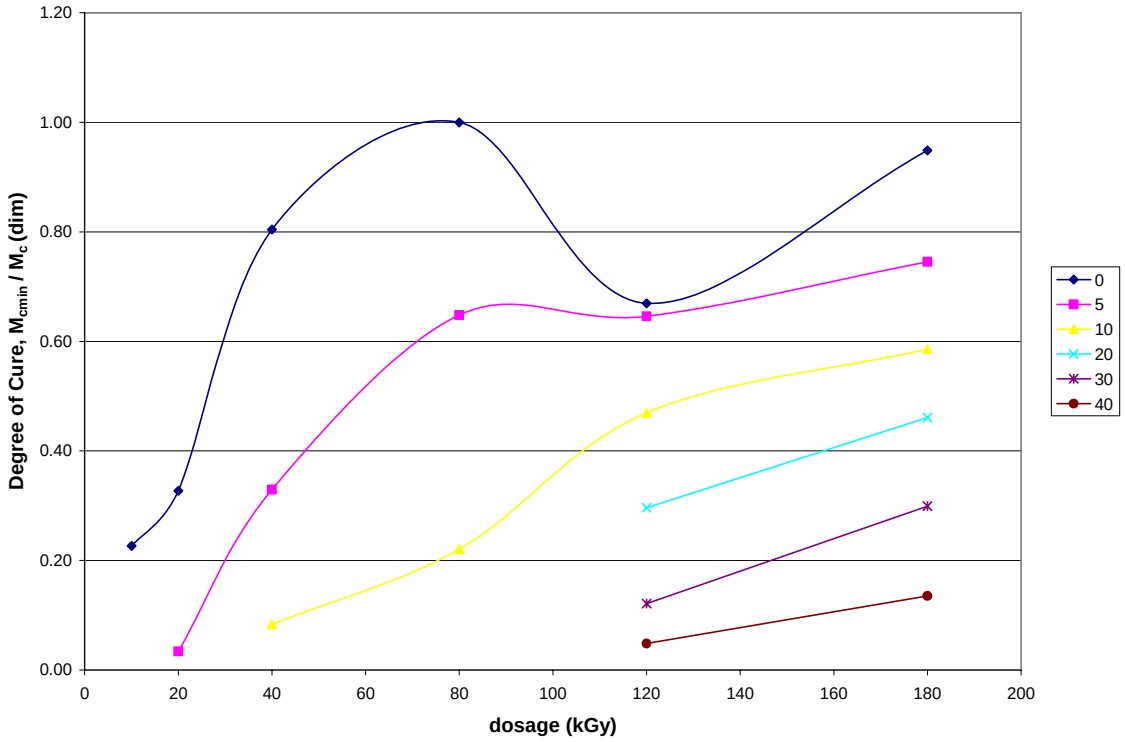

Figure 41: Degree of cure for R67 samples at various concentrations of lignin by cure dosage.

4.4 FT-IR Testing of R46 and R67 Composites

The samples considered are separated by three different parameters: resin, weight percent of lignin present and dosage of e-beam applied for cure. In the following sections, results from PCA and PLS will be used to determine which of these parameters represent significant statistical difference within the spectral data, beginning first with resin and then weight percent lignin and then dosage of e-beam. The reason for ordering the analysis in this way (rather than swapping the last two parameters) comes from the physical testing, most notably the degree of cure with increasing dosage of e-beam. From this property it is evident that the different concentrations of lignin are simply not on the same 'scale' with respect to cure with increasing dosages of e-beam radiation. Having broken the data down, results of PLS regression will be presented to correlate the spectra during cure and show the functional groups which are significant to developing that model for each composite (resin and concentration of lignin specific).

4.4.1 FT-IR Spectra

In gathering spectra for R46 and R67, all dosages (10, 20, 40, 80, 120 and 180 kGy) provided excellent data for statistical analysis. Figure 42 shows the spectra of R46, 20% lignin by dosage of e-beam radiation. This is done by way of example. Of interest to this investigation is the small peak or 'shoulder' at about 810 cm^{-1}, which corresponds to the C=C bond in the acrylate resin. Figure 43 shows this shoulder close up. It is apparent from this image that the absorbance of this peak is diminishing with increasing dosage. This result is consistent with all other R46 spectra. Figure 44 shows the FT-IR spectra of R67, 5% lignin. It is clear here that the far right peak (810 cm^{-1}) is diminishing with increased dosage of e-beam. Figure 45 shows the same spectra with a view of 1160 cm^{-1} close up. This wavenumber corresponds to the stretching of the -CH2-CH2- bond, which is the product of the saturation of two acrylate C=C bonds. It is clear in Figure 45 that a peak is forming at this wavenumber with increasing dosage of e-beam radiation.

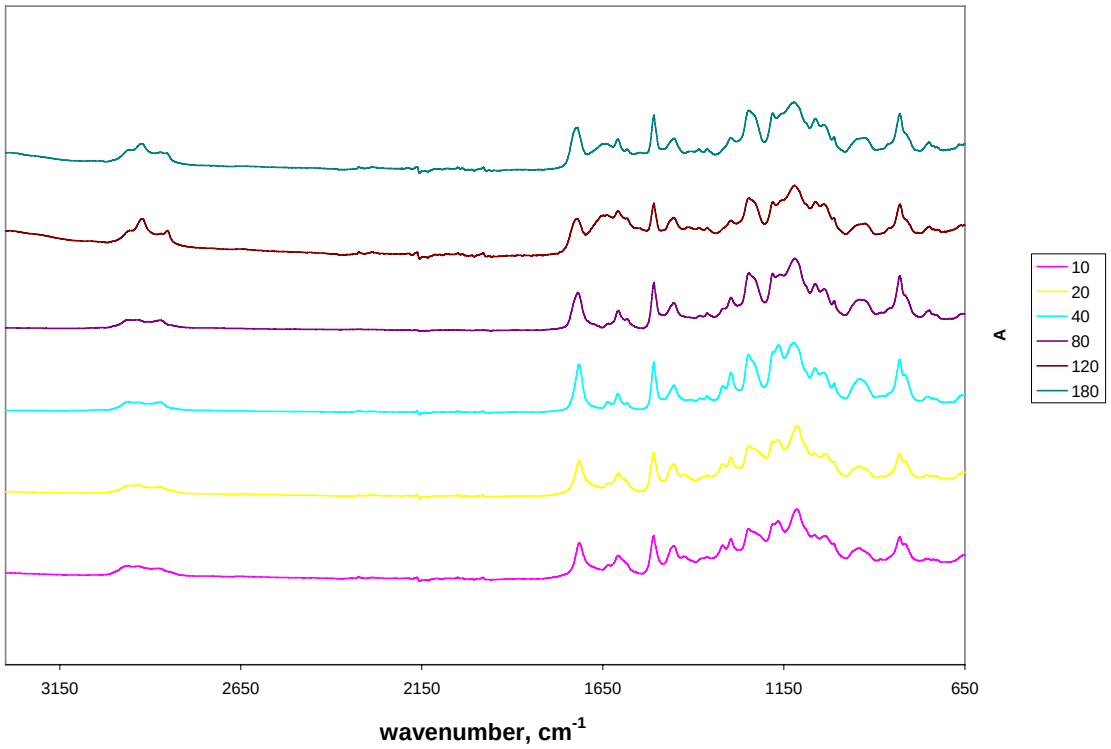

Figure 42: FT-IR spectra of R46, 20% lignin samples for various dosages of e-beam radiation.

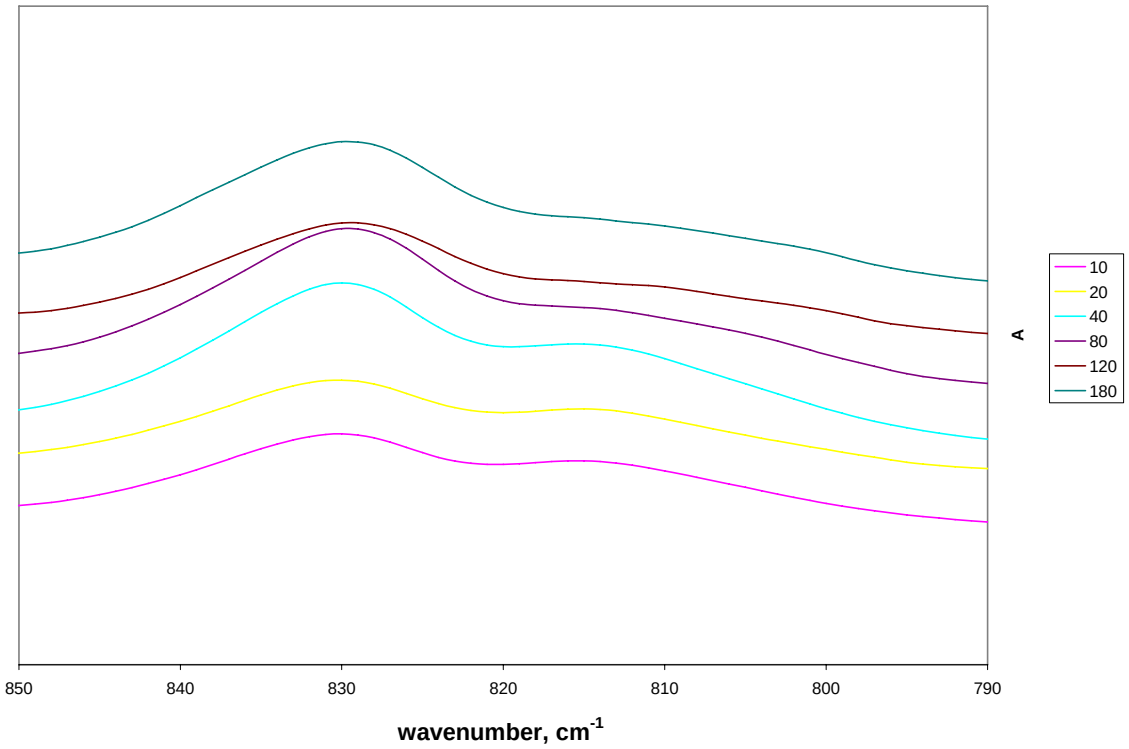

Figure 43: FT-IR spectra of R46, 20% lignin for various dosages of e-beam radiation. Notice the disappearance of the peak at about 810 cm^{-1}.

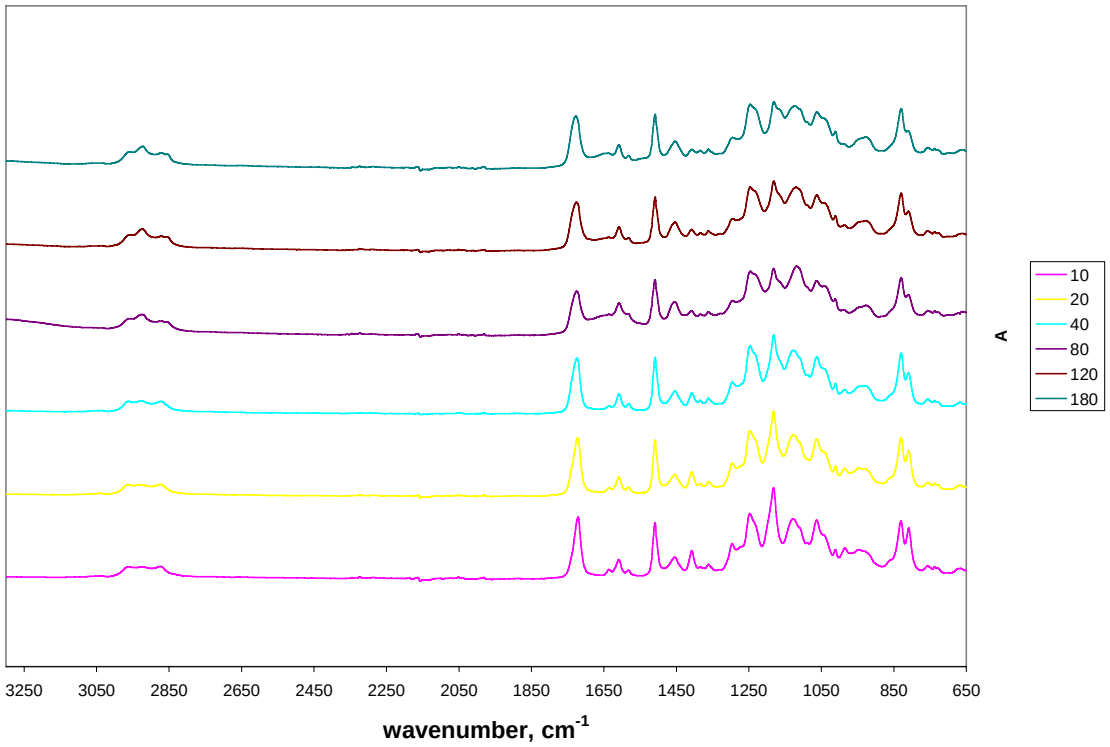

Figure 44: FT-IR spectra of R67, 5% lignin samples by various dosages of e-beam. Note the disappearance of the far right peak (810 cm^{-1}) with increasing dosage.

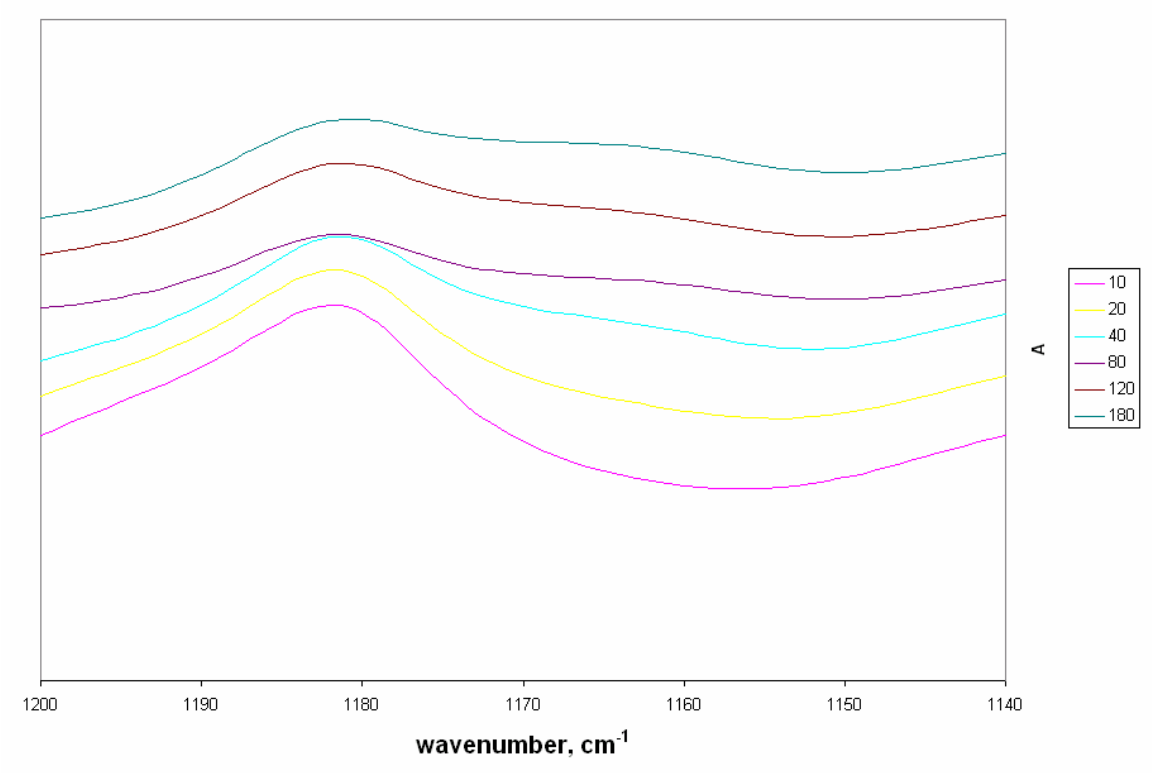

Figure 45: FT-IR spectra of R67, 5% lignin samples at various dosages of e-beam radiation. Notice the formation of a peak or 'shoulder' at 1160 cm^{-1} with increasing dosage.

4.4.2 Principal Component Analysis of All Samples with Replicants Averaged and the Effect of Resin

PCA was first employed on a collection of all sample sets with replicants averaged together. The first results of this analysis are shown below in Figures 46 and 47. Figure 46 is the scores of PC1 (42% of explained variance) versus PC3 (14% of explained variance). A clear distinction between the two resins can be made by PC1. This indicates that there exist statistically significant differences between the spectra of the two resins. For this reason in further statistical analysis the two resins will be treated separately.

Figure 47 shows the loadings for PC1 for this analysis by wavenumber, which is an indication of which wavenumbers are significant in distinguishing the two resins (R46 and R67). The height of the band at about 1160 cm^{-1} indicates that this wavenumber is very significant in classifying the differences present. This wavenumber is assigned to the stretching of the -CH2-CH2- bond, formed during saturation of the C=C bond in the acrylate. It may also be an indication of interactions between the lignin and resin phenolic groups. Additionally, the small band at 810 cm^{-1}, indicates that the presence of C=C acrylate bonds is also significant in classification of the differences between the two resins.

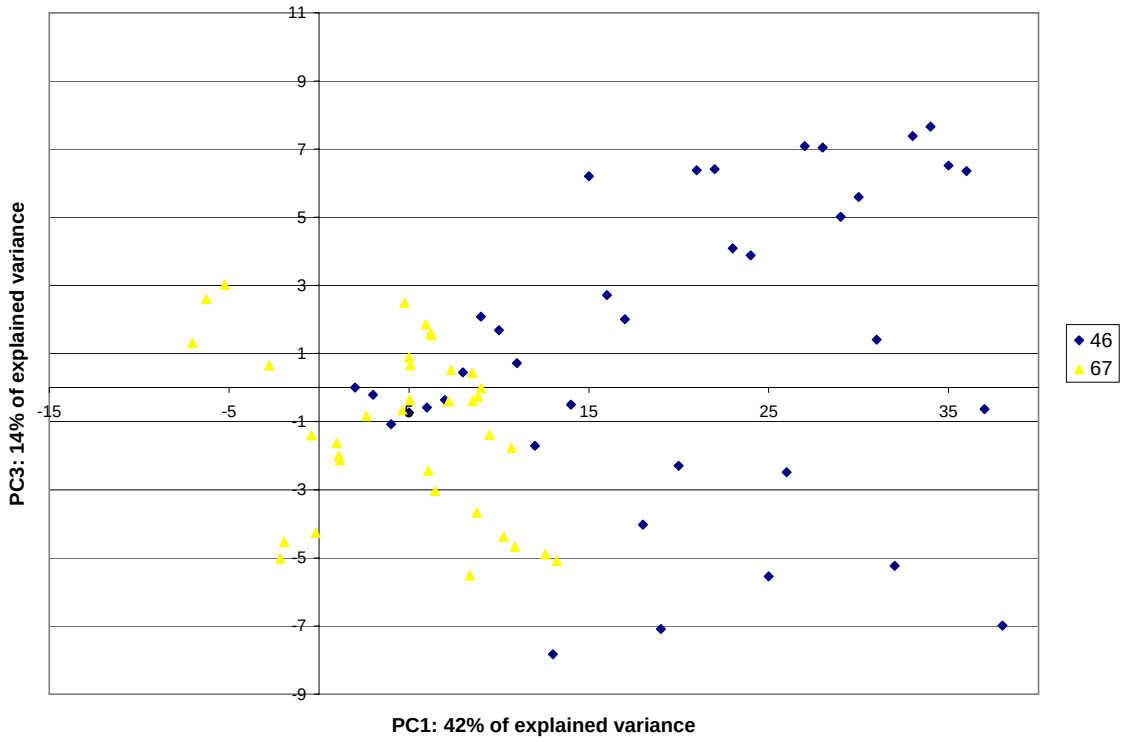

Figure 46: Graph of PCA scores for PC1 and PC3 for all samples by resin. Note the grouping by resin used.

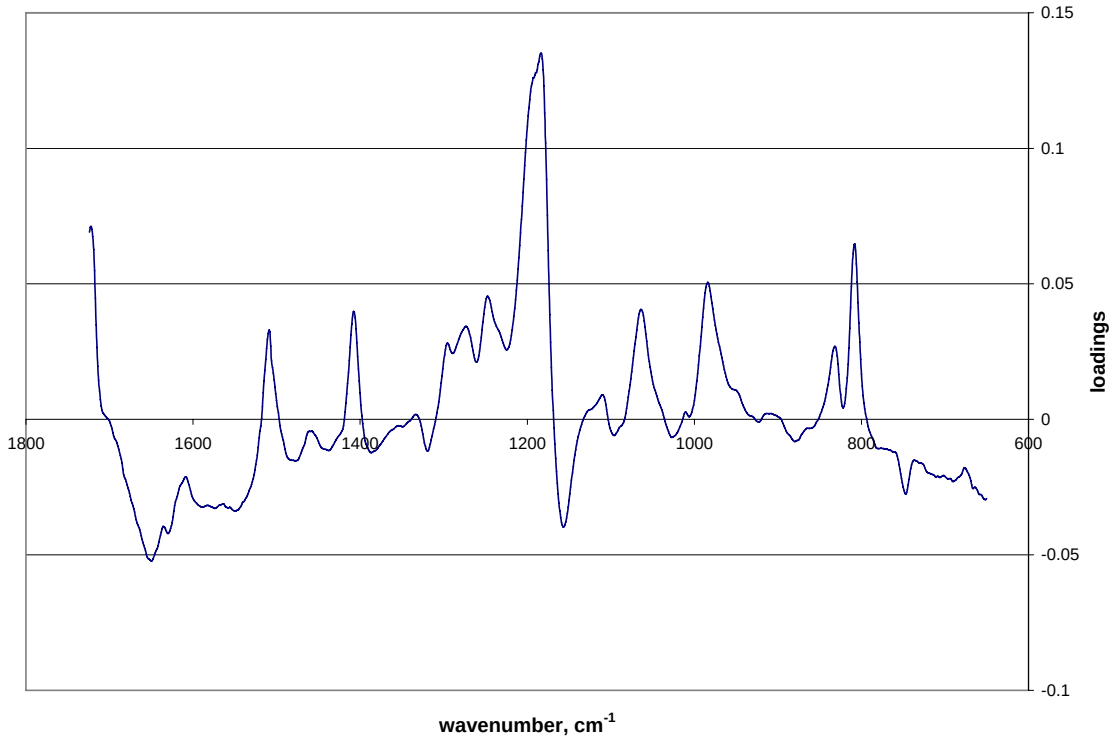

Figure 47: PCA loadings of PC1 by wavenumber for all sample sets. Note the peak at 810 cm^{-1}.

4.4.3 Analysis of R46 Samples with Replicants Averaged and the Affect of Concentration of Lignin

From the previous analysis, it is apparent that the type of resin used is statistically significant in analyzing the available samples. In this section the question of whether the concentration of lignin present is also a statistically significant parameter in analyzing spectral data will be answered. For R46 samples, PCA was again applied, this time to analyze the statistical differences between different concentrations of lignin. Figure 48 shows the scores for PC1 and PC2 for this analysis. Note the gradual change in PC2 between the different concentrations of lignin. Also, notice that nearly all samples with concentrations of lignin less than 20% are negative by PC2. Figure 49 shows the loadings versus wavenumber for PC2. Again notice the inverse peak about 810 cm^{-1}, indicating that the C=C bond in the acrylate is a significant parameter in the analysis.

In order to more fully characterize the changes occurring by concentration of lignin and dosage of e-beam, a PLS analysis was performed for R46 samples. The results of this regression are presented below. The results of the same model for R67 are nearly identical both in fit of the data and regression coefficients significant to developing the model.

The PLS regression response for R46 samples by dosage of e-beam radiation is characterized by Figures 50 and 51. An R value of 0.89 at 6 PC's indicates a reasonable model; however an error of 27 is quite high with the smallest gap between variables being only 10 at 10-20 kGy (Figure 50).

The regression coefficients for the response to dosage of the model show a considerable band at 1720 cm^{-1}, which likely correspond to the stretch of the C=O bond in the ketone. There is also observed a band at 810 cm^{-1}, the C=O bond in the acrylate. This indicates that these wavenumbers are significant in developing the model (Figure 51).

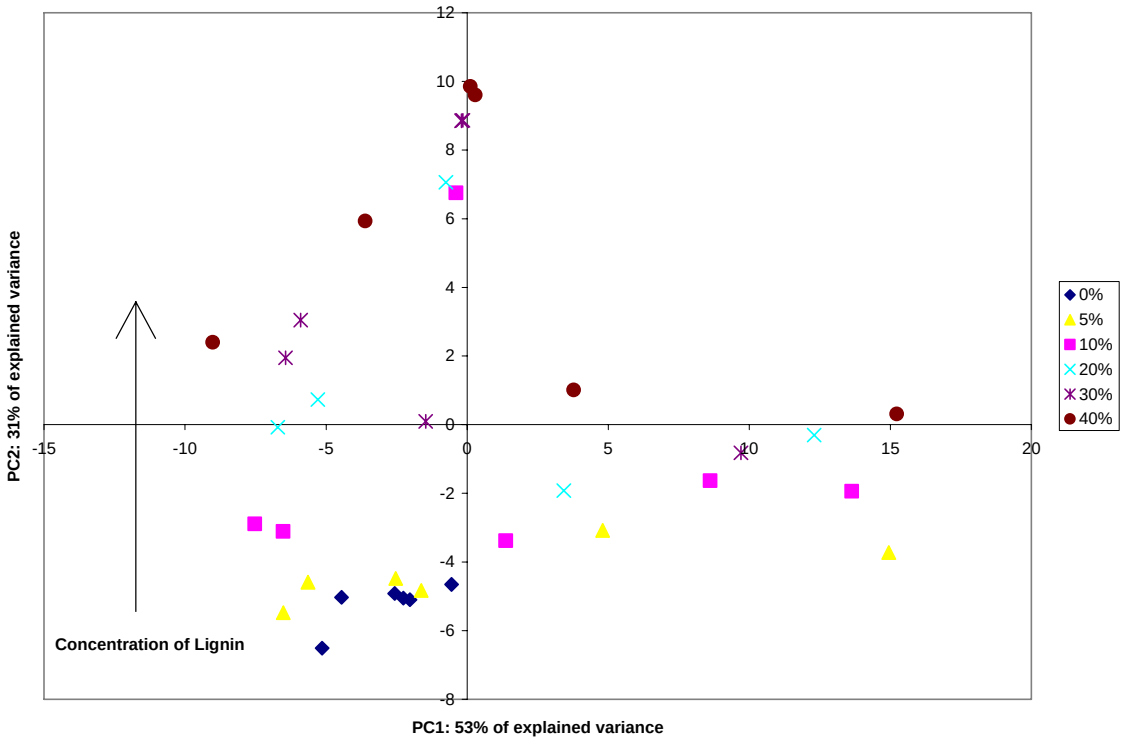

Figure 48: PCA scores for R46 samples. Note the gradual drift in PC1 between the various concentrations of lignin.

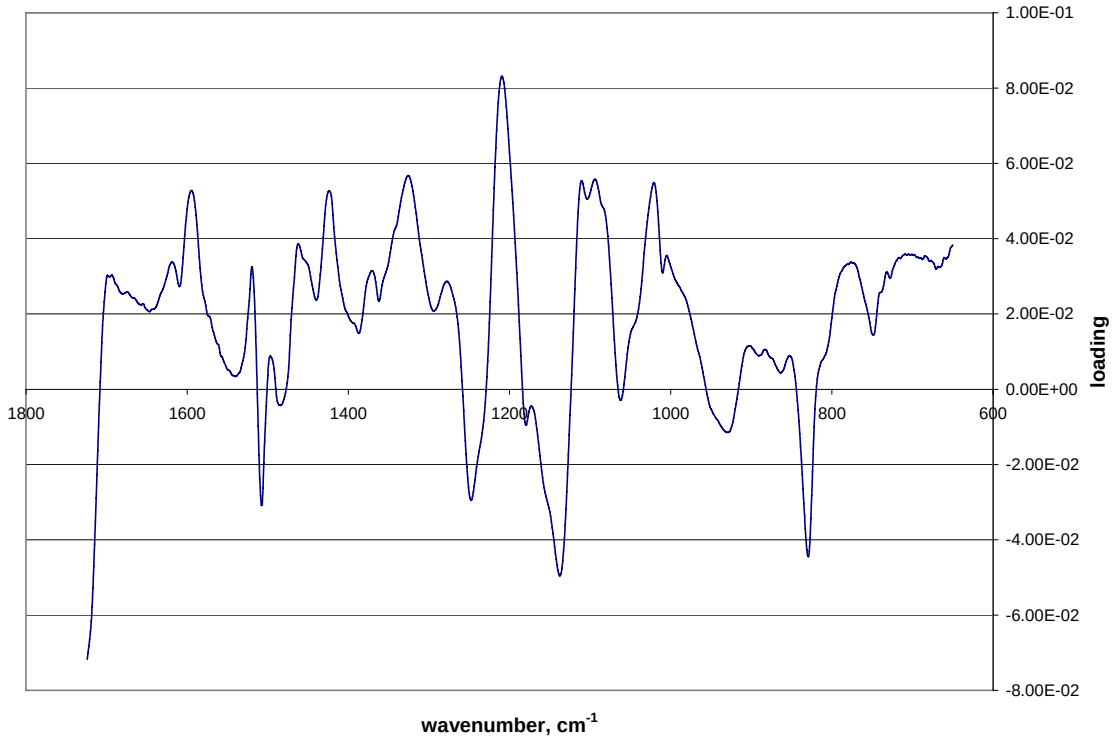

Figure 49: Loadings of PC2 for all R46 spectra.

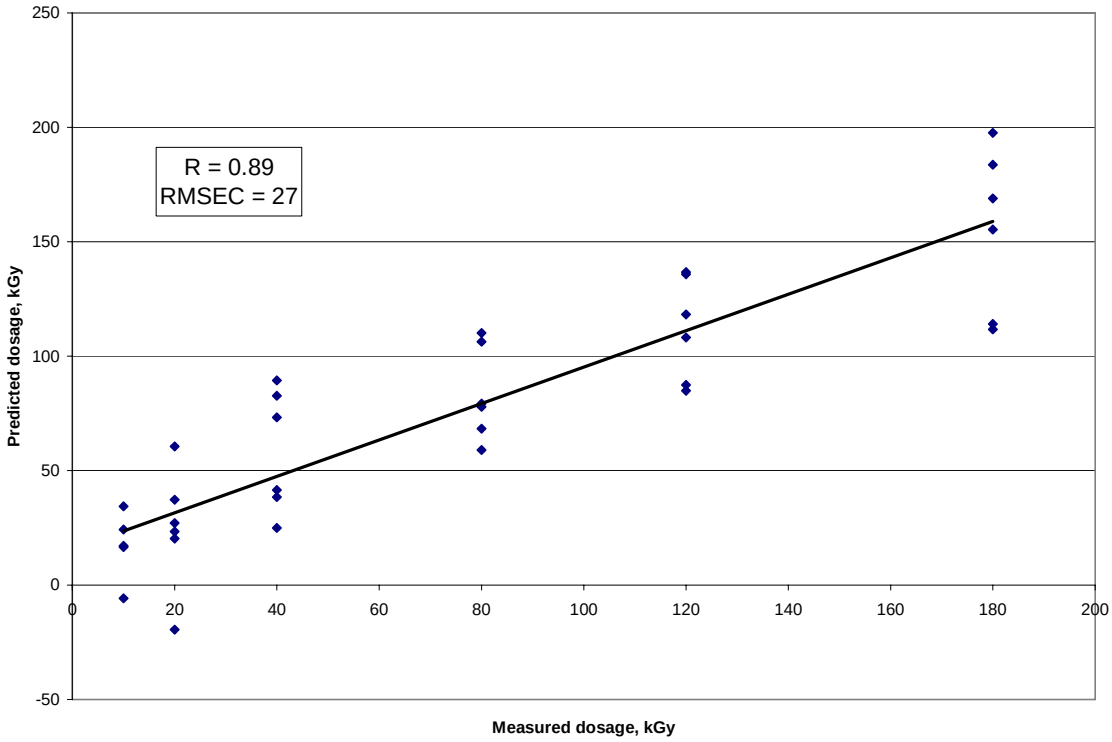

Figure 50: PLS predicted versus measured values by dosage of e-beam radiation for spectra of all R46 composite samples

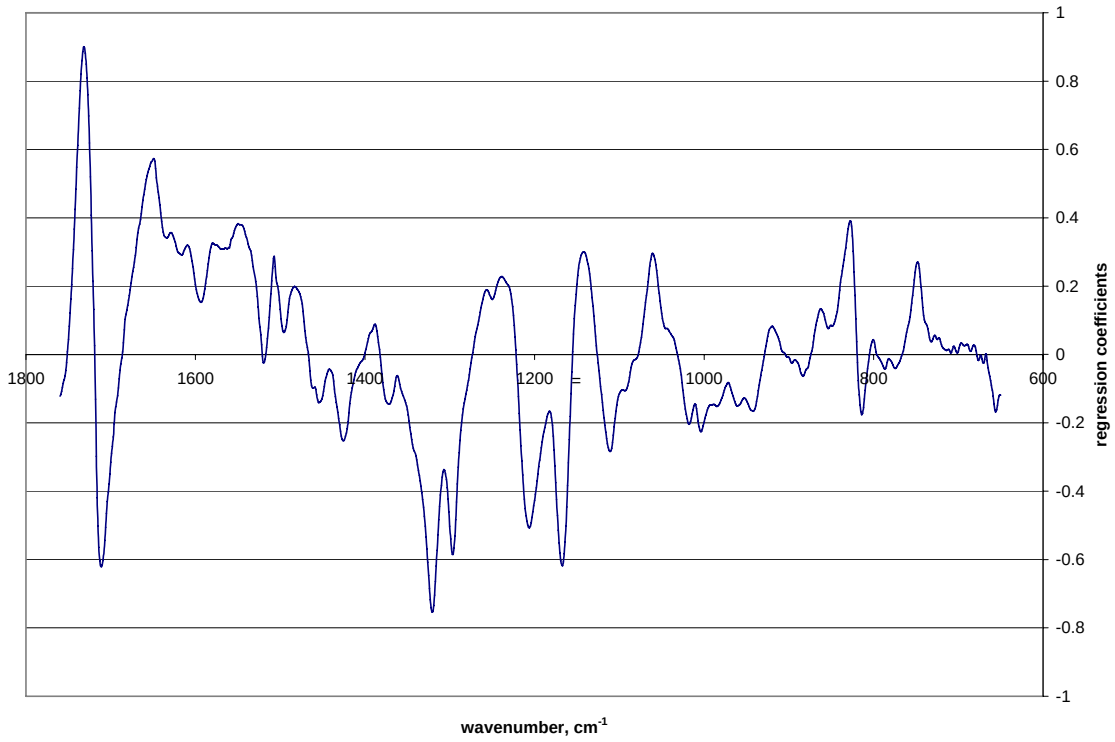

Figure 51: PLS regression coefficients by dosage of e-beam for spectra of all R46 composite samples.

For PLS regression based on concentration of lignin, a better regression coefficient (R) value of 0.94 is shown with a root mean squared (RMSEC) error of 5. This is an acceptable level of error, although the minimum interval for concentration of lignin is also 5 at 5 to 10% (Figure 52)

Regression coefficients for the same regression (Figure 53) show a strong band at 1110 cm^{-1}, which corresponds to stretches in the C-O-C bond in the ether, indicating that this wavenumber is significant in developing the model. It is logical that this functional group would be significant in developing this model, since the variable of interest is increasing concentrations of lignin, and the lignin molecule contains several ether groups. Of importance to the cure process is the band at 810 cm^{-1} corresponding to the C=O bond in the acrylate.

This analysis would indicate that for R46, concentration of lignin might be a more significant parameter than dosage of e-beam radiation in developing a model for statistical differences present within the data set.

4.4.4 Analysis of R67 Samples with Replicants Averaged and the Affect of Concentration of Lignin

PCA was performed for R67 across all concentrations of lignin in order to determine statistical differences. These differences are evident through a graph of their scores in Figure 50. Here PC1 accounts for 53% of total variance while PC2 accounts for 37%. Although clear grouping is not evident, the change across concentrations of lignin is apparent by PC2 (Figure 54). In addition, all the 0-10% samples are positive by PC2, whereas the higher concentrations are negative.

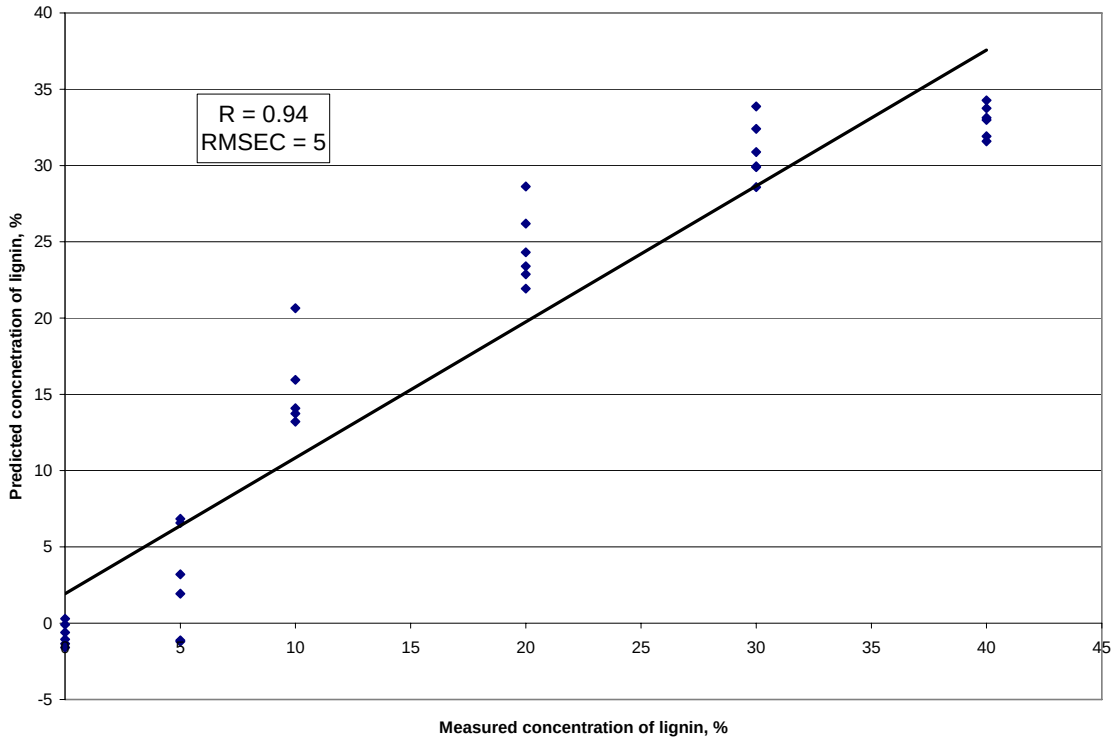

Figure 52: PLS predicted versus measured concentration of lignin for spectra of all R46 samples

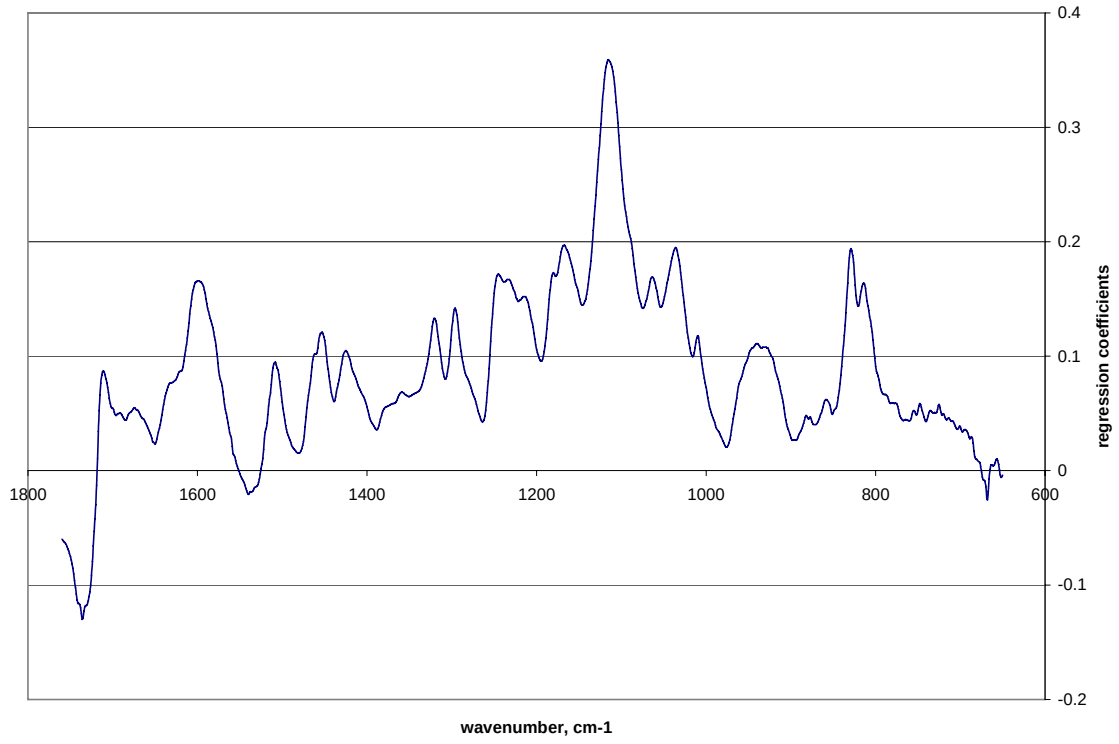

Figure 53: PLS regression coefficients for concentration of lignin for spectra of all R46 samples.

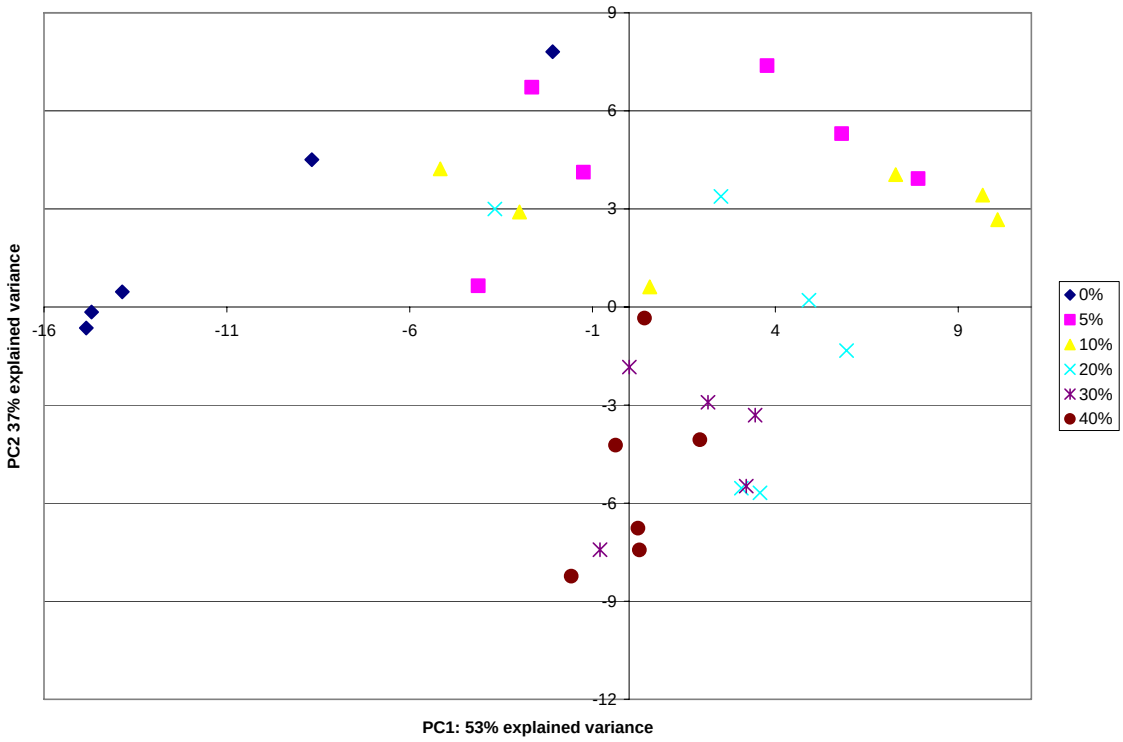

Figure 54: PCA scores of R67 spectra with various concentrations of lignin.

The graph of loadings for PC2 shown in Figure 55 is significant in that the peak at 810 cm^{-1} shows that the saturation of acrylate double bonds is contributing to the model. In this case, changes in the bending of the C=O bond present in the carbonyl group are also evident by the band at 1720 cm^{-1}. This is logical since the carbonyl functionality is a key characteristic of mid-IR spectra of lignin, and with samples in this set having different concentrations of lignin present it should be expected that changes would be evident at this wavenumber. PLS regression was performed for R67 for dosage of e-beam radiation and concentration of lignin. Results were nearly identical to those of R46, with a better model fit to changes in the spectral data based on concentration of lignin being more significant to the two variable regression than dosage of e-beam radiation. In order to represent the change occurring within each composite, samples need to be broken down into individual composites (resin and concentration) and analyzed. This will be done in the next section.

4.4.5 Component Analysis of Individual Composites

PCA was performed individually for each concentration, with individual replicants considered. This was done in order to determine the behavior of each composite during the curing process. Once the results have been used to eliminate outliers, grouping by dosage is generally clear for all composites (Figure 56). For R46, in low concentrations of lignin, dosages above 40 kGy in most cases form overlapping groups separated mostly by PC2. The lower dosages, 10 and 20 kGy are clearly separated by PC1 and PC2. It is likely that this is the range over which actual cure is taking place, where as dosages from 80 to 180 kGy represent something else, likely a decay of the polymer chain. Physical testing, showing a decrease in desirable properties after 80 kGy, largely support this assertion. Figure 56 is the PCA scores for R46, 0% lignin. Here PC1 accounts for 66% of total variance and PC2 accounts for 33%. Note the greater separation between 10 and 20 kGy than the remaining dosages. Figure 57 is the PCA loadings for PC2 for the same analysis. Note the largest band at 1160 cm^{-1} and the much smaller band at 810 cm^{-1}, both indicating that the saturation of the C=C acrylate bonds is significant in the analysis.

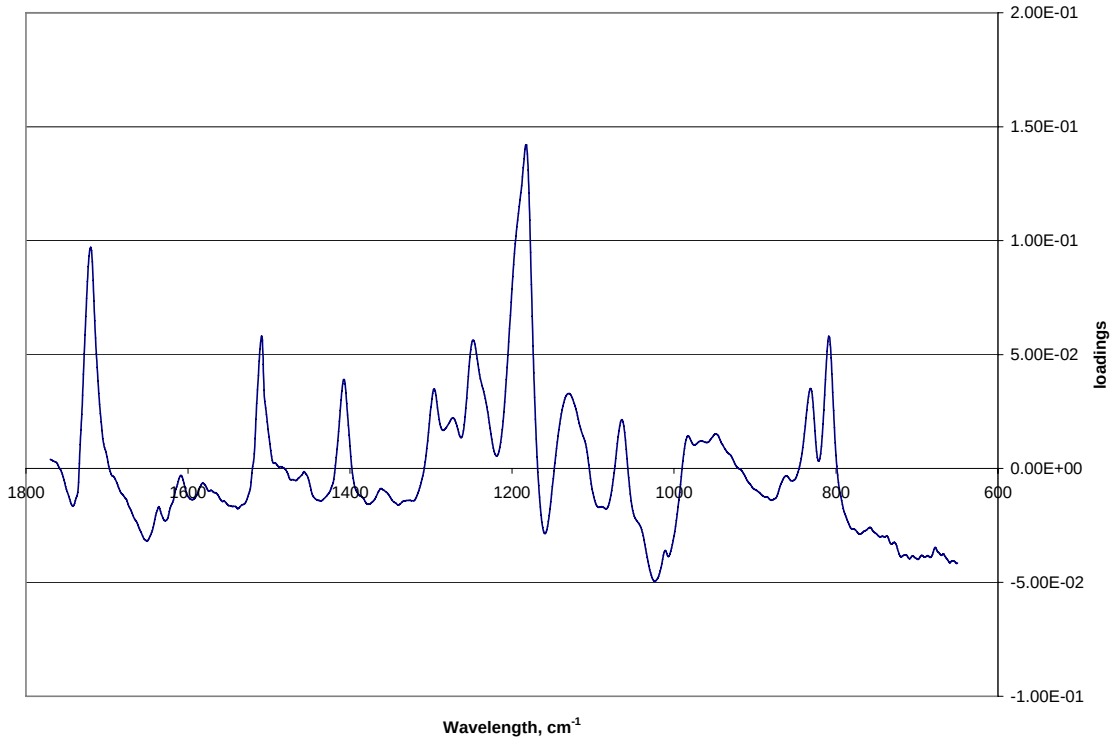

Figure 55: PCA loadings for PC2 from spectra of R67 samples at with various concentrations of lignin and dosage of e-beam.

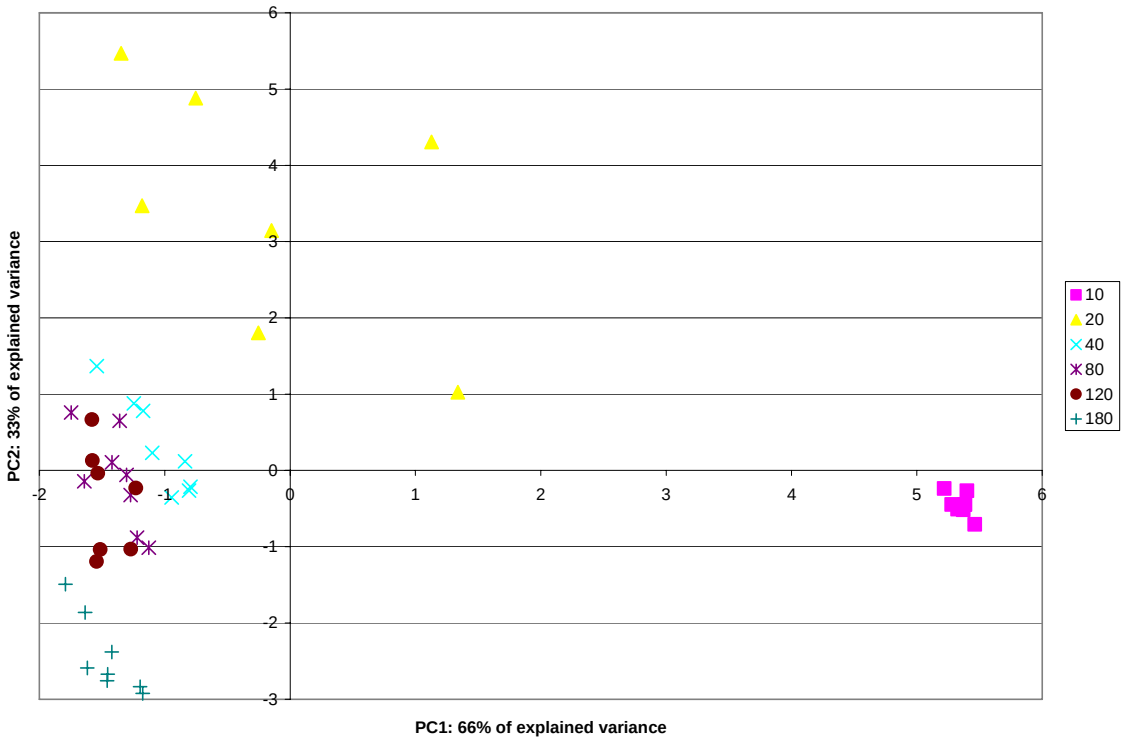

Figure 56: PCA scores for R46, 0% lignin spectra

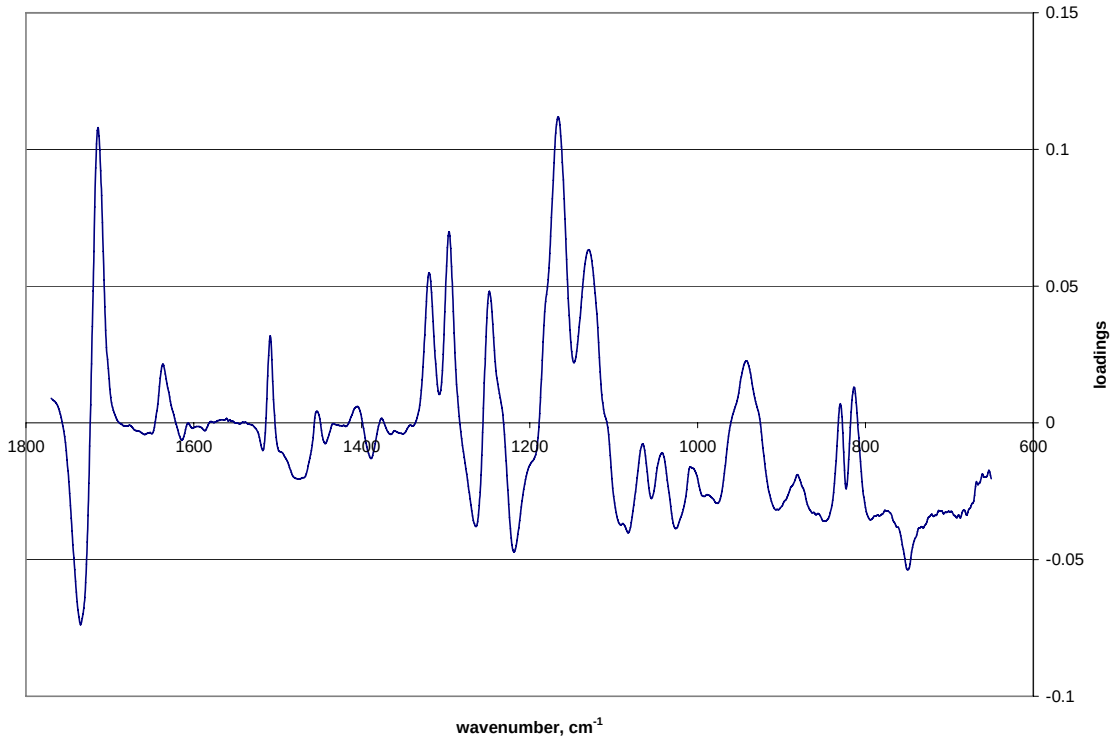

Figure 57: PCA loadings of PC1 for spectra of R46, 0% lignin.

By contrast, for R46 at high concentrations of lignin, the opposite is observed. Cure dosages up to 40kGy show very little variation by PC1, whereas higher dosages show a great deal of difference in their groupings by the same (Figure 58): 10 and 20 kGy are not differentiable; 40 and 80 appear clustered by PC2, and 120 and 180 kGy are largely separated by PC1. Again, it is likely (and confirmed by physical testing of cure-related properties) that the different behavior of this sample set versus that of the lower concentrations of lignin are due to a much-delayed cure mechanism in higher concentrations of lignin. Figure 58 below shows PCA scores for R46 at 40% lignin, given by way of an example. Here, PC1 accounts for 74% of the total variance, while PC2 accounts for 24%. Figure 59 is the PCA loadings for PC2 for the same analysis. The carbonyl functionality is significant for this analysis, as indicated by the band at 1720 cm^{-1}. This is due to the concentration of lignin (40%) and the accompanying carbonyl groups. Note also the largest band at about 1160 cm^{-1}, significant to the -CH2-CH2- bond, a product of the cure process, and also again the small peak at 810 cm^{-1}.

For R60, no such discrepancy between concentrations exists. Changes in the amount of grouping occur with respect to both high and low dosages at a more or less equivalent rate for both PCs. Figure 60 is a PCA for R67 at 10% lignin. PC1 accounts for 84% of the total variance, while PC2 only accounts for 9%. Progression with dosage follows PC1 fairly strongly over the entire range of dosage.

Figure 61 shows the loadings by PC1 for the same analysis. The band at 1160 cm^{-1} is again the strongest, indicating that the curing process is significant in the analysis. The band at 1720 cm^{-1} is also present, again indicating changes in the C=O bond bending. Note also the strong peak at 810 cm^{-1}, indicating that the acrylate C=C bond is important here as well. From the graph of scores for R46 and R67, we see that in R46 at low concentrations of lignin the lower dosages (10 and 20 kGy) are much more statistically dissimilar than R67 at low concentrations. It is likely that this is an indication of a different (likely slower) curing mechanism occurring for R67 than for R46.

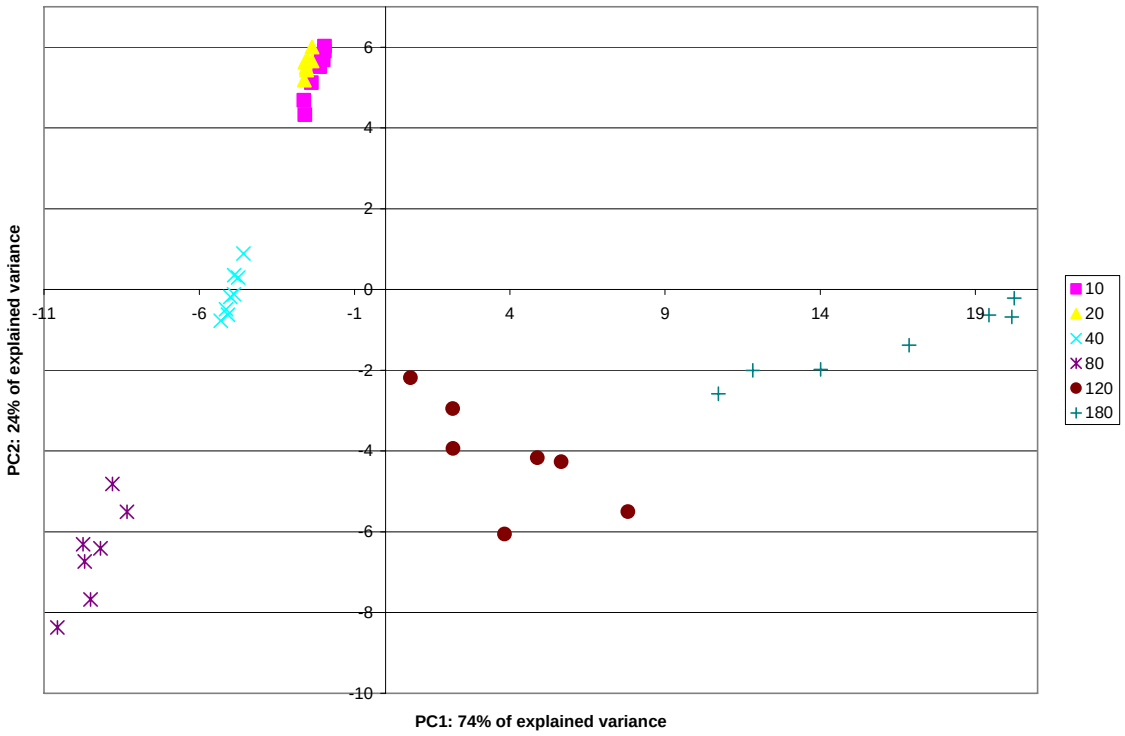

Figure 58: PCA scores for R46, 40% lignin

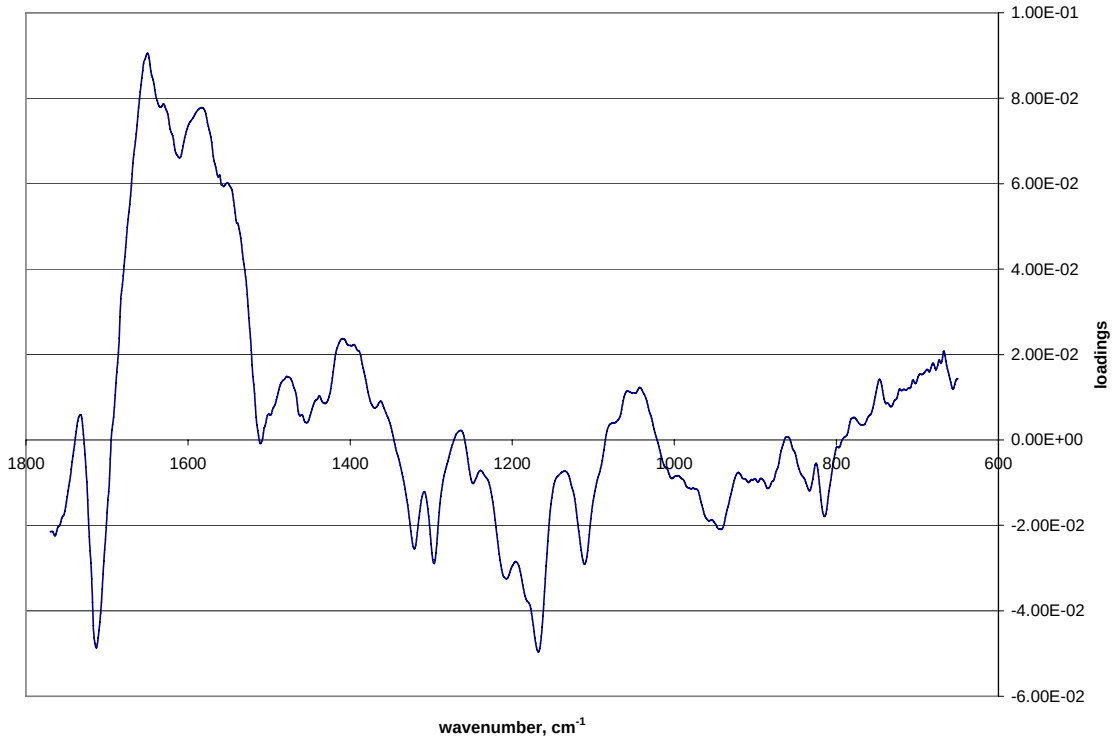

Figure 59: PCA loadings of PC1 for spectra of R46, 40% lignin.

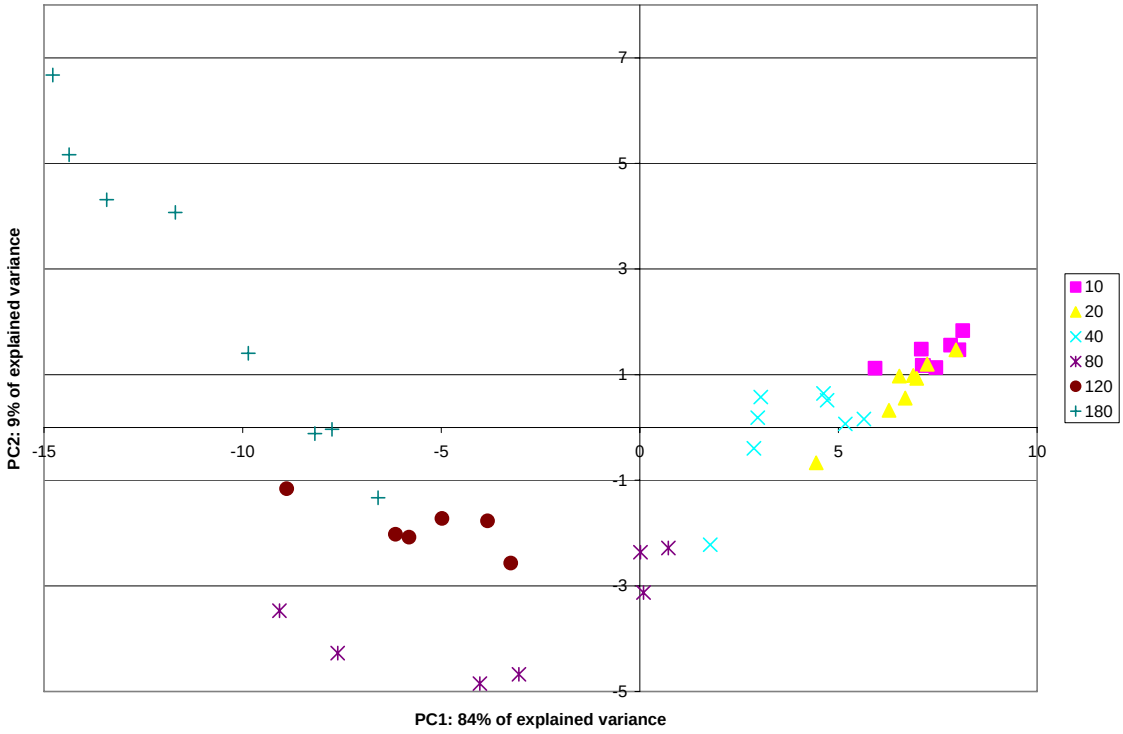

Figure 60: PCA scores for spectra of R67, 10% lignin

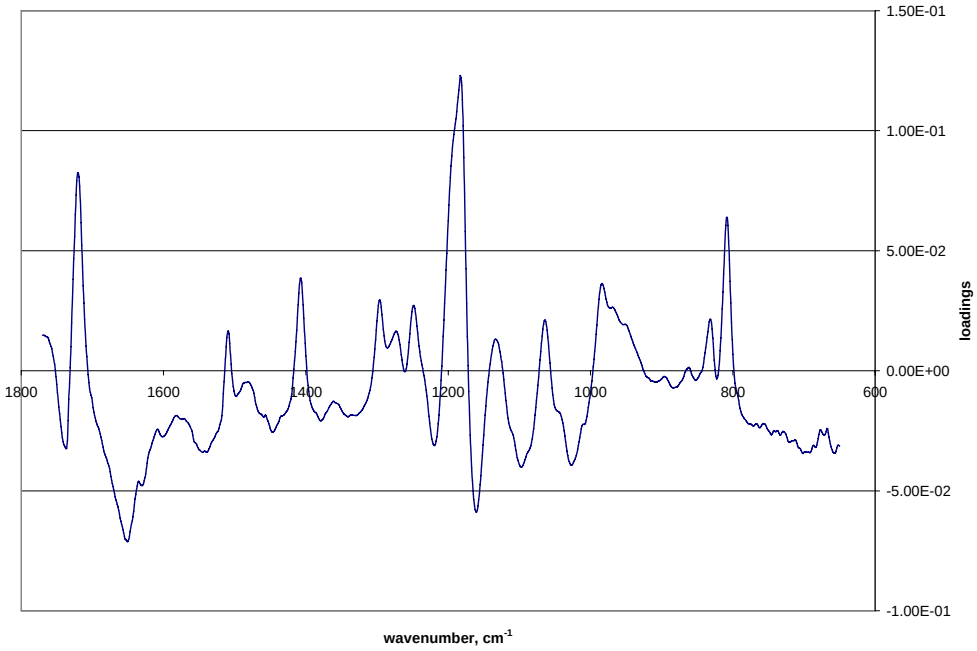

Figure 61: PCA loadings for PC1 for spectra of R67, 10% lignin.

4.4.6 PLS Regression of Individual Composites and the Affect of E-beam Radiation

Using PLS regression, a model was developed for each composite (resin and concentration of lignin specific). The model is developed by 2/3 of the samples in the data set, chosen randomly (calibration). The remaining 1/3 are then used to validate the model (prediction).

From the regression coefficients, each concentration showed a change at the C=O bend within the carbonyl functionality as indicated by a band at 1720 cm^{-1}, -CH2-CH2- bonds as indicated by a band at about 1160 cm^{-1}, and C=C acrylate bonds as indicated by a lesser band at 810 cm^{-1}, again where the regression is done based on dosage. This behavior indicates that these wavenumbers are important parameters in configuring the model. Figure 62 is such a graph of regression coefficients for R46, 30% lignin at 4 PCs. Figure 63 is the calibration and prediction graph of predicted dosage versus measured dosage for this model. The results of both calibration and prediction show acceptable root-mean squared error values (RMSEC and RMSEP) of 7.9 at only 4 PC's. The remaining data relating to the spectral analysis of all composites can be found in Appendix A.

Each concentration of lignin is shown to have a strong correlation between measured and predicted dosage of e-beam radiation. Table 1 below shows correlation coefficient values (R) obtained by PLS for each composite. These indicate a very good model with R values from .99 to .98 showing extremely strong correlation between predicted dosage of e-beam radiation and measured dosage for all composites. With values of e-beam dosage ranging from 10 to 180 kGy, an error (RMSEC for calibration and RMSEP for prediction) below 10 would be reasonable, since this is the smallest difference between dosages (10 kGy and 20 kGy). An error above 20 would be rather high, however note that with regard to the prediction error values, this portion of the model is based on only 16 separate values, which may be a limiting factor in its development.

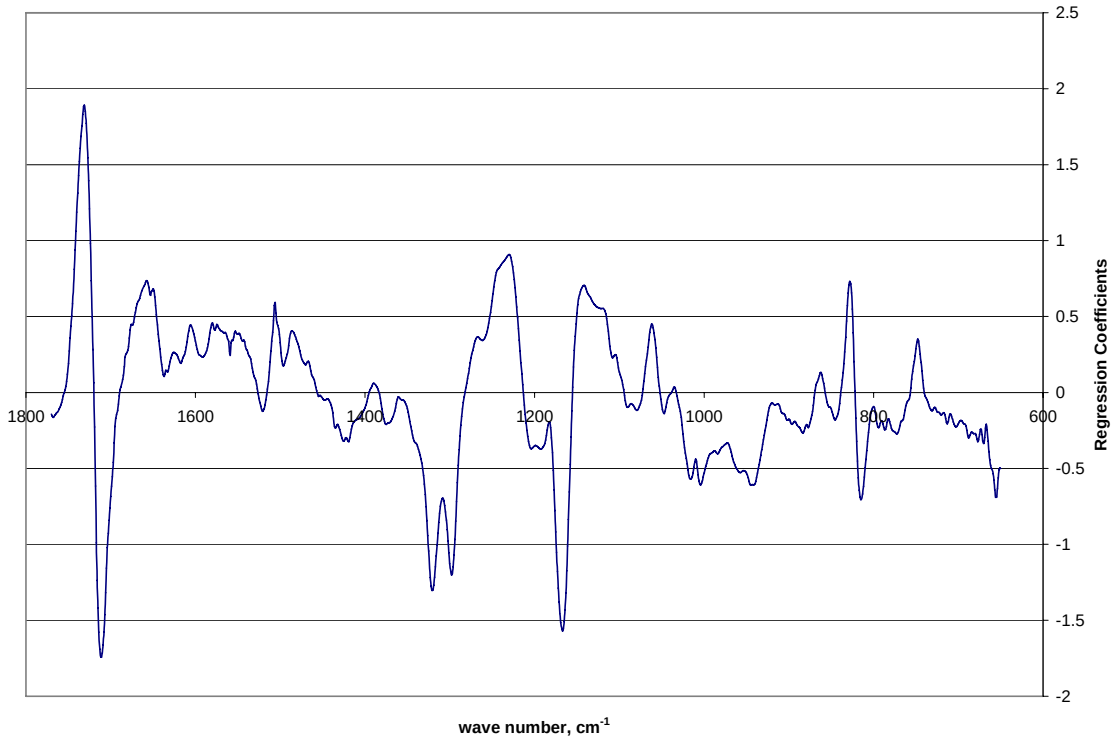

Figure 62: PLS regression coefficients at 4 PC's for R46, 30% lignin for regression by cure dosage. Note the inverse peak at 810 cm^{-1}.

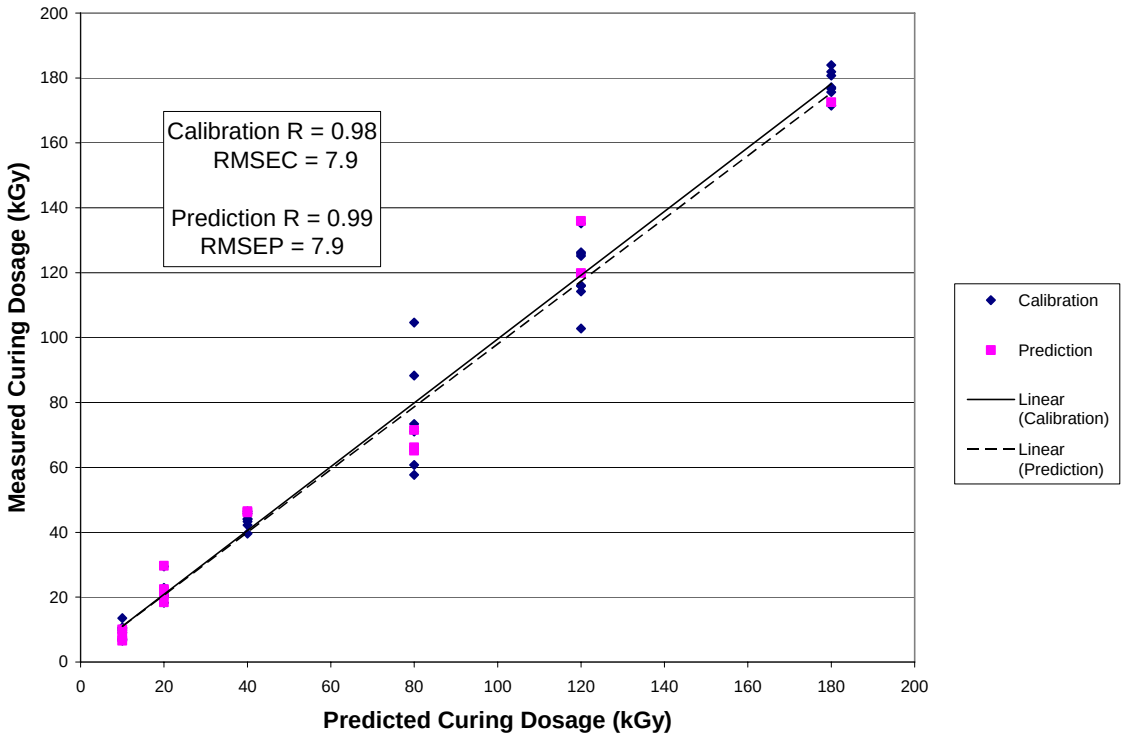

Figure 63: PLS calibration and prediction both at 4 PC's of R46, 30% lignin samples.

Table 1: Correlation of predicted versus measured dosage of e-beam radiation

Composite	# PC's Used	R	RMSEC	RMSEP
R46, 0% Lignin	7	0.99	9.1	12.3
R46, 5% Lignin	9	0.99	7.7	22.8
R46, 10% Lignin	7	0.99	9.9	19.3
R46, 20% Lignin	4	0.99	10.1	16.4
R46, 30% Lignin	4	0.99	7.9	7.9
R46, 40% Lignin	2	0.99	9.2	9.3
R67, 0% Lignin	8	0.98	10.9	35.0
R67, 5% Lignin	6	0.99	9.1	30.0
R67, 10% Lignin	6	0.99	8.6	18.6
R67, 20% Lignin	2	0.99	8.3	11.2
R67, 30% Lignin	3	0.98	11.2	16.7
R67, 40% Lignin	2	0.99	9.5	17.6

Chapter 5: Conclusions

As anticipated, for the composite materials increasing dosages of e-beam radiation have increased the degree of cure. Also, increasing concentrations of lignin have severely hindered the cure. This is most evident in Figures 40 and 41, which show degree of cure for R46 and R67, respectively. The degree to which increasing concentrations of lignin (particularly 30 and 40%) retard the cure is particularly apparent in the T_g, since most of these composites were too gelatinous or liquid to be tested, and the values at higher dosages of e-beam (120, 180) appeared to be in the exponential stage of cure. The primary significance of micrograph and SEM imagery is clearly the anomalous 'skin-core' effect. This effect might be used effectively in future product-development initiatives to provide better control in final production. Further study should focus upon experiments to determine the cause of this effect, and analytical testing to determine the concentrations of lignin associated with each phase.

Physical properties correlate well to chemical changes, as studied by DMA and FT-IR respectively. From FT-IR we have a model for each composite to predict dosage of e-beam with a regression coefficient of .98 or better. In each model the regression coefficients show a moderate peak at 810 cm^{-1}, which is an indication of change in the acrylate C=C bond. From DMA it appears storage modulus (E') increases dramatically with increasing dosage of e-beam radiation, but for increasing concentration of lignin it appears to be out of phase or on a different scale. In fact, the final storage modulus values at high dosage for the higher concentrations are at or about that of the lower concentrations. Again, it is likely that higher concentrations are simply on a different scale of e-beam dosage requirements for cure; a more true comparison might be to cure all composites to a 'fully cured' state and then back-out properties from there, comparing composites at different dosages of e-beam radiation. By extrapolating the data it is

apparent that a ‘fully cured’ 30 or 40% lignin composite will exhibit a significantly higher E’ than those at lower concentrations, giving higher concentrations at a ‘fully cured’ state a much more brittle appearance and behavior.

From DMA data and SEM it appears a two phase system exists for several sample sets. This is likely due to either shear stress at the wall of the syringe during sample preparation or temperature variations during shipping to SteriGenics lab. During sample preparation, samples are heated to 45 degree C. This is unavoidable since the heat is necessary to decrease the viscosity of the resin for mixing. Cooling to 25 degree C is also unavoidable since at that temperature the samples are cured at SteriGenics.

For the pure lignin samples, it appears as if many mechanisms are occurring at once during the cure. This was predicted by literature, and so should be little surprise. It is possible, that the response of lignin might be more accurately examined by breaking the sample set down into an exponential and linear response region, since response to radiation is generally an exponential while the PLS attempts to fit a linear regression, albeit a very sophisticated one. Future study might focus on changes up to say, 20 kGy with multiple intermediary variables in order to determin the response within that first exponential stage.

For the pure cellulose samples very little change is apparent with increasing dosage. That which is contributing to the model occurs at or about the 1000-1260 cm-1 range. This corresponds to the C-O bond in the alcohol as well as the dialkyl-ether stretch.

Bibliography

1) Chuaqui, C. A., Rajagopal, S., Kovacs, A., Stepanik, T., (1993). Radiation-Induced Effects In Lignin Model Compounds: A Pulse and Steady-State Radiolysis Study. *Tetrahedron,* **49**, 9689-9698

2) Mcarthy, J.L., Islam, A., "Lignin Chemistry, Technology and Utilization: A Brief History", ACS Symposium Series, 1999, 98

3) Kosbar, L.L., Japp, R.M., (2001).Introducing Bio-based Materials Into the Electronics Industry. *Journal of Industrial Ecology*, **4**, 93-105

4) Czvikovsky, T., (1996). Electron-Beam Processing of Wood Fiber Reinforced Polypropylene. *Radiat. Phys. Chem,* **47***,* 425-430.

5) Griffith, W. L., Dorsey, G. F., Moschler, W. W., Rials, T. G., Song, T., Winistorfer, P. M., Song, C., "Resin Systems for Wood Composites Rapidly E-Beam Cured At Low Temperatures", Oak Ridge National Lab, 2005

6) Lepifre, S., Froment, M., Cazaux, F., (2004). Lignin Incorporation Combined with Electron-Beam Irradiation Improves the Surface Water Resistance of Starch Films. *Biomacromolecules*, **5**, 1678-1686 1678-1682

7) Ghosh, I., Jain, R.K., Glasser, W.G., (2000). Blends of Biodegradable Thermoplastics with Lignin Ethers. *Lignin: Historical, Biological and Matrials Perspective*. **10**, 331-349

8) Pascu, Mihaela, Vasile, Cornelia, Gheorghiu, Mariana. (2002). Modification of Polymer Blend Properties by Argon Plasma/Electron Beam Treatment: Surface Properties. *Materials Chemistry and Physics*, **80**, 548-554

9) Stepanik, T. M., Rajagopal, S., Ewing, D., Whitehouse, R., (1998). Electron Processing Technology: A Promising Application for the Viscose Industry. *Radiat. Phys. Chem.,* **52**, 505-509

10) Burst, Ellen., "Structure and Properties of Dimethacrylate-Styrene Resins and Networks", Virginia Polytechnic Institute, 2000, 2.5-2

11) Griffith, W.L., Dorsey, G.F., Harper, D.P., Moschler, W.W., Rials, T.G., Song, Ting, Winistorfer, P.M., Chang, Song, "Electron-Beam Cured Resin Systems for Wood Composites", Oak Ridge National Lab, 2005

12) Hon, D. N., Chang, S.-T. (1984). Surface Degradation of Wood by Ultraviolet Light. *Journal of Polymer Science: Polymer Chemistry Edition,* **22**, 2227-2241.

Appendices

Appendix A: Results of FT-IR Testing of R46 and R67

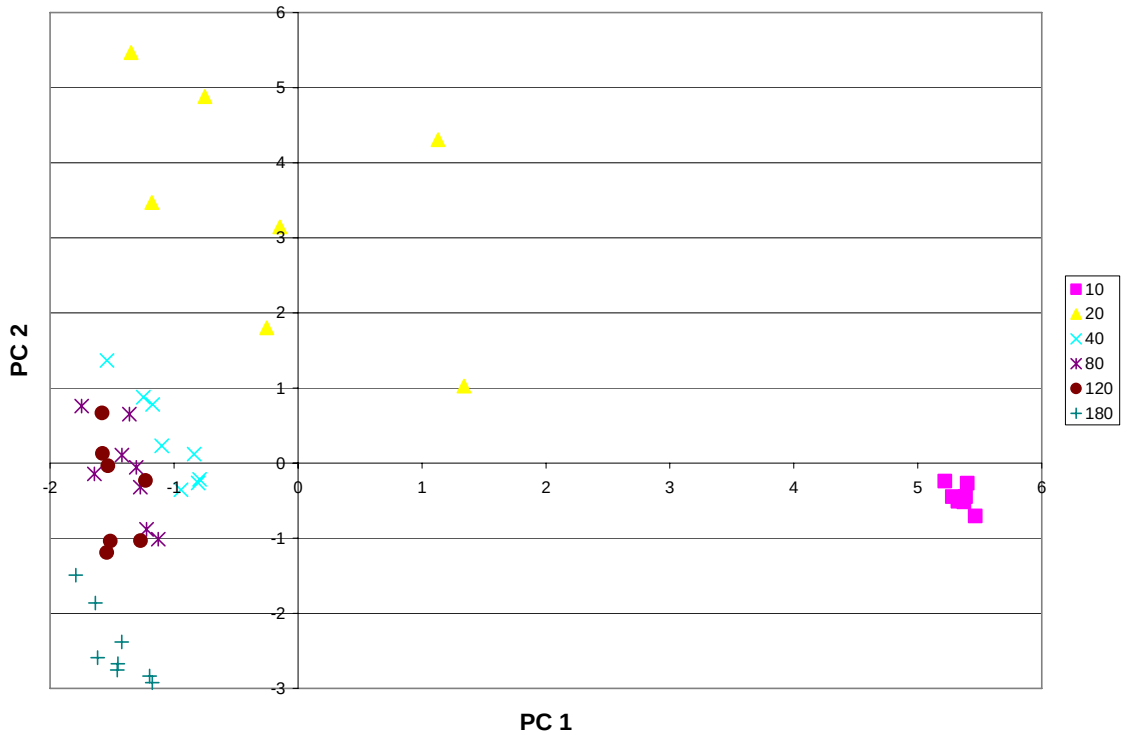

Figure A1: PCA scores for R46, 0% lignin spectra

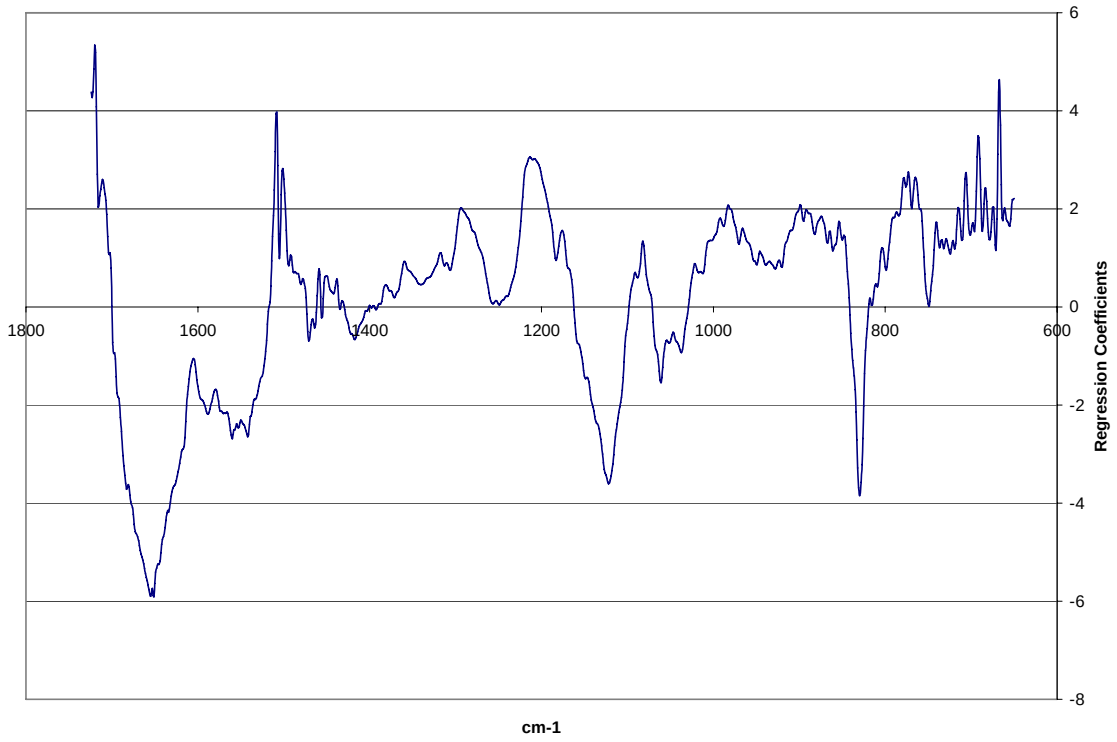

Figure A2: PLS regression coefficients for R46, 0% lignin

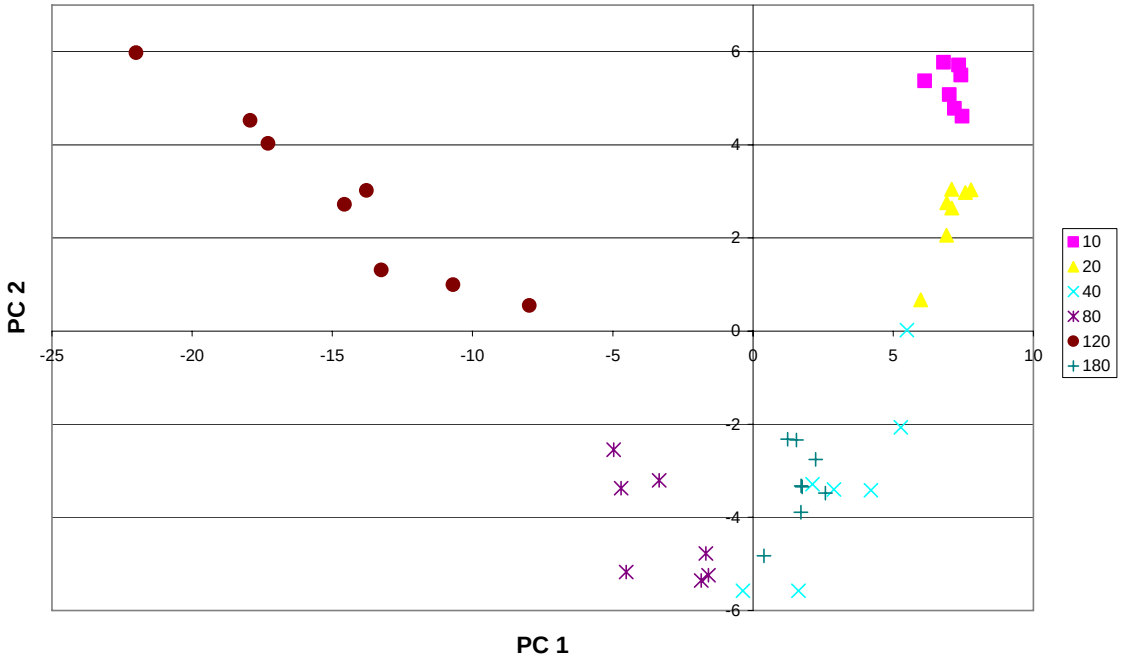

Figure A3: PCA scores for R46, 5% lignin spectra

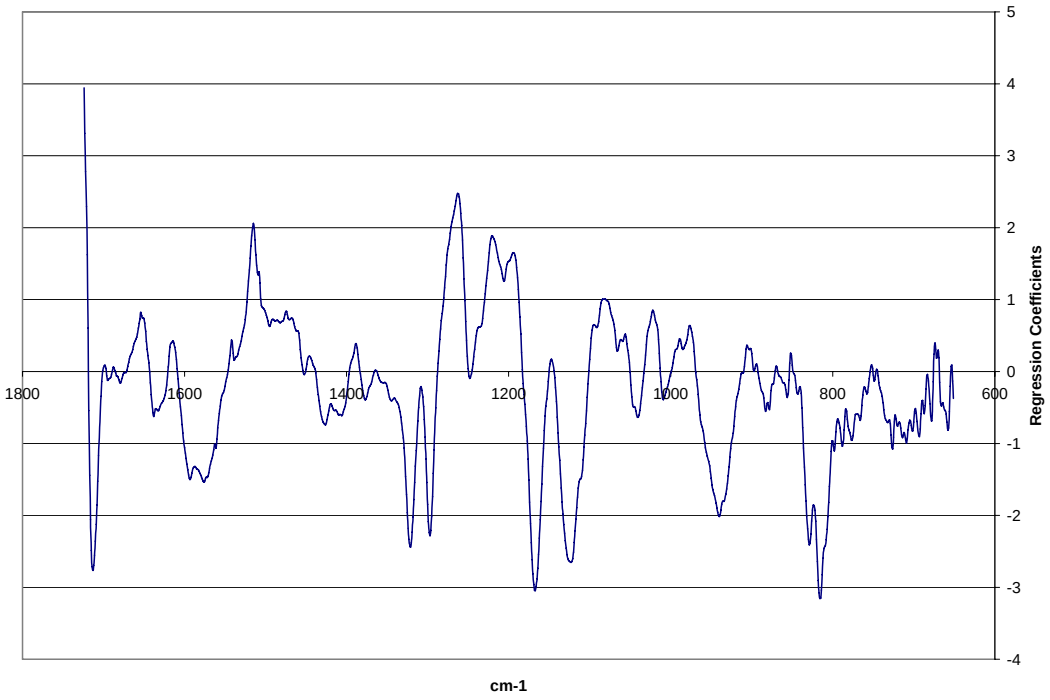

Figure A4: PLS regression coefficients for R46 5% lignin spectra

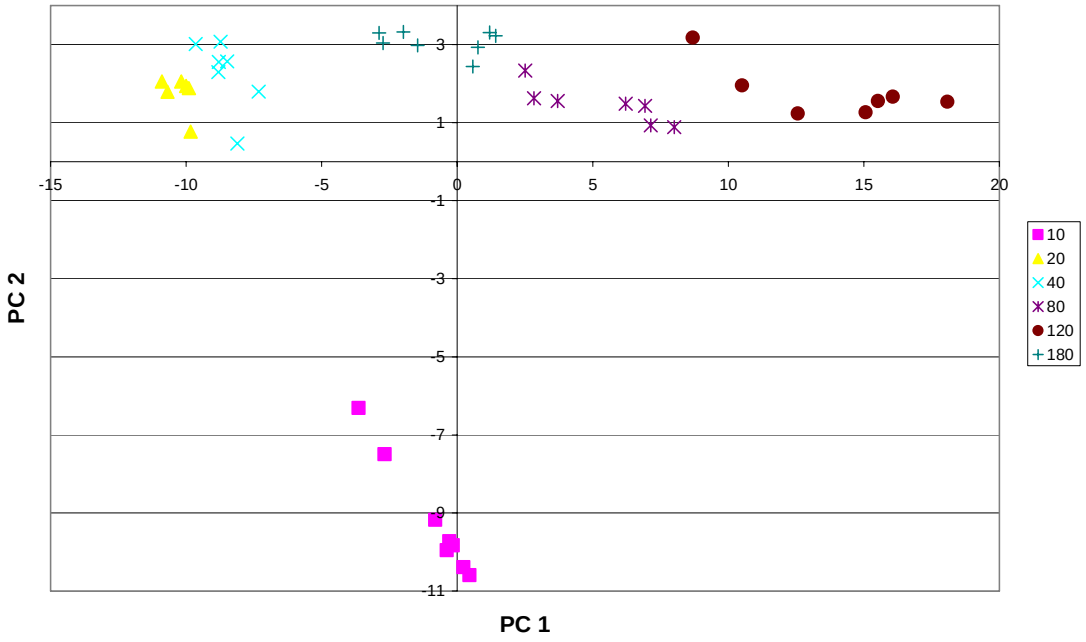

Figure A5: PCA scores for R46, 10% lignin spectra

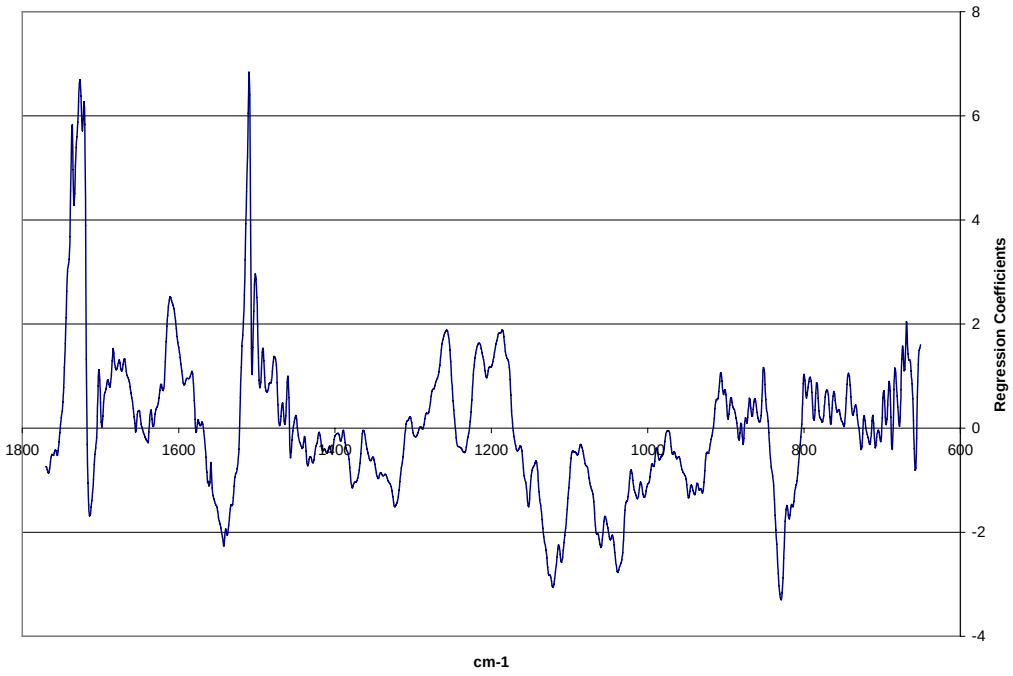

Figure A6: PLS regression coefficients for R46, 10% lignin spectra

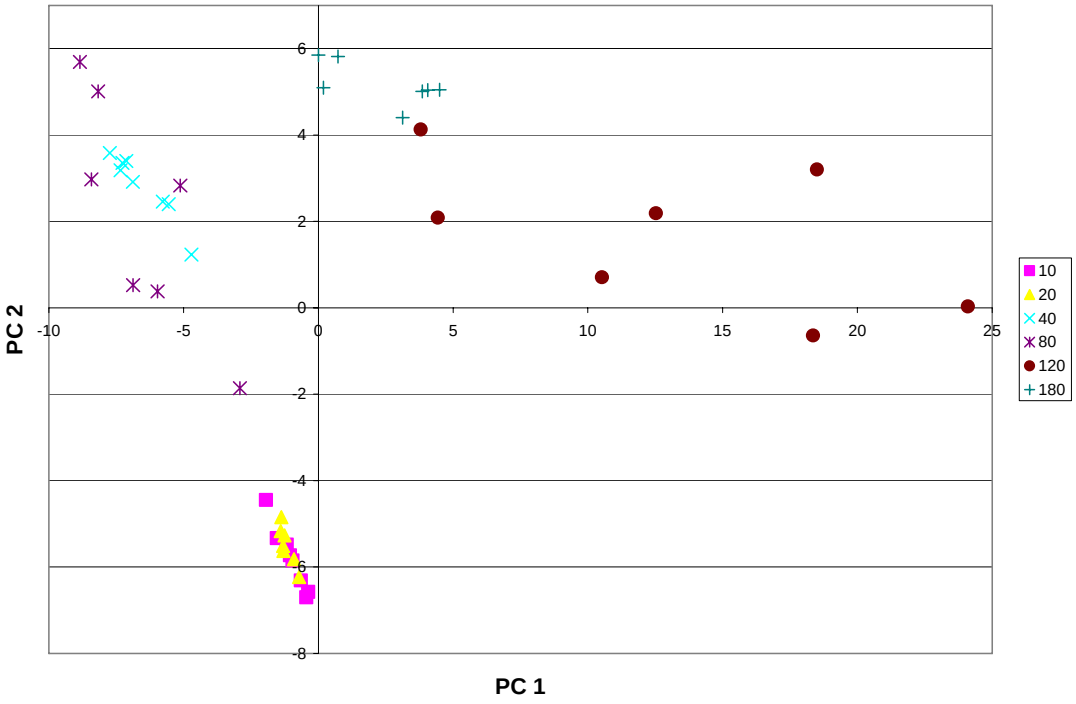

Figure A7: PCA scores for R46, 20% lignin spectra

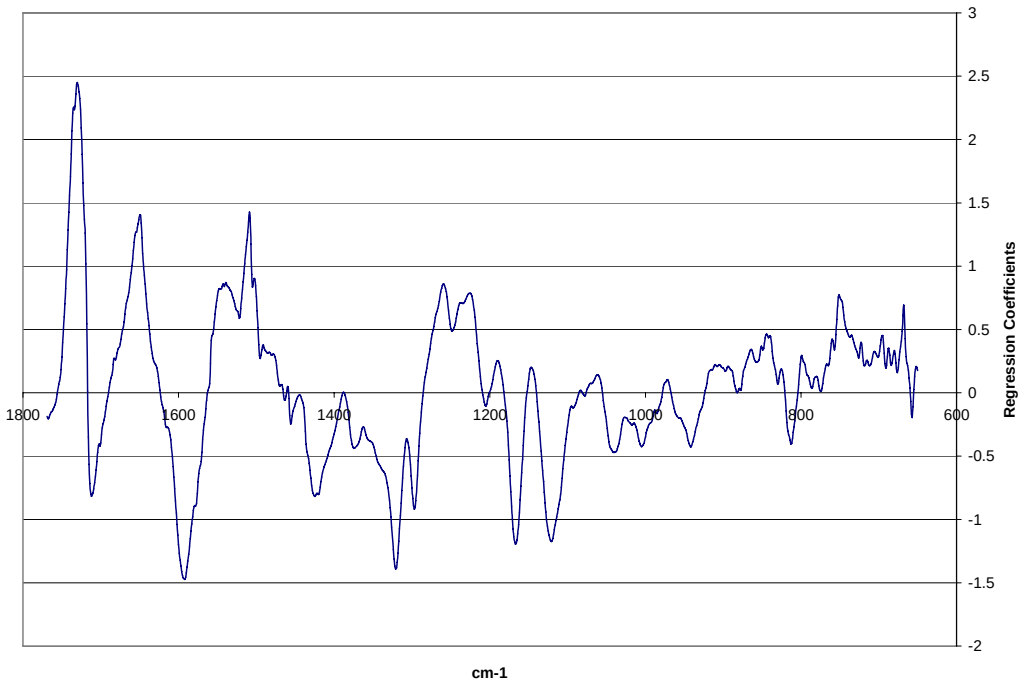

Figure A8: PLS regression coefficients for R46, 20% lignin spectra

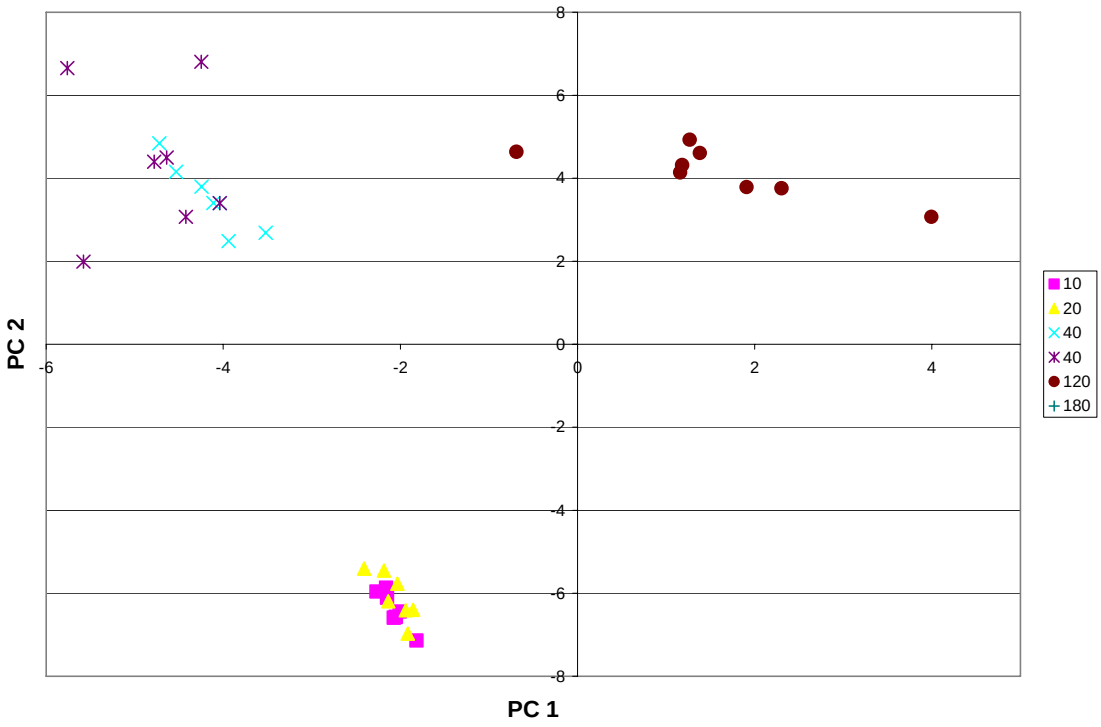

Figure A9: PCA scores for R46, 30% lignin spectra

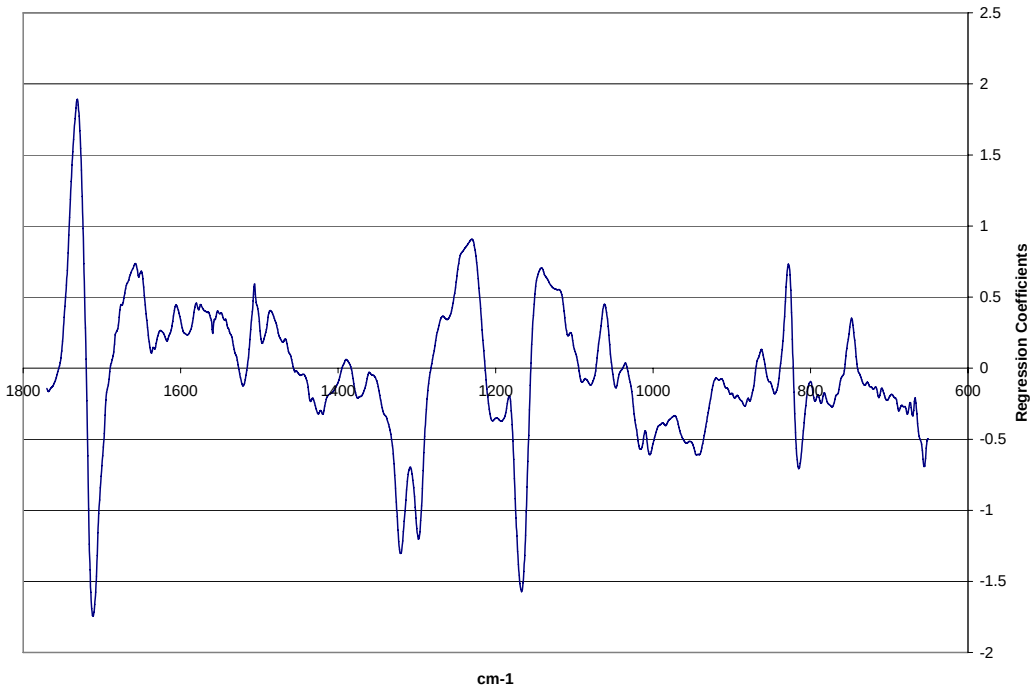

Figure A10: PLS regression coefficients for R46, 30% lignin spectra

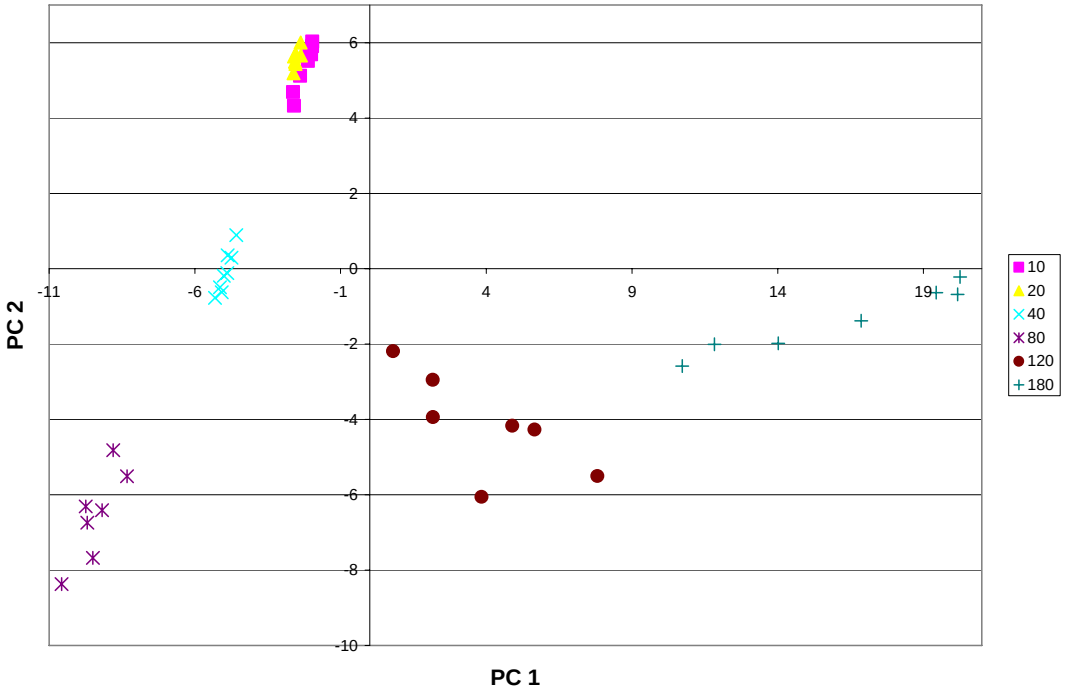

Figure A11: PCA scores for R46, 40% lignin spectra

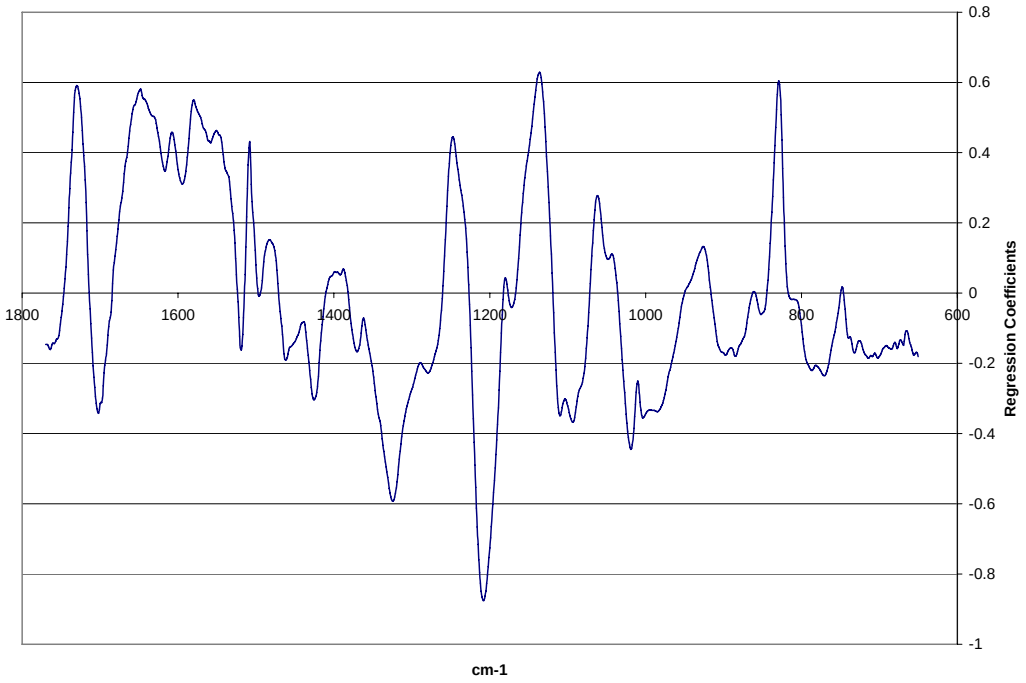

Figure A12: PLS regression coefficients for R46, 40% lignin spectra

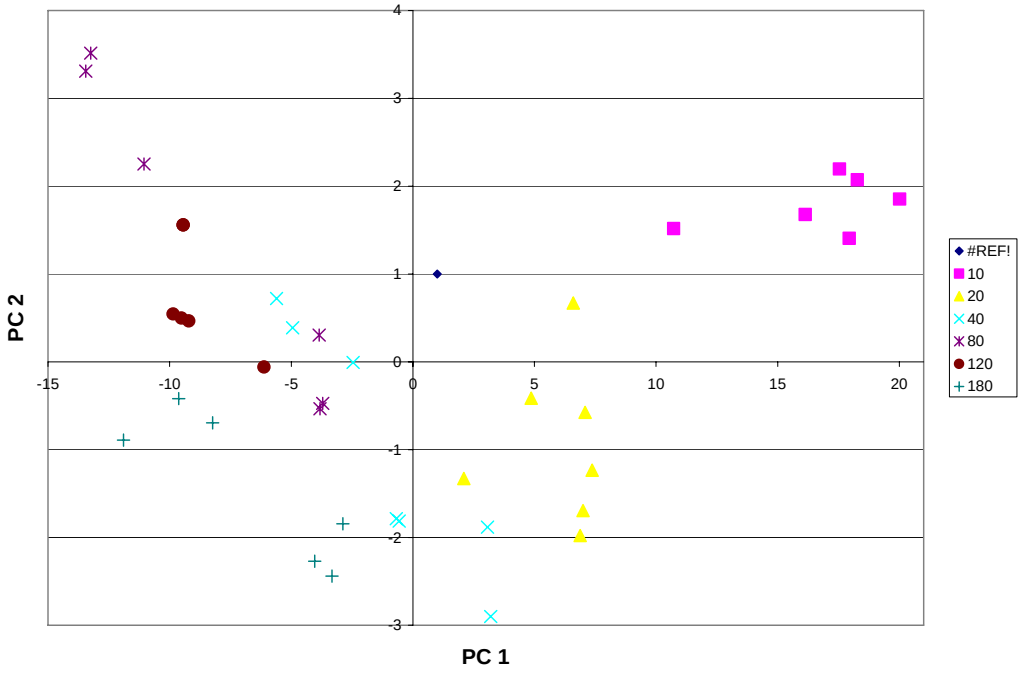

Figure A13: PCA scores for R67, 0% lignin spectra

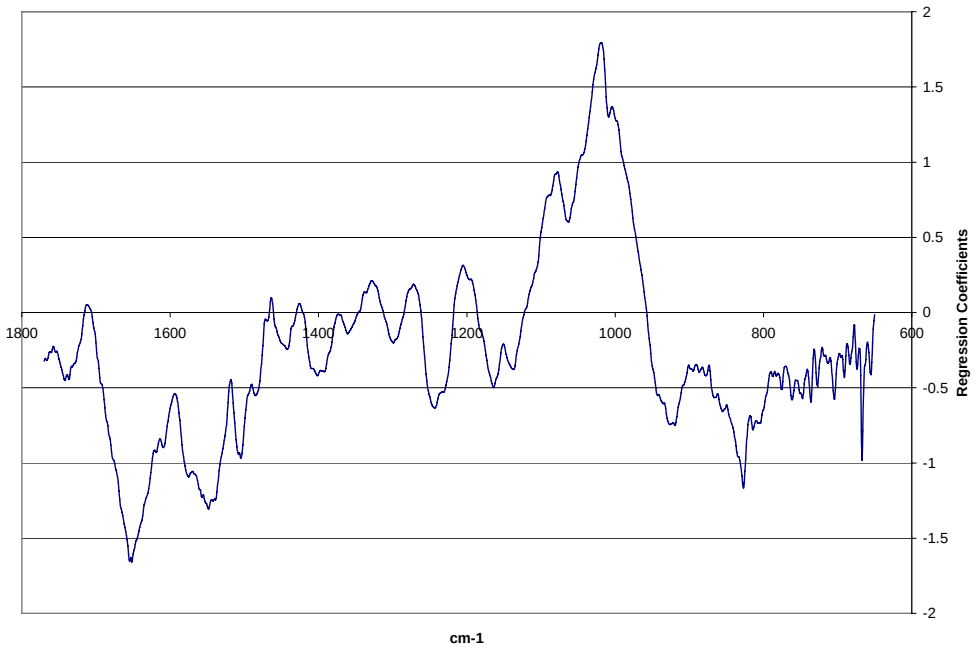

Figure A14: PLS regression coefficients for R67, 0% lignin spectra

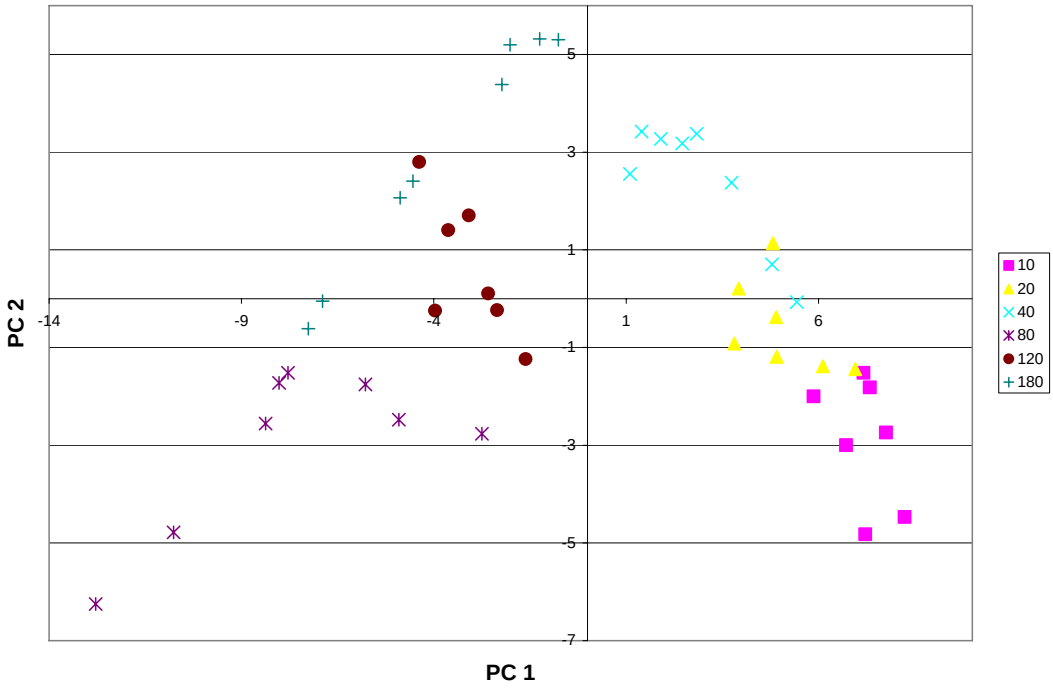

Figure A15: PCA scores for R67, 5% lignin spectra

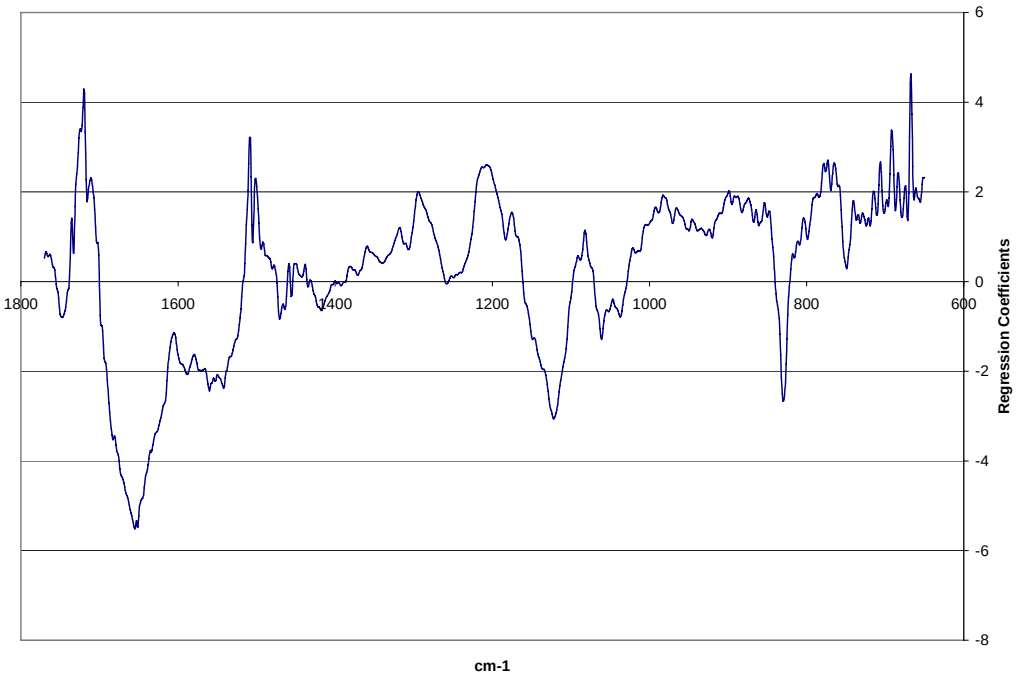

Figure A16: PLS regression coefficients for R67, 5% lignin spectra

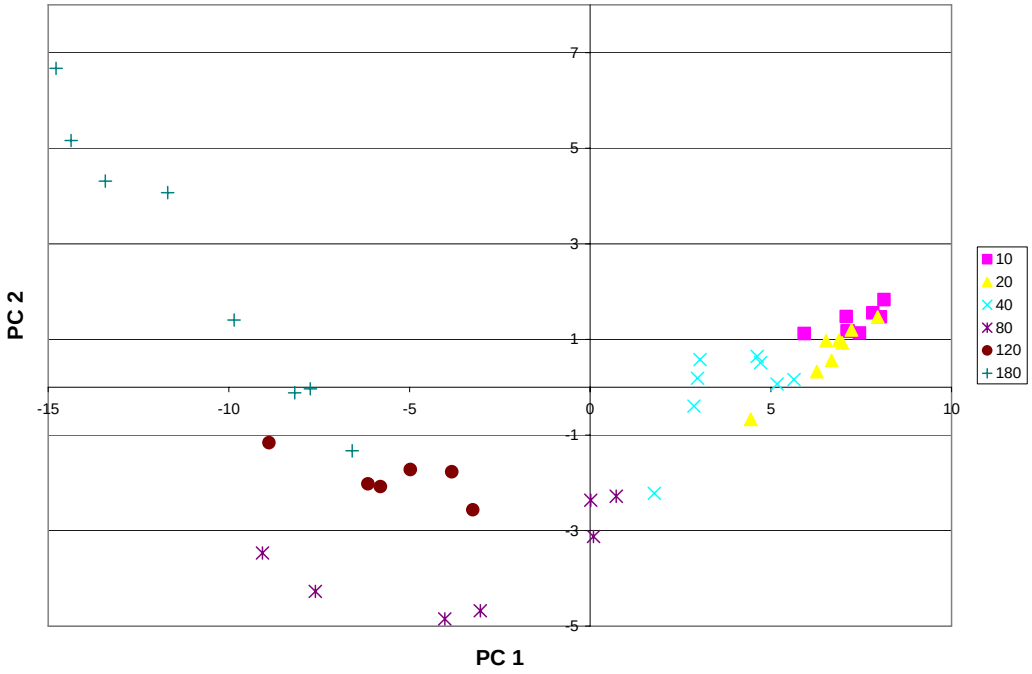

Figure A17: PCA scores for R67, 10% lignin spectra

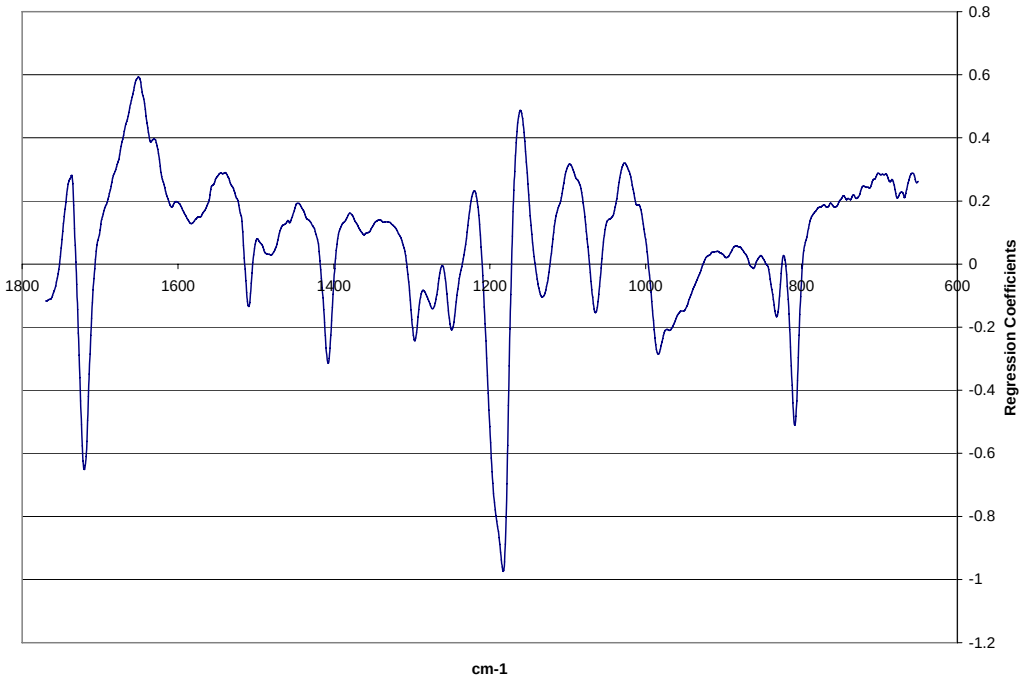

Figure A18: PLS regression coefficients for R67, 10% lignin spectra

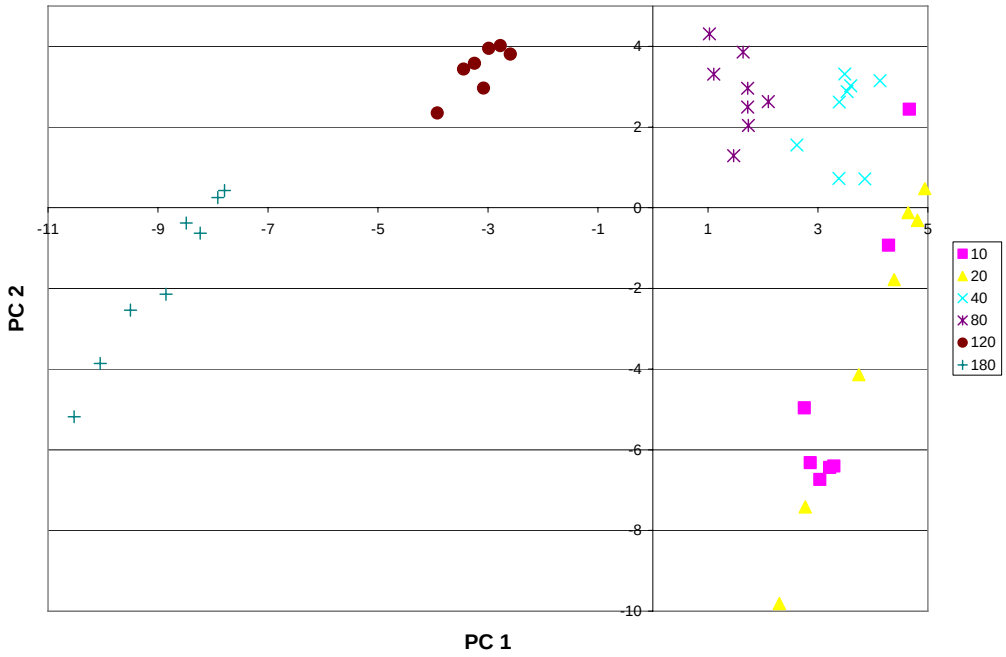

Figure A19: PCA scores for R67, 20% lignin spectra

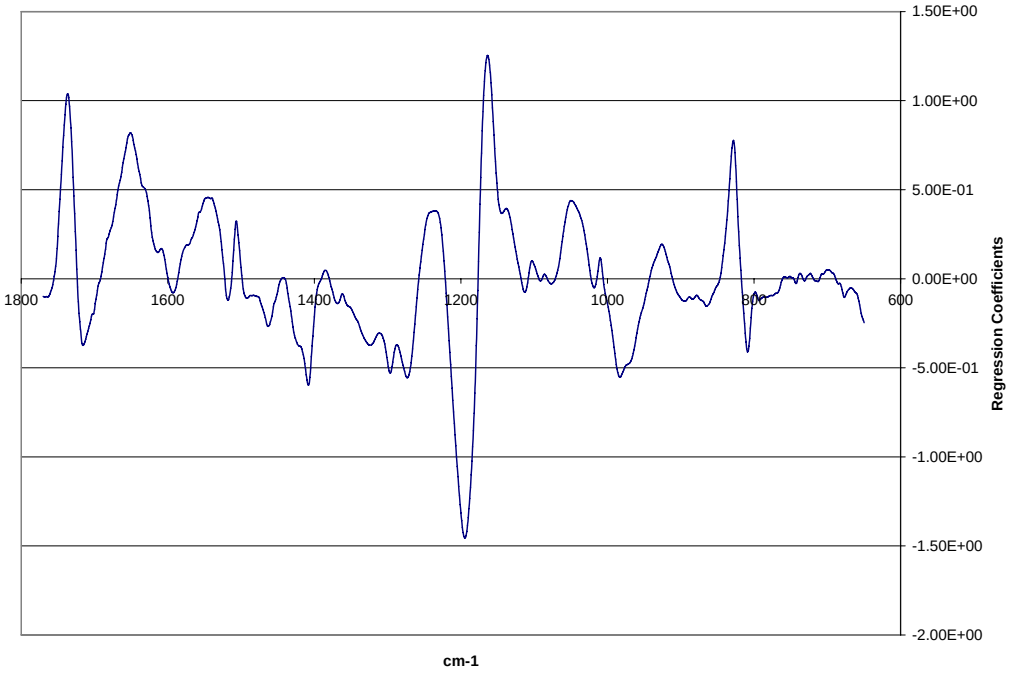

Figure A20: PLS regression coefficients for R67, 20% lignin spectra

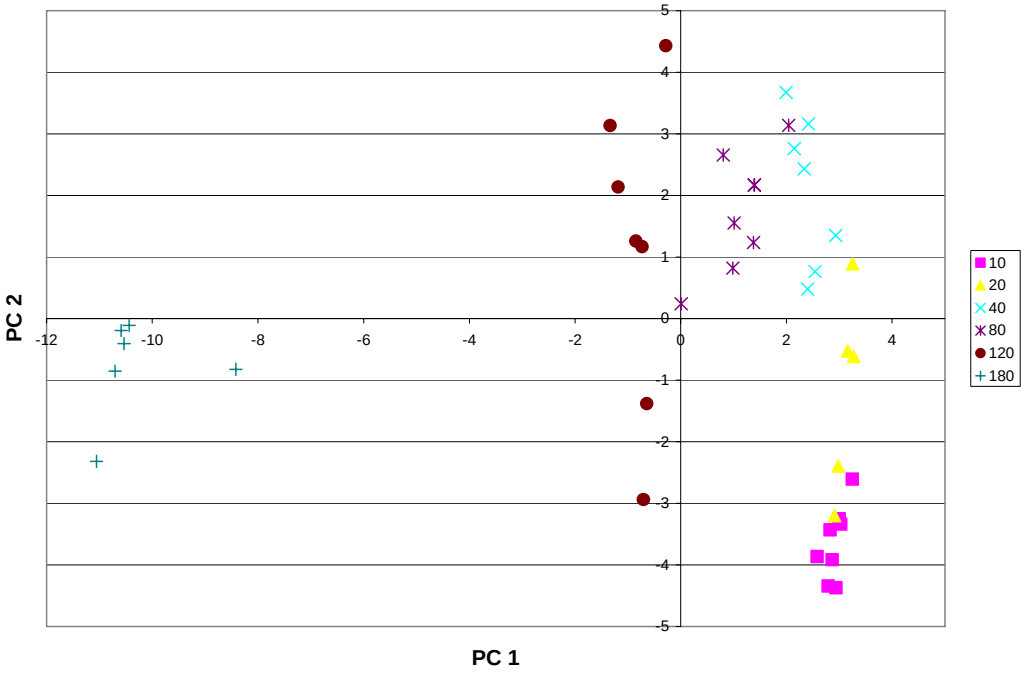

Figure A21: PCA score for R67, 30% lignin spectra

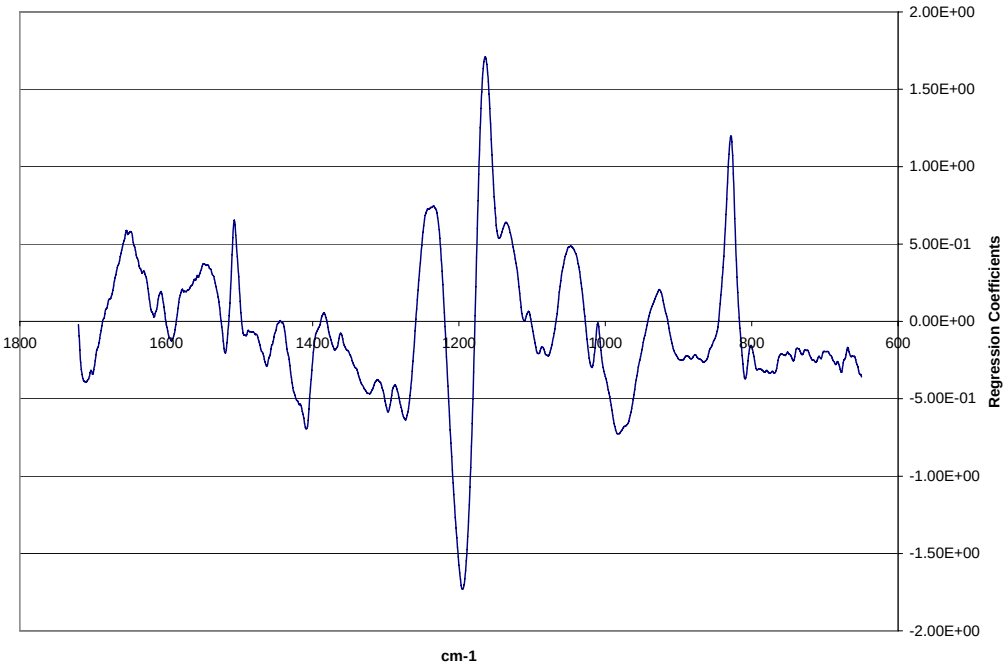

Figure A22: PLS regression coefficients for R67, 30% lignin spectra

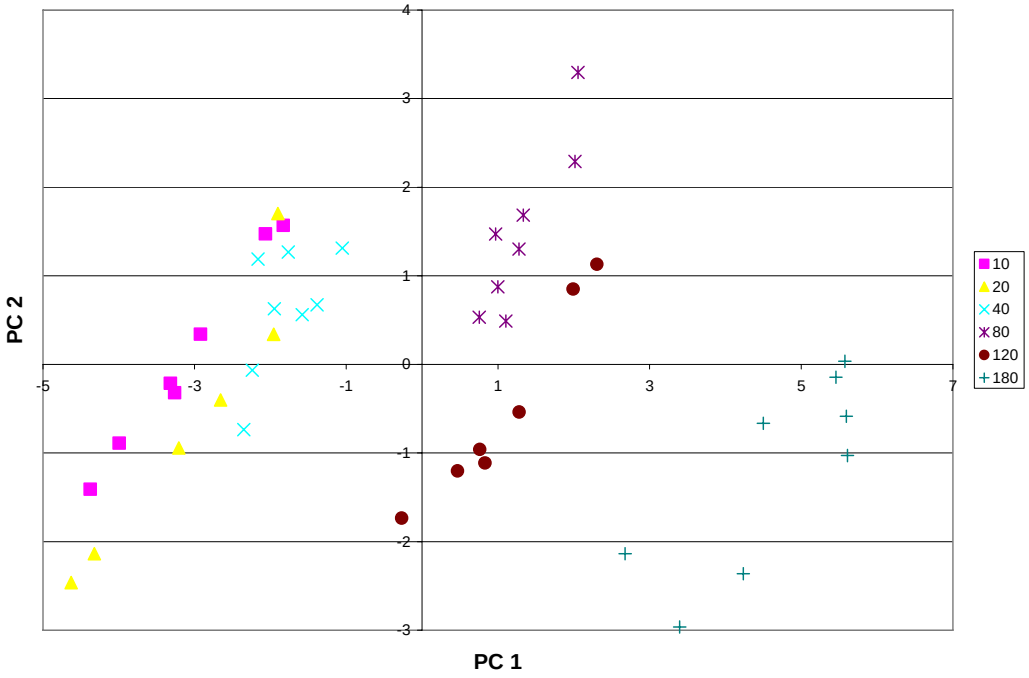

Figure A23: PCA scores for R67, 40% lignin spectra

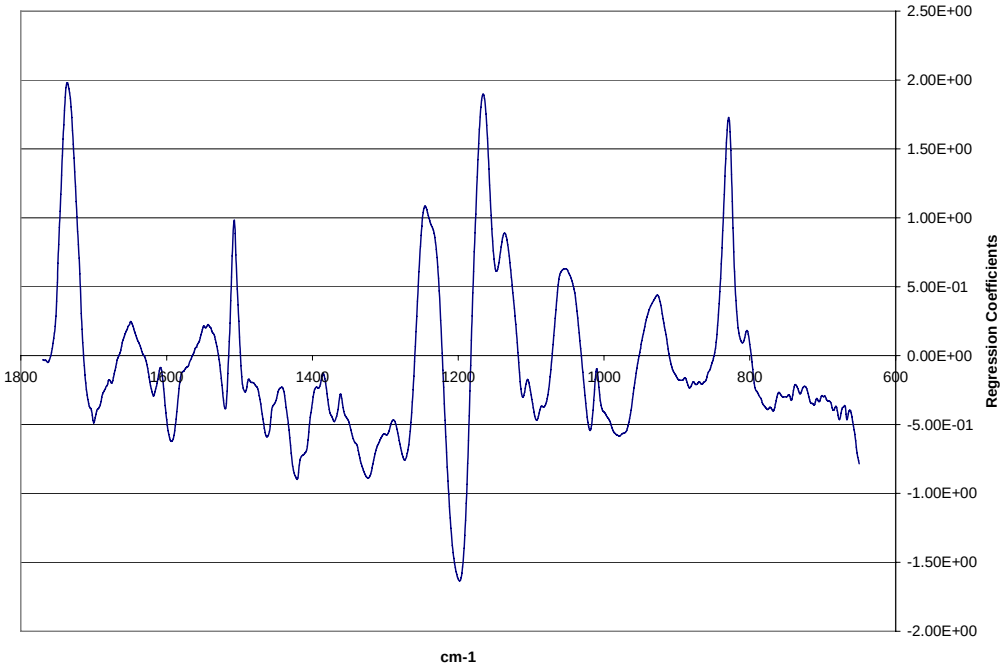

Figure A24: PLS regression coefficients for R67, 40% lignin spectra

Appendix B: DMA Results for R46 and R67 Composites

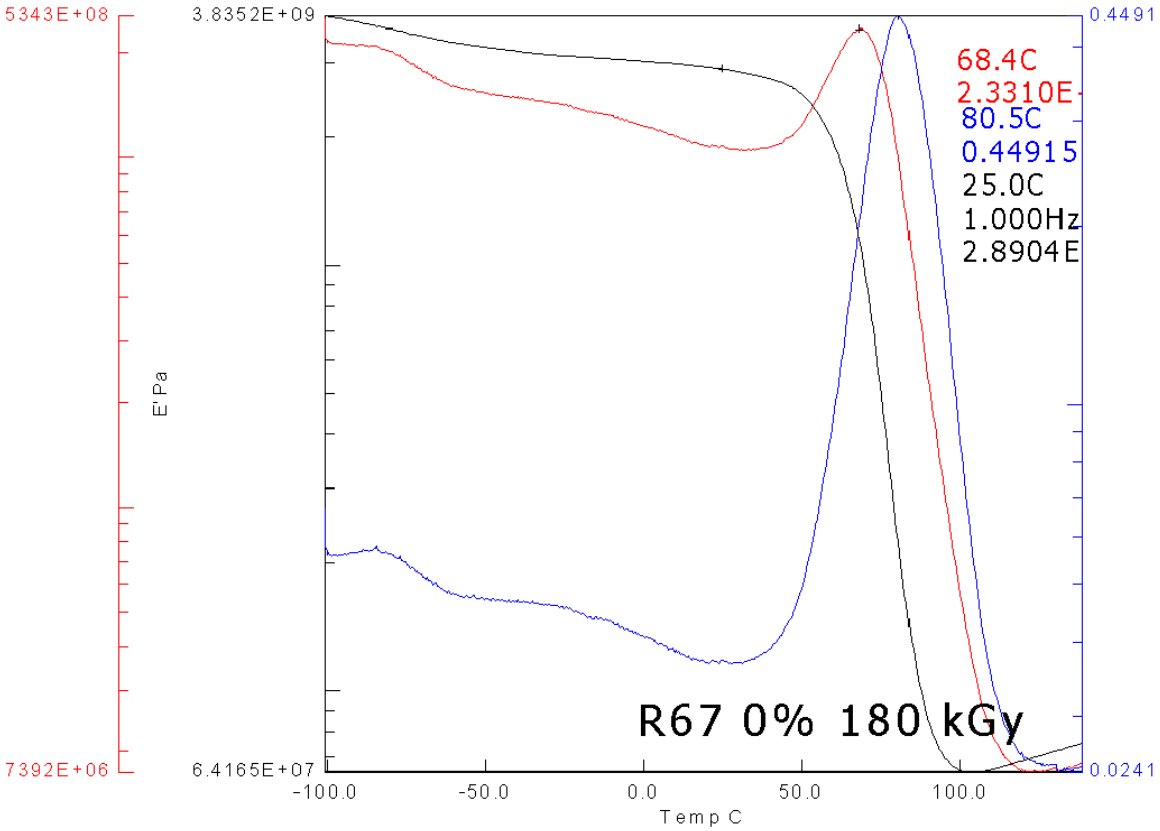

Figure B1: DMA output R67 at 180 kGy

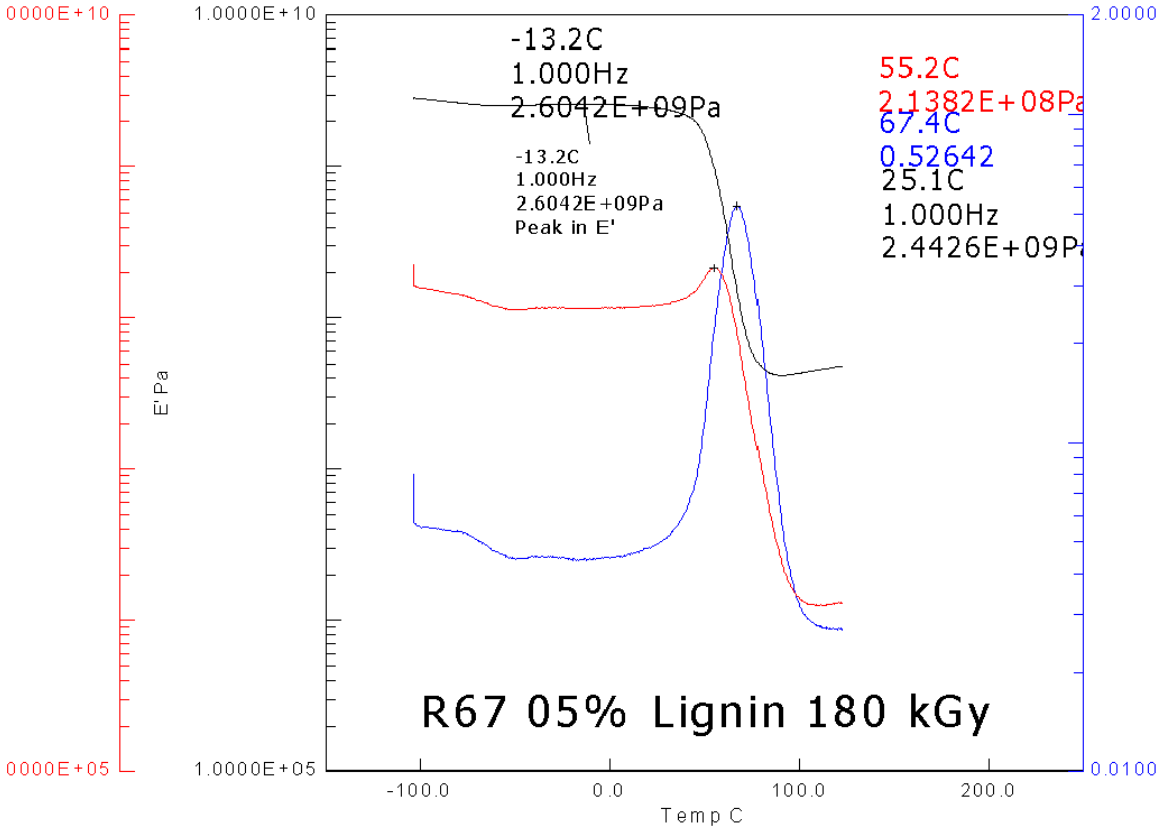

Figure B2: DMA output R67 05% Lignin Cured at 180 kGy

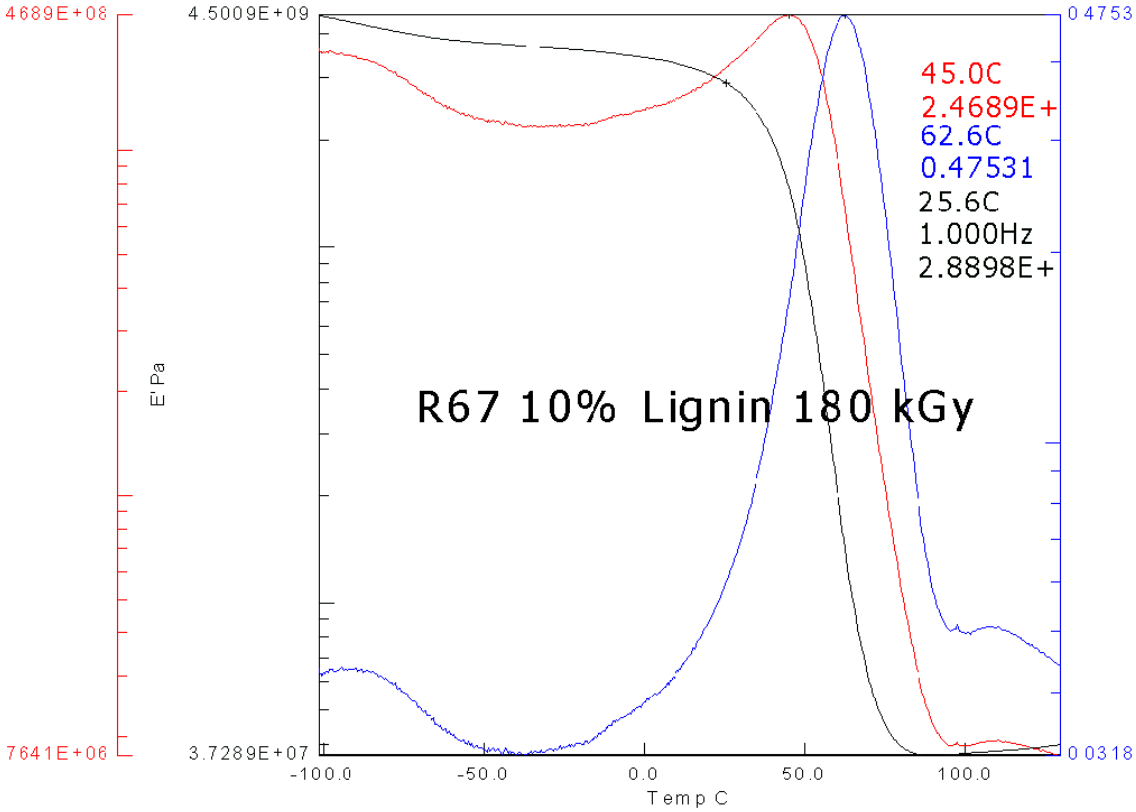

Figure B3: DMA output R67 10% Lignin Cured at 180 kGy

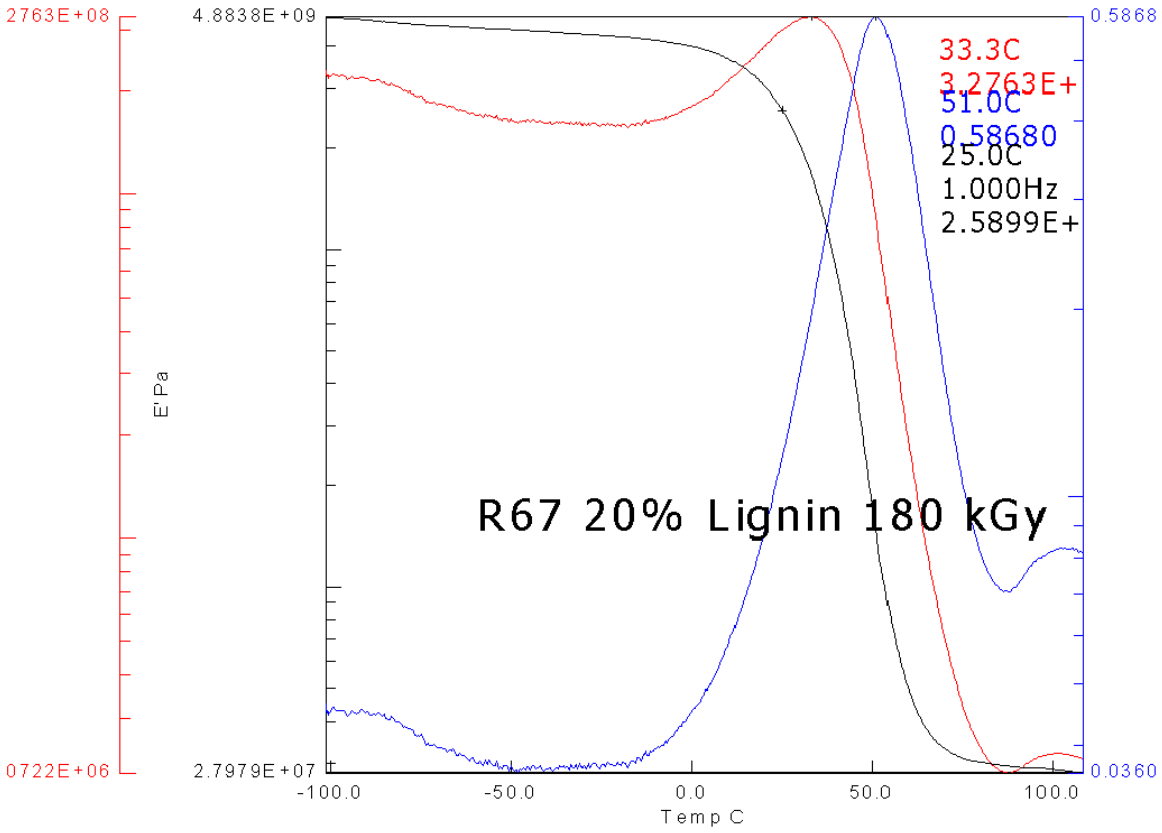

Figure B4: DMA output R67 20% Lignin Cured at 180 kGy

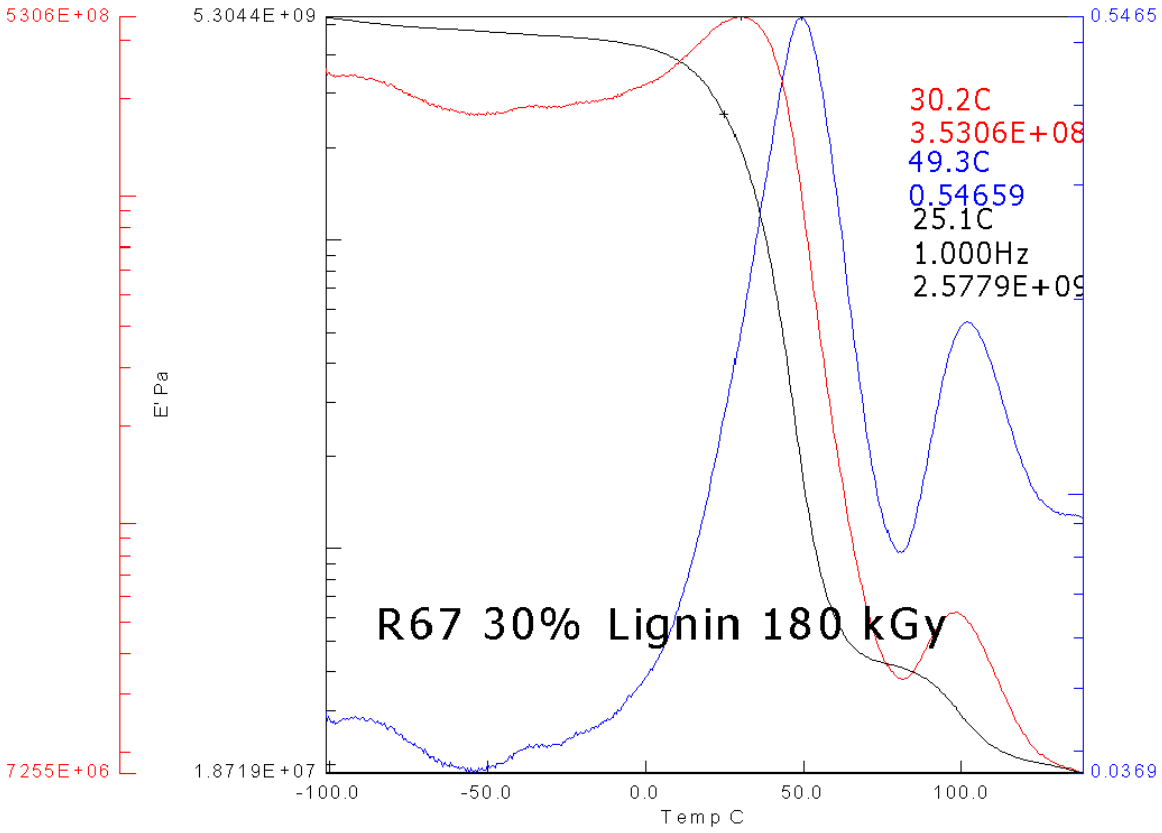

Figure B5: DMA output R67 30% Lignin Cured at 180 kGy

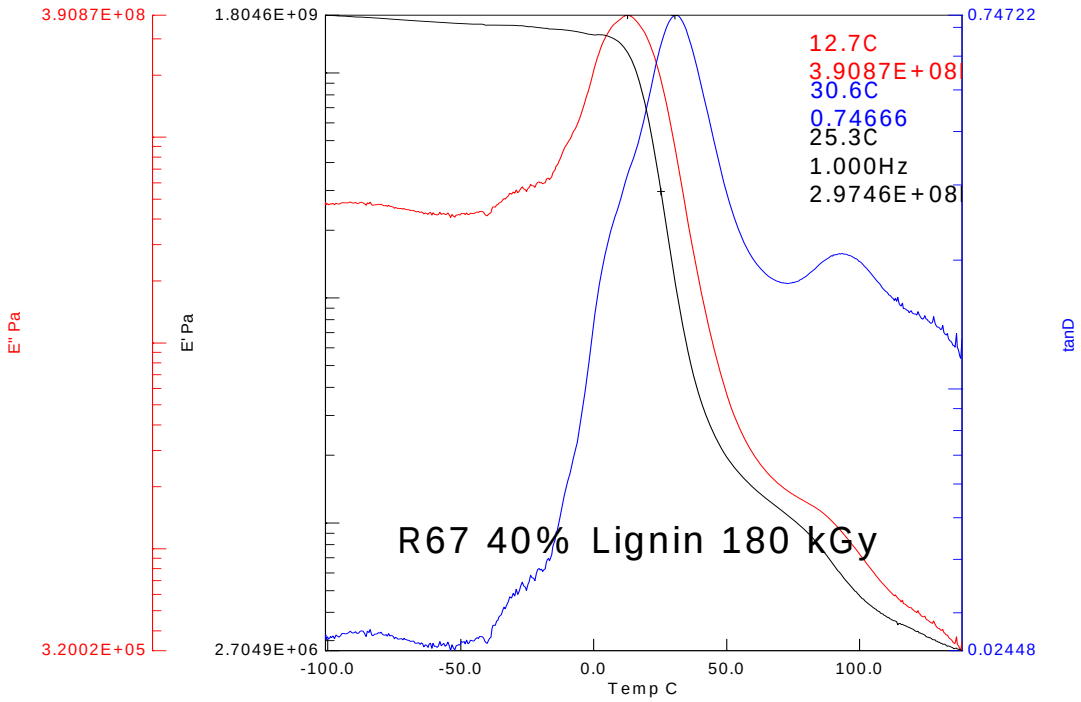

Figure B6: DMA output R67 40% Lignin Cured at 180 kGy

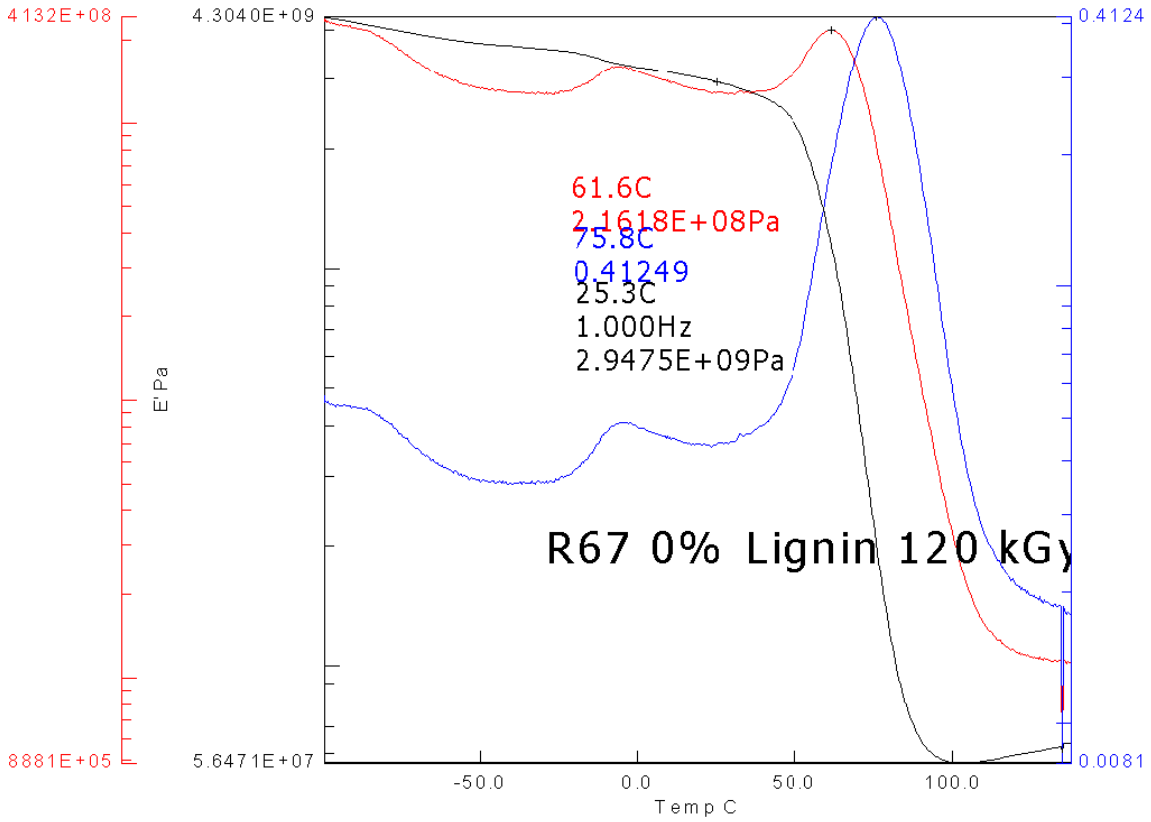

Figure B7: DMA output R67 Cured at 120 kGy

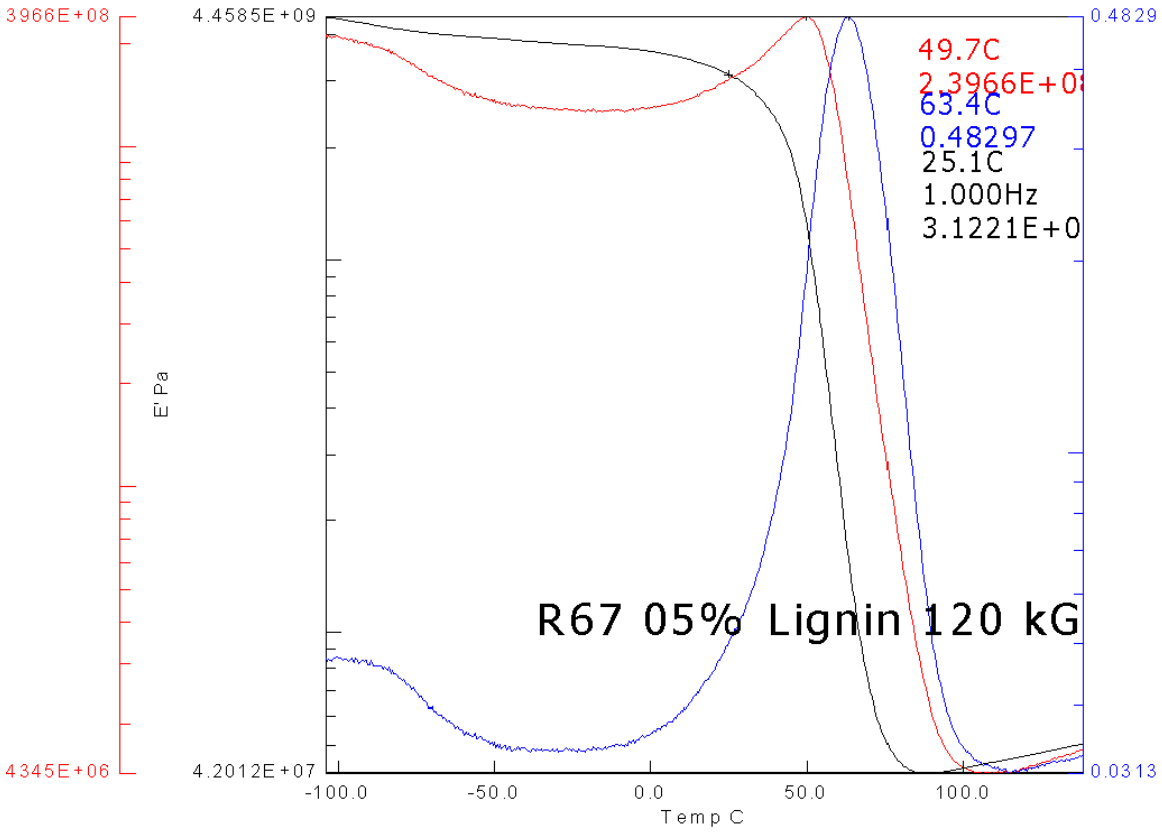

Figure B8: DMA output R67 05% Lignin Cured at 120 kGy

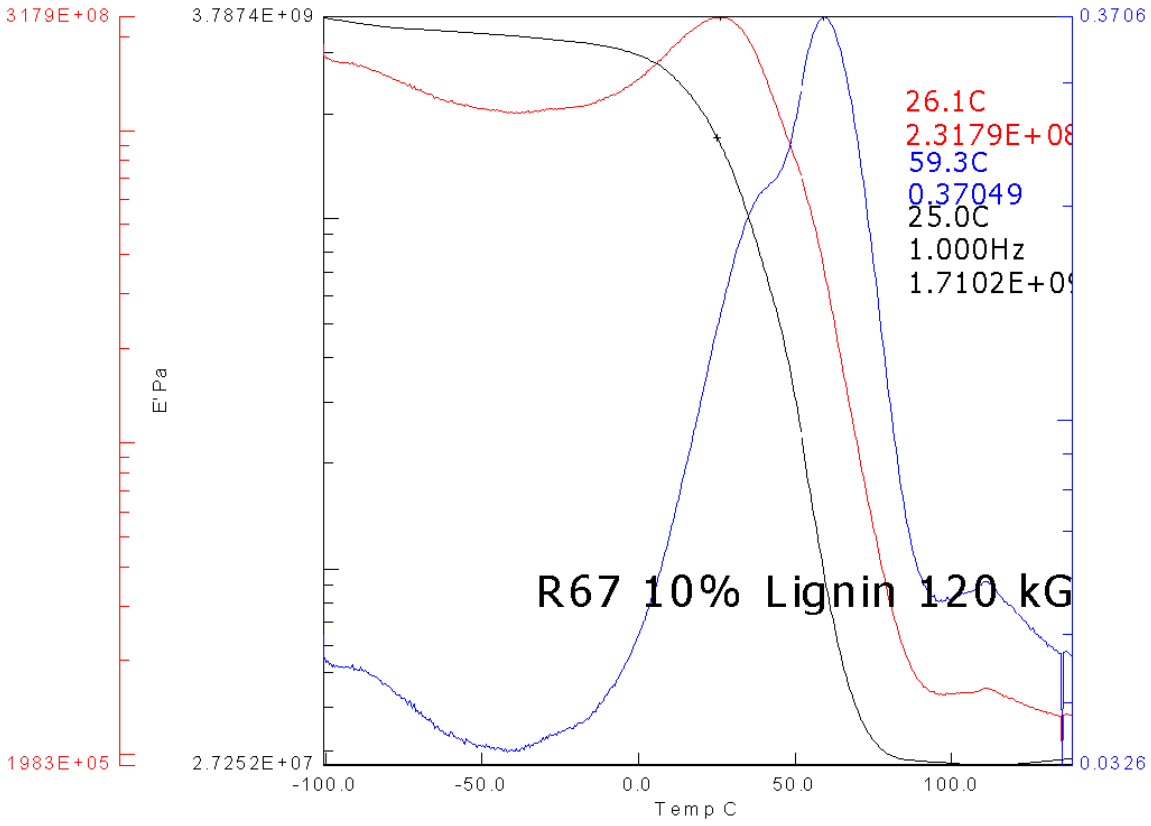

Figure B9: DMA output R67 10% Lignin Cured at 120 kGy

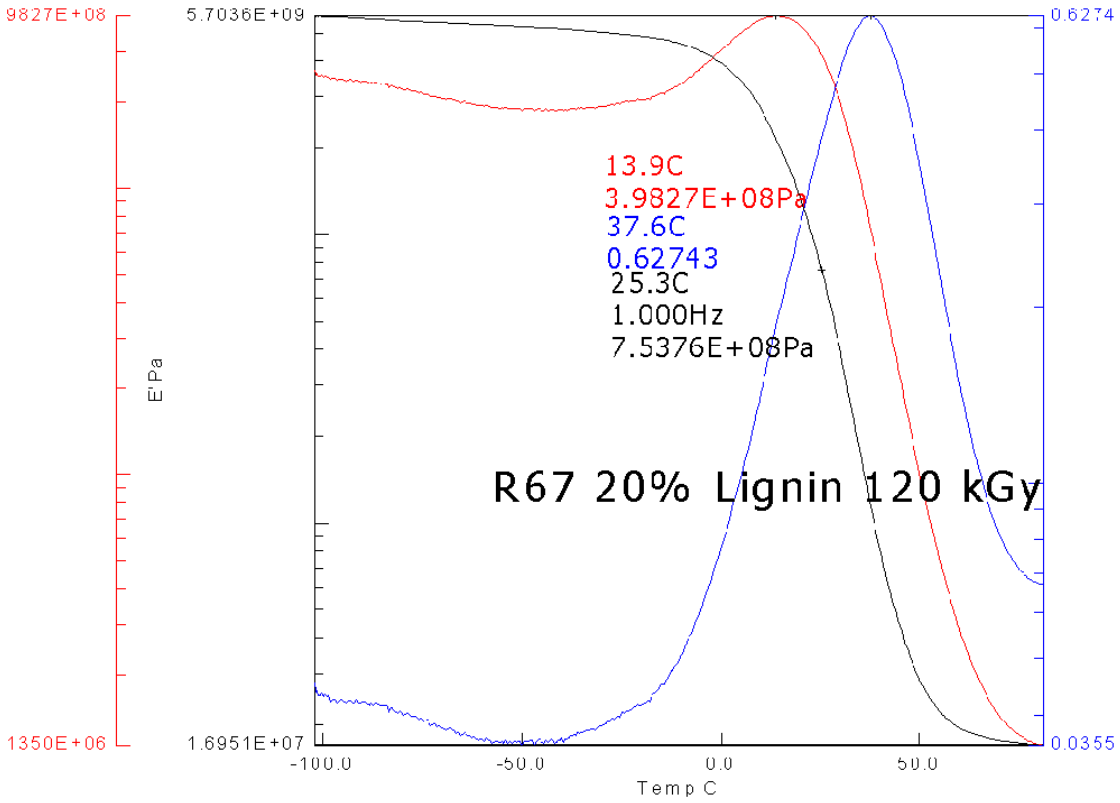

Figure B10: DMA output R67 20% Lignin Cured at 120 kGy

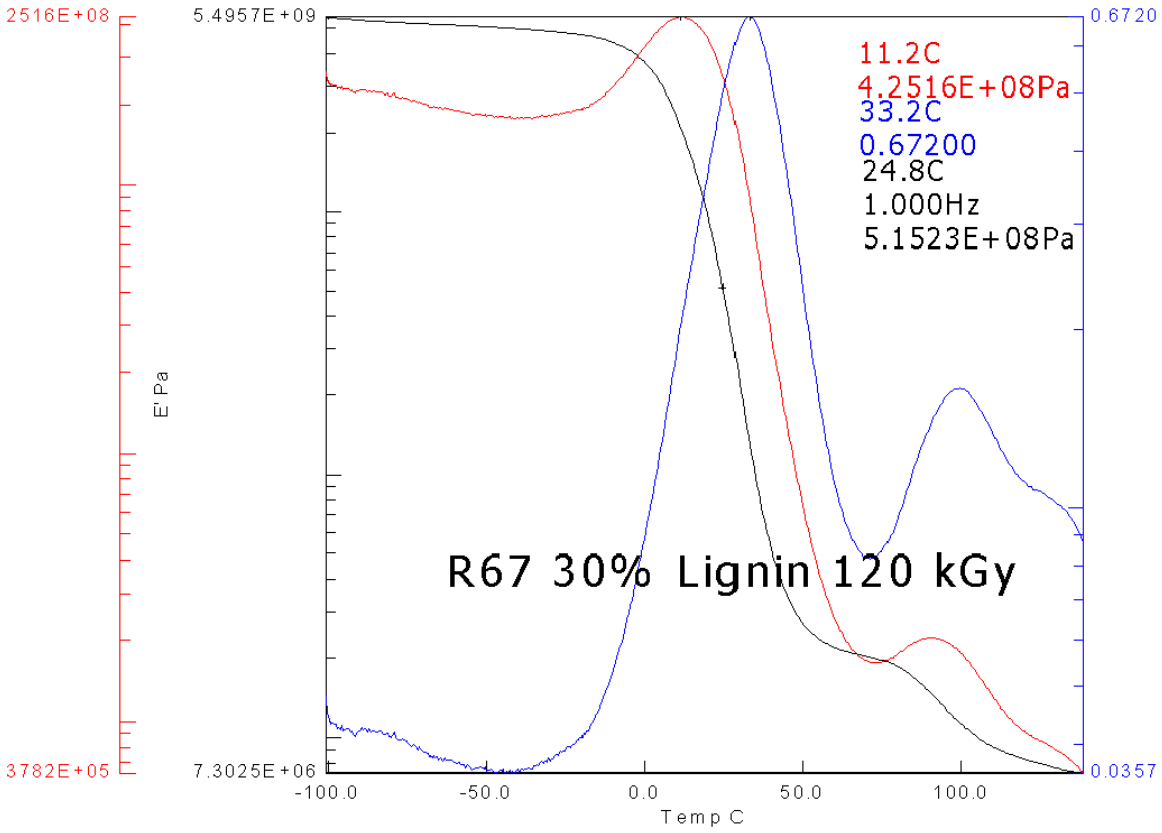

Figure B11: DMA output R67 30% Lignin Cured at 120 kGy

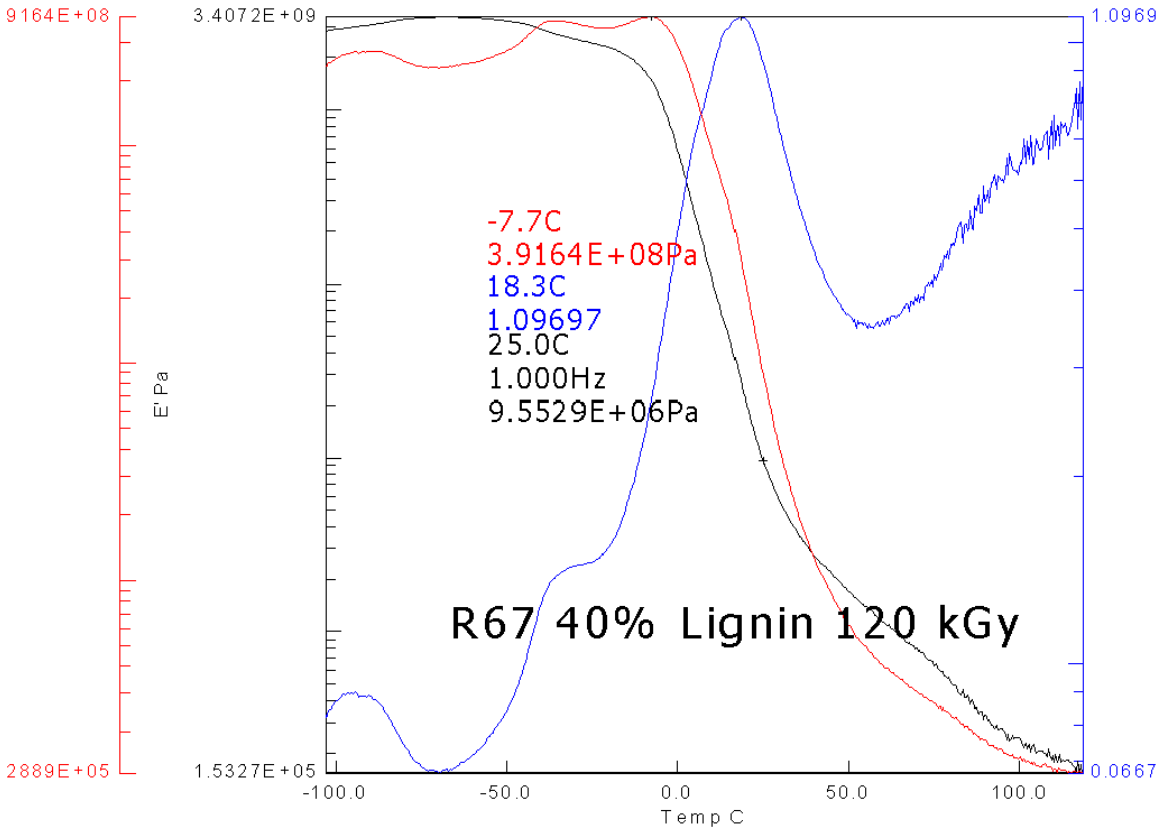

Figure B12: DMA output R67 40% Lignin Cured at 120 kGy

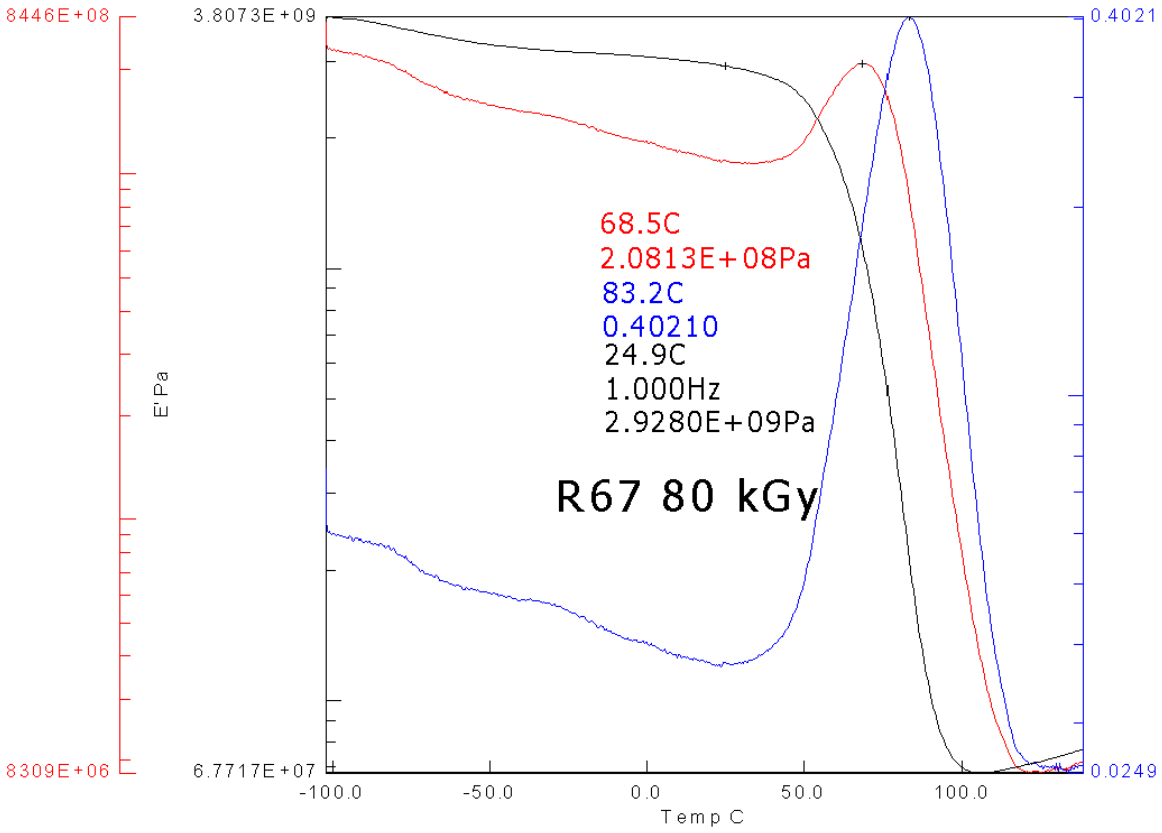

Figure B13: DMA output R67 0% Lignin Cured at 80 kGy

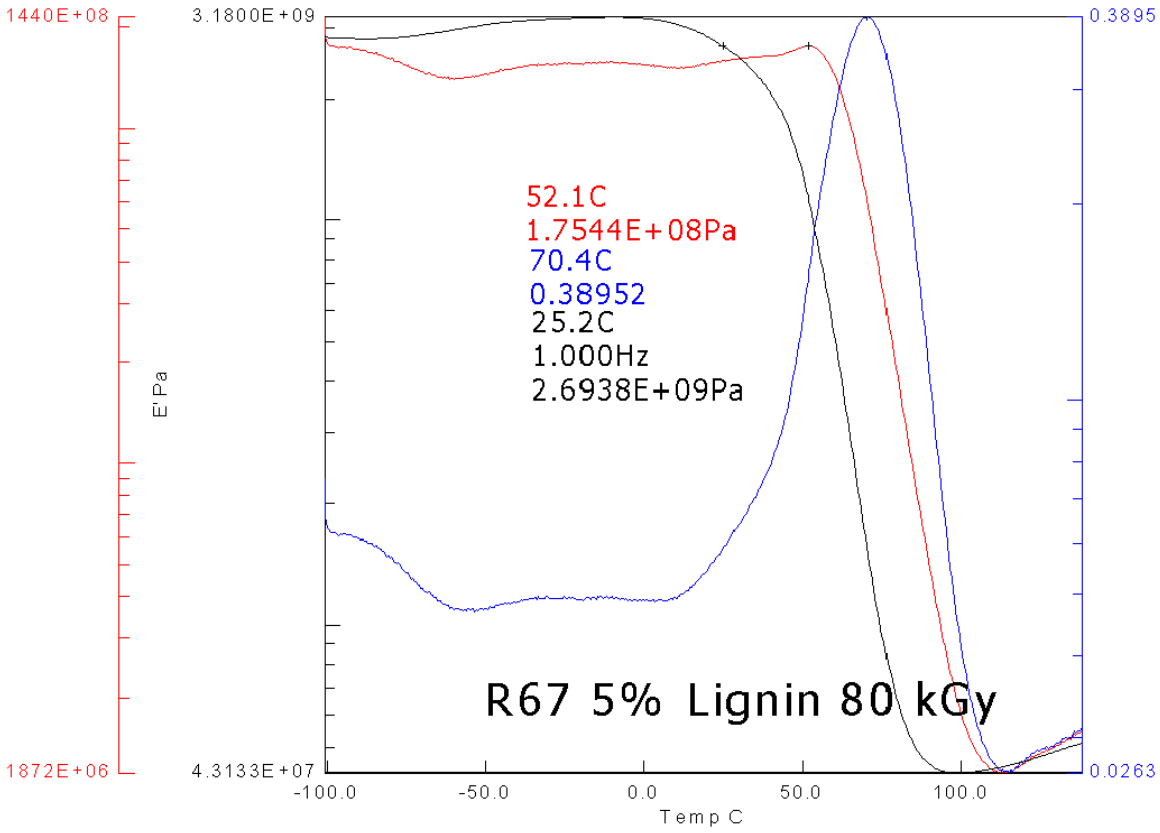

Figure B14: DMA output R67 5% Lignin Cured at 80 kGy

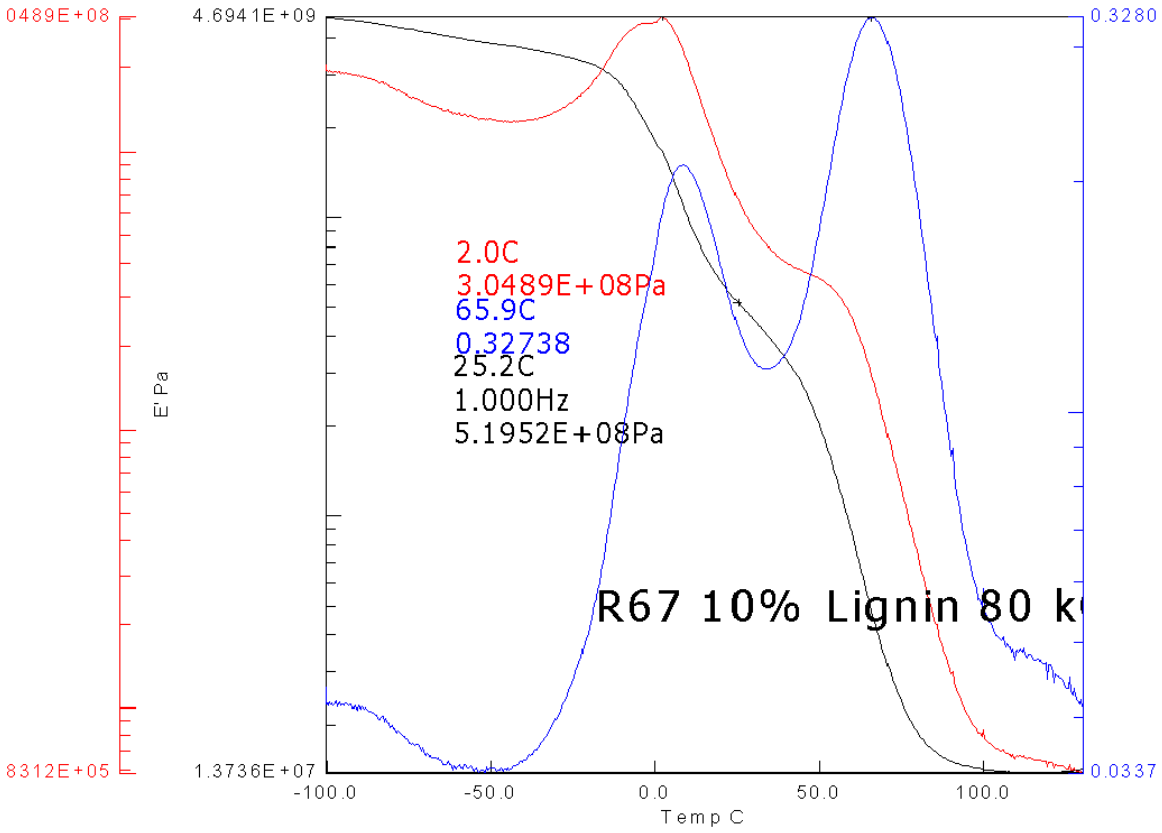

Figure B15: DMA output R67 10% Lignin Cured at 80 kGy

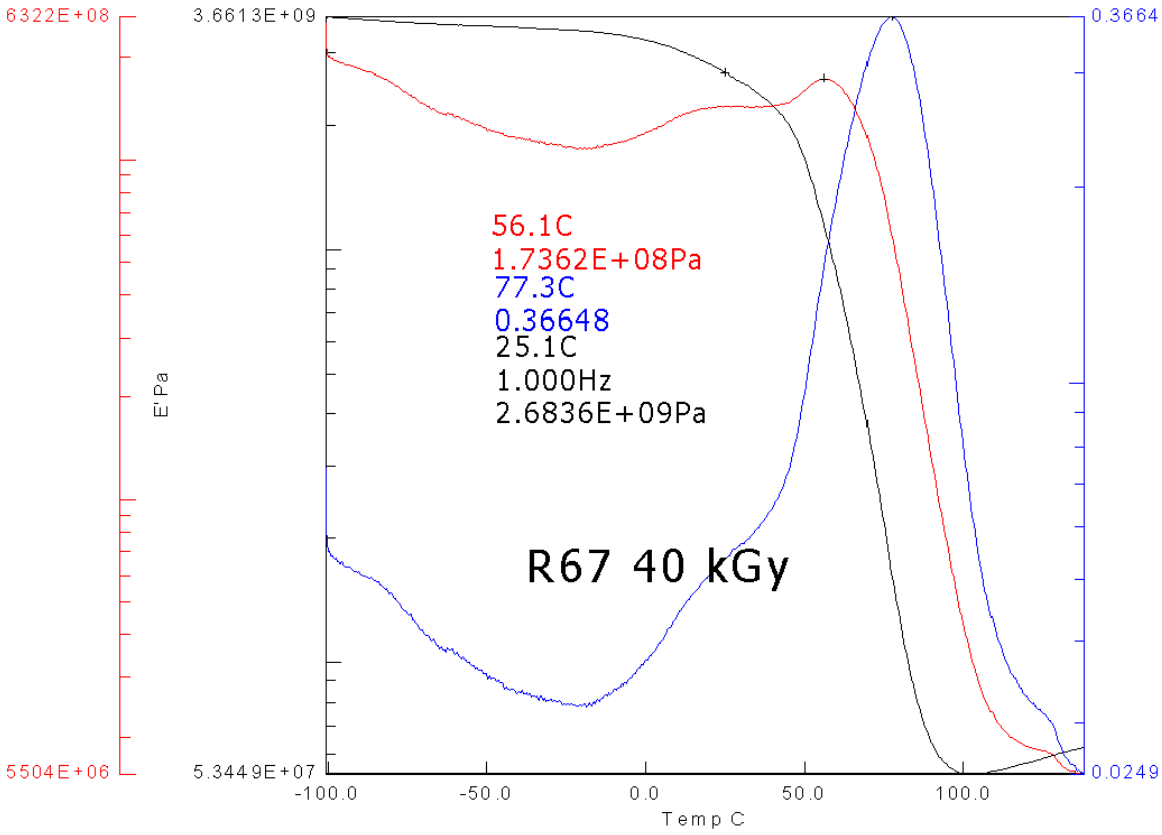

Figure B16: DMA output R67 0% Lignin Cured at 40 kGy

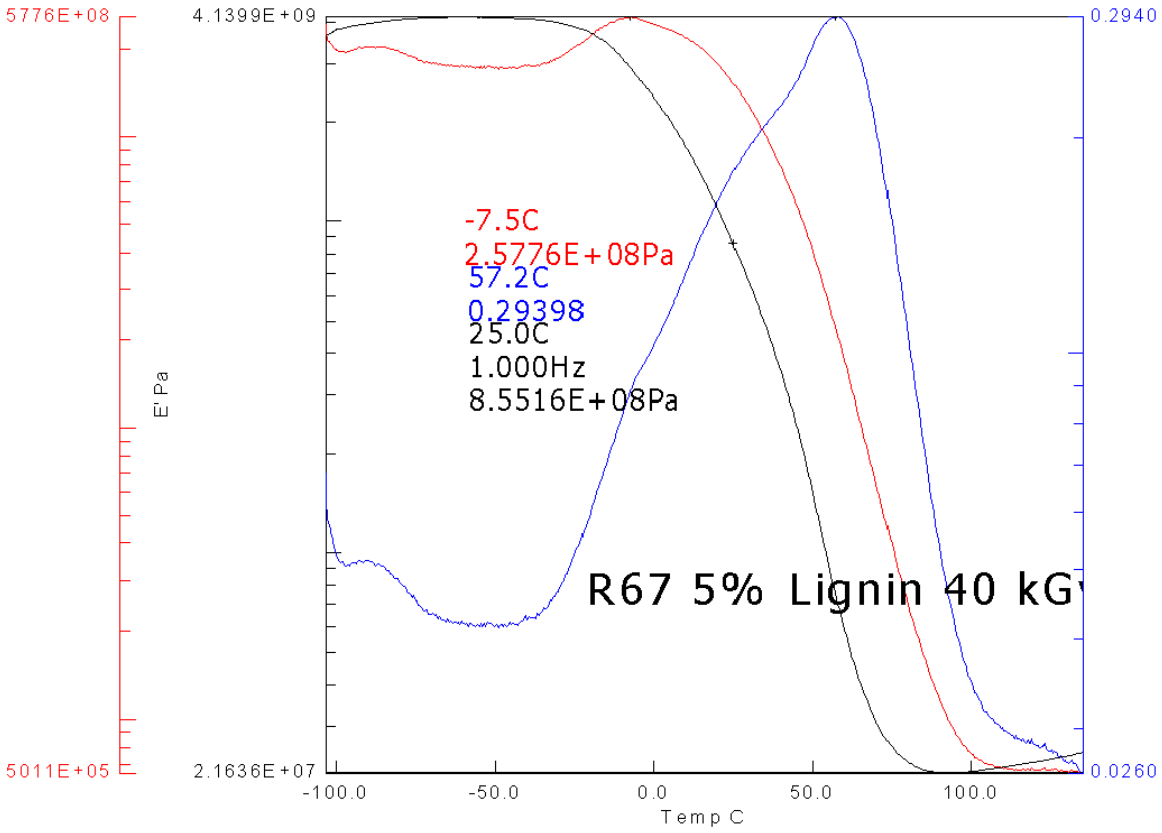

Figure B17: DMA output R67 5% Lignin Cured at 40 kGy

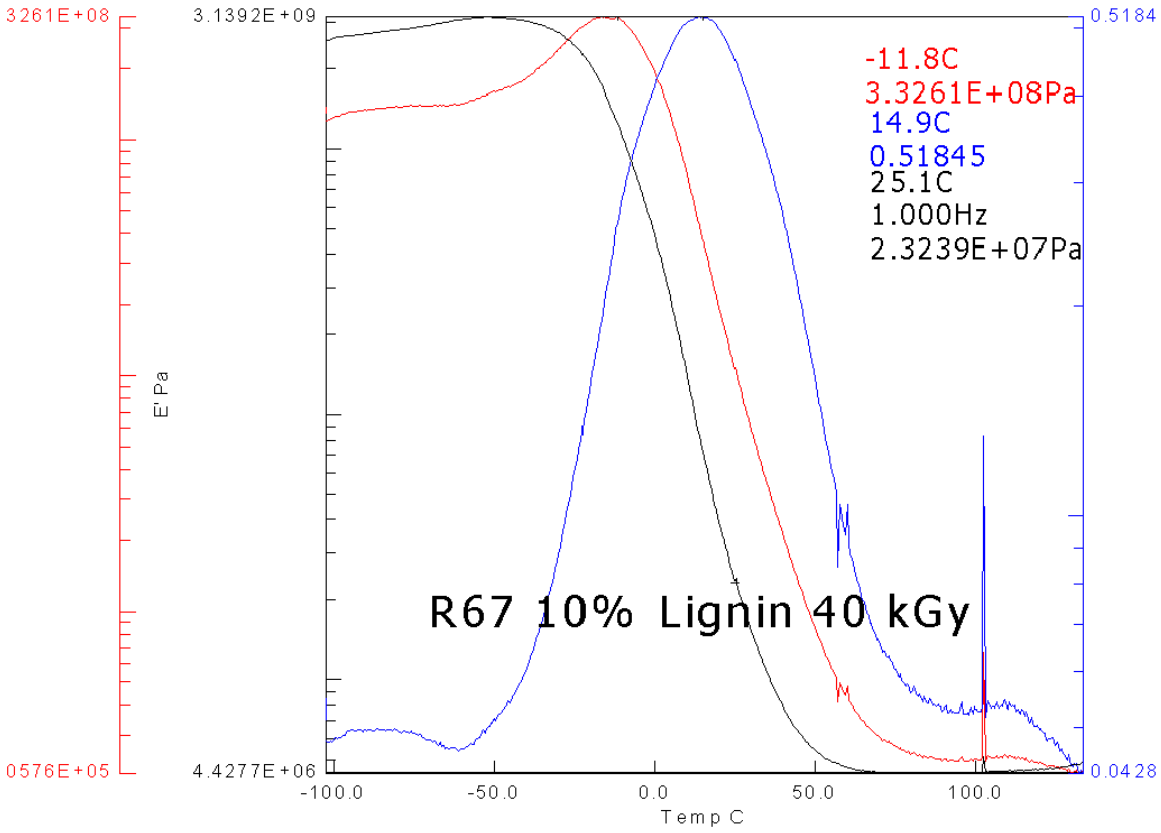

Figure B18: DMA output R67 10% Lignin Cured at 40 kGy

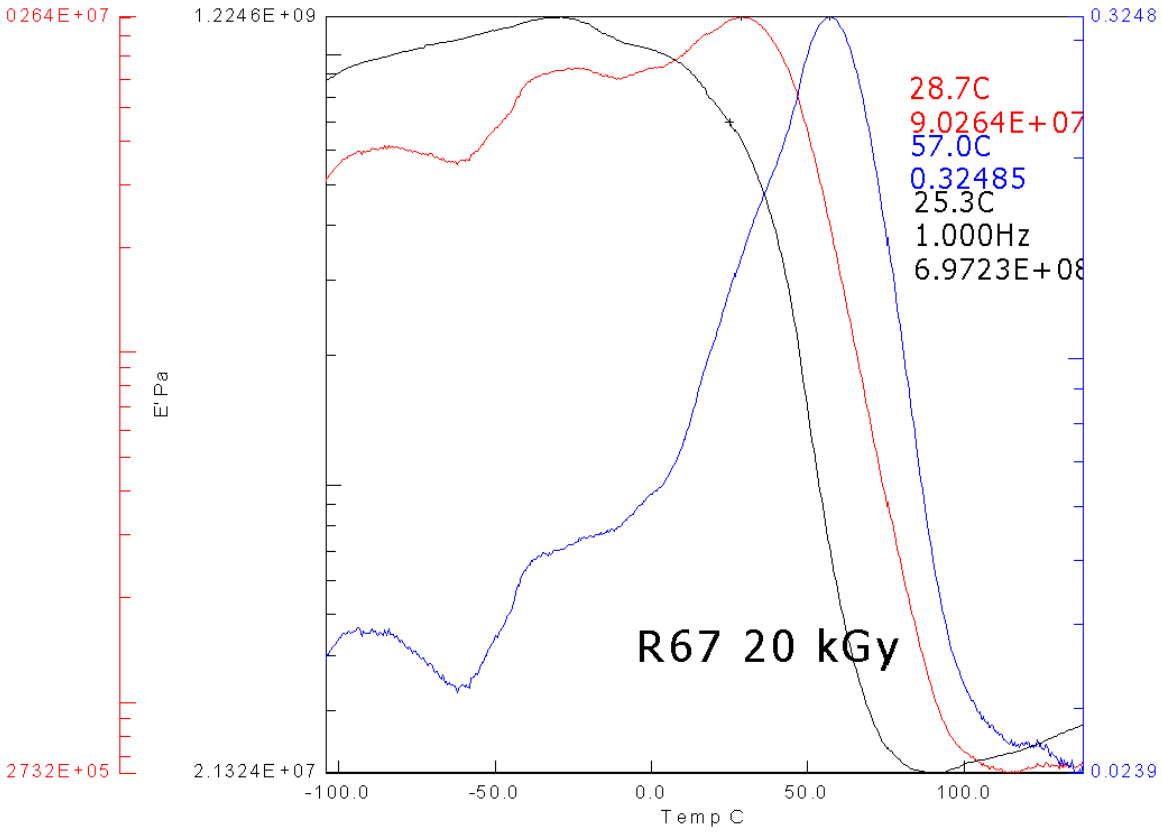

Figure B19: DMA output R67 0% Lignin Cured at 20 kGy

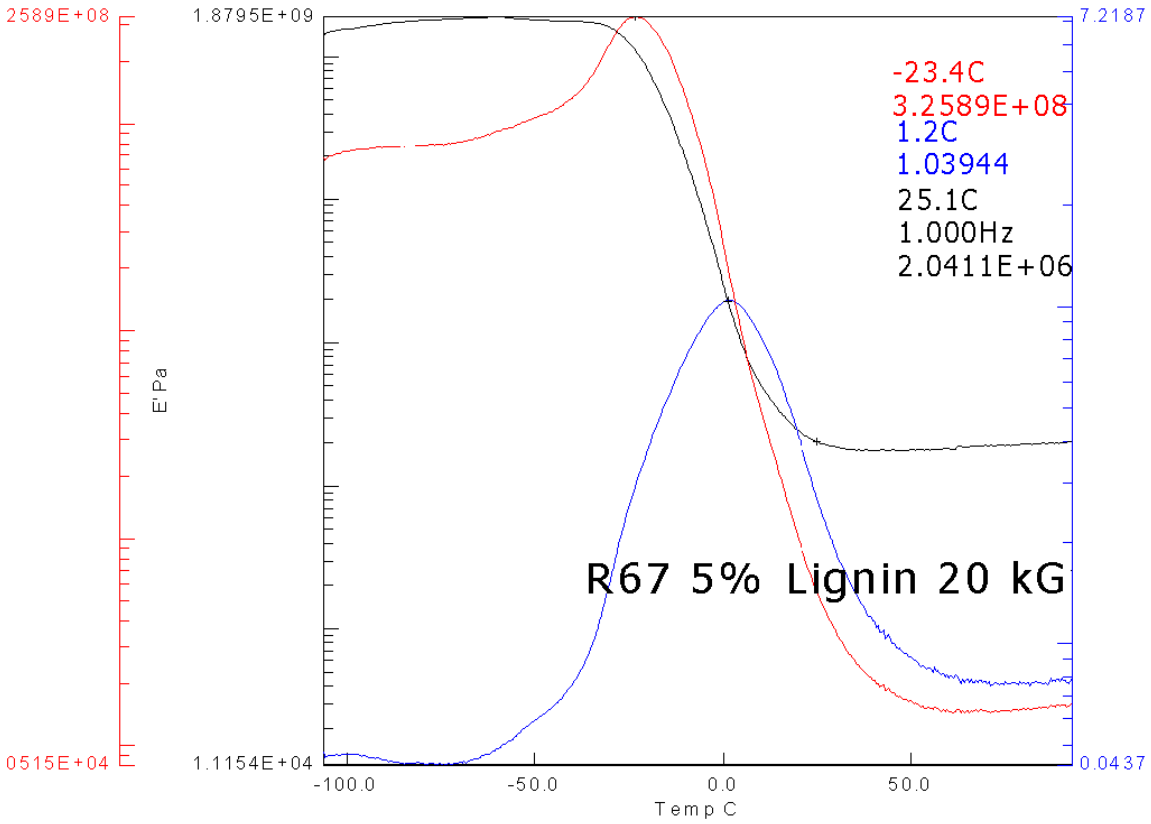

Figure B20: DMA output R67 5% Lignin Cured at 20 kGy

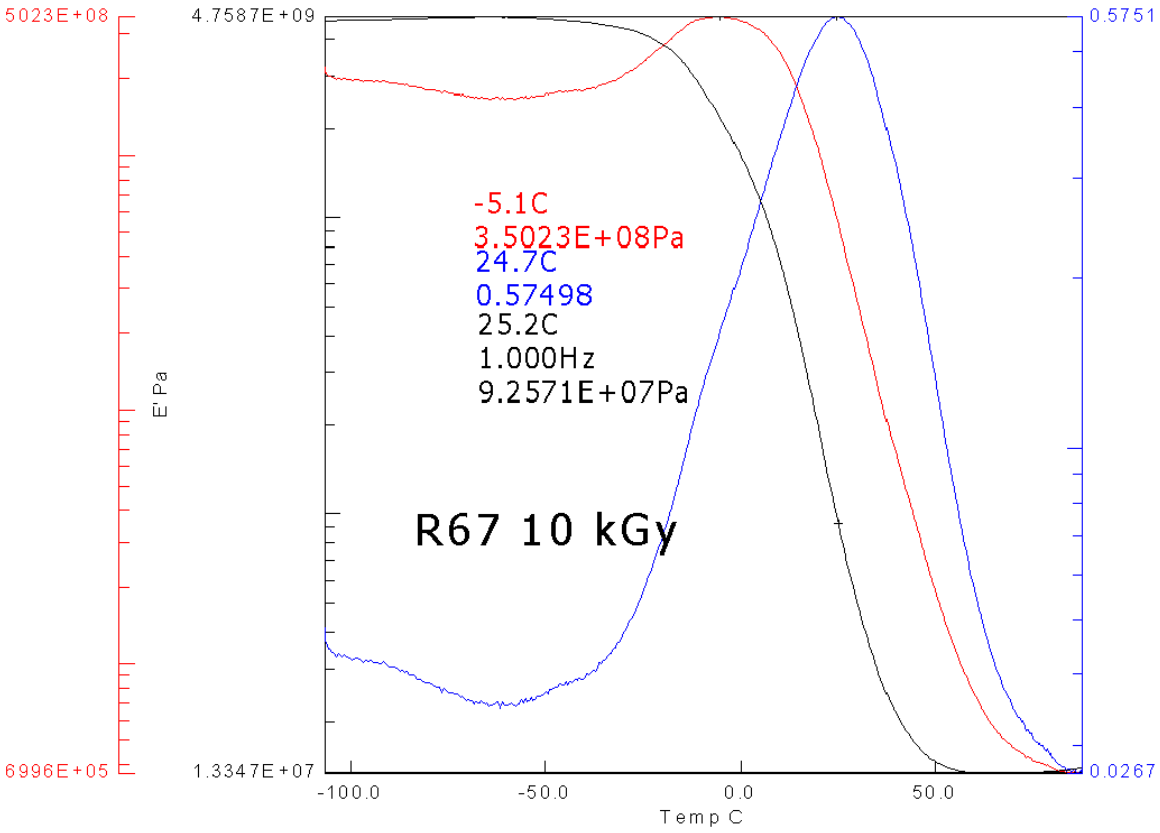

Figure B21: DMA output R67 0% Lignin Cured at 10 kGy

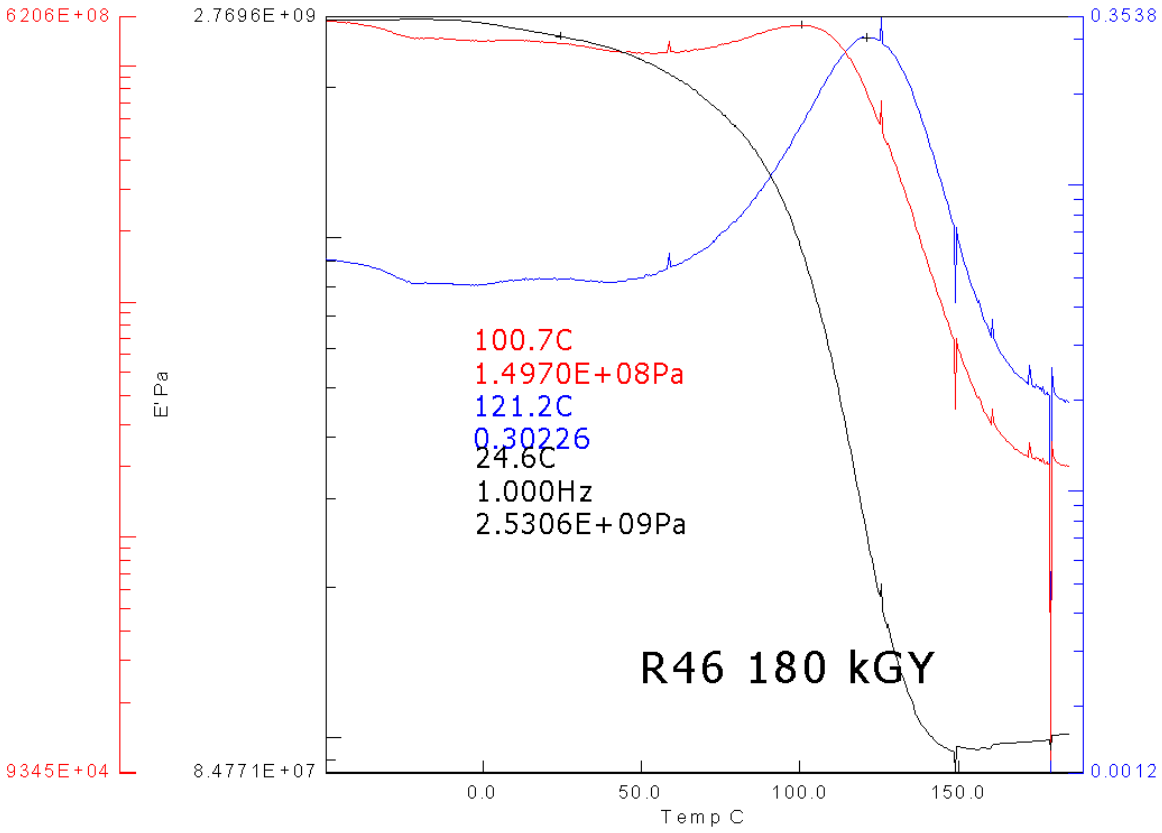

Figure B22: DMA output R46 0% Lignin Cured at 180 kGy

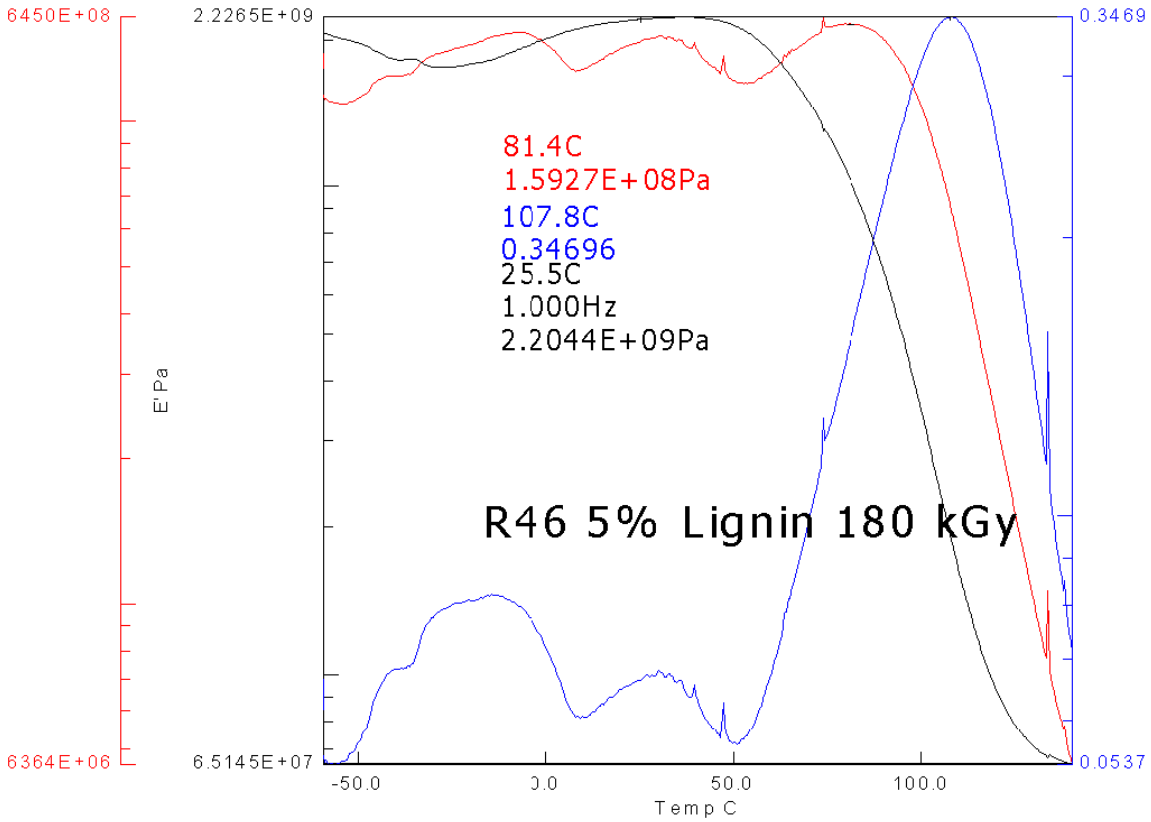

Figure B23: DMA output R46 5% Lignin Cured at 180 kGy

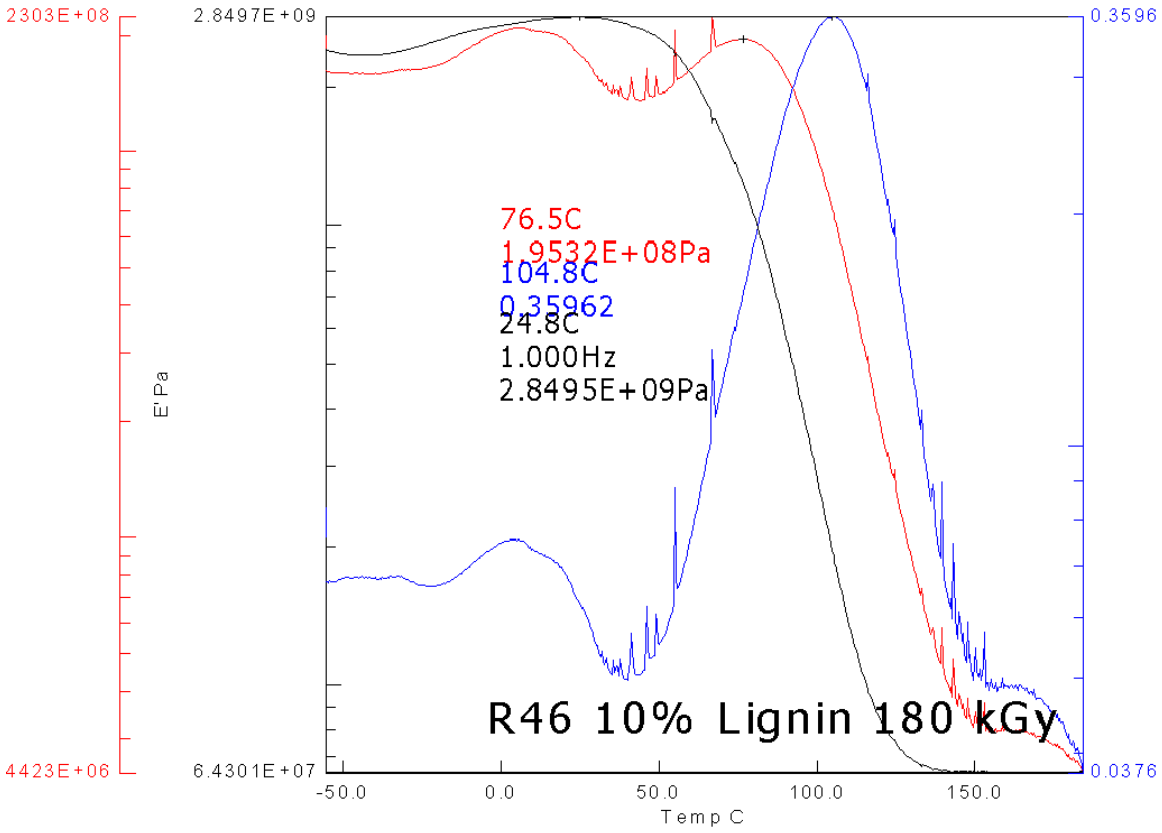

Figure B24: DMA output R46 10% Lignin Cured at 180 kGy

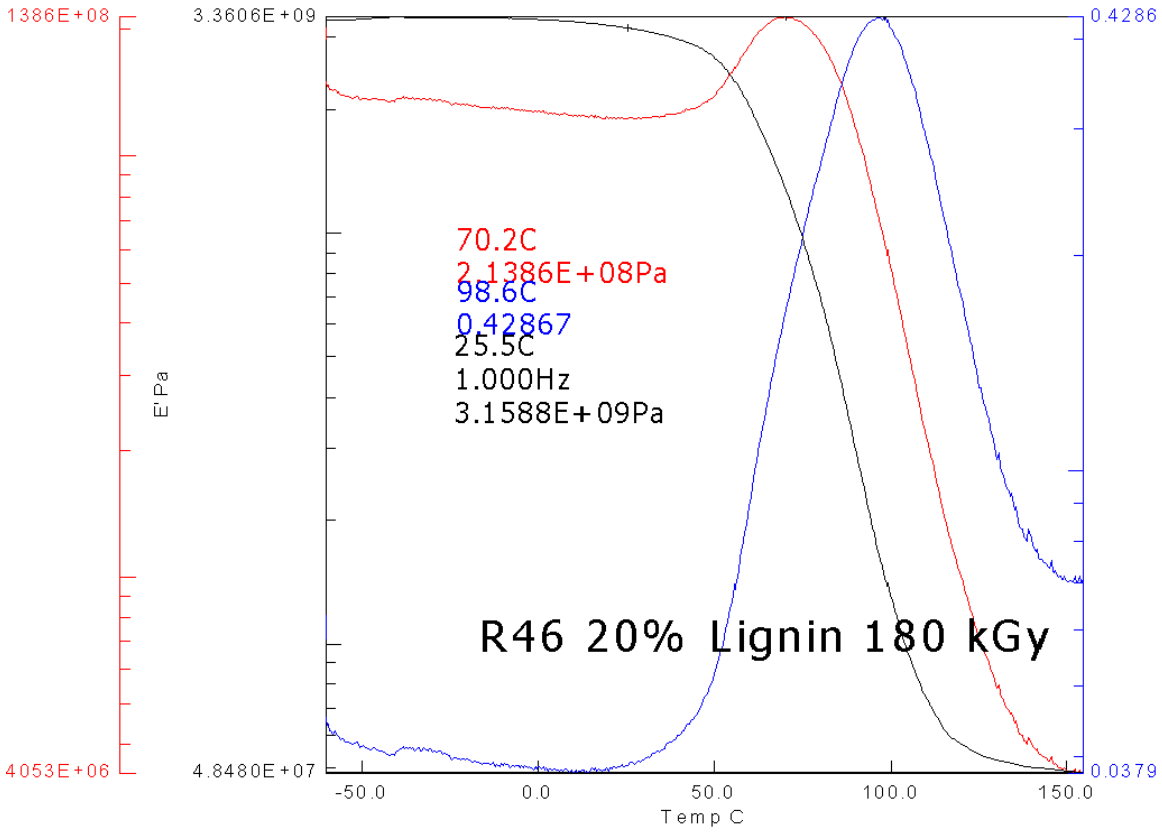

Figure B25: DMA output R46 20% Lignin Cured at 180 kGy

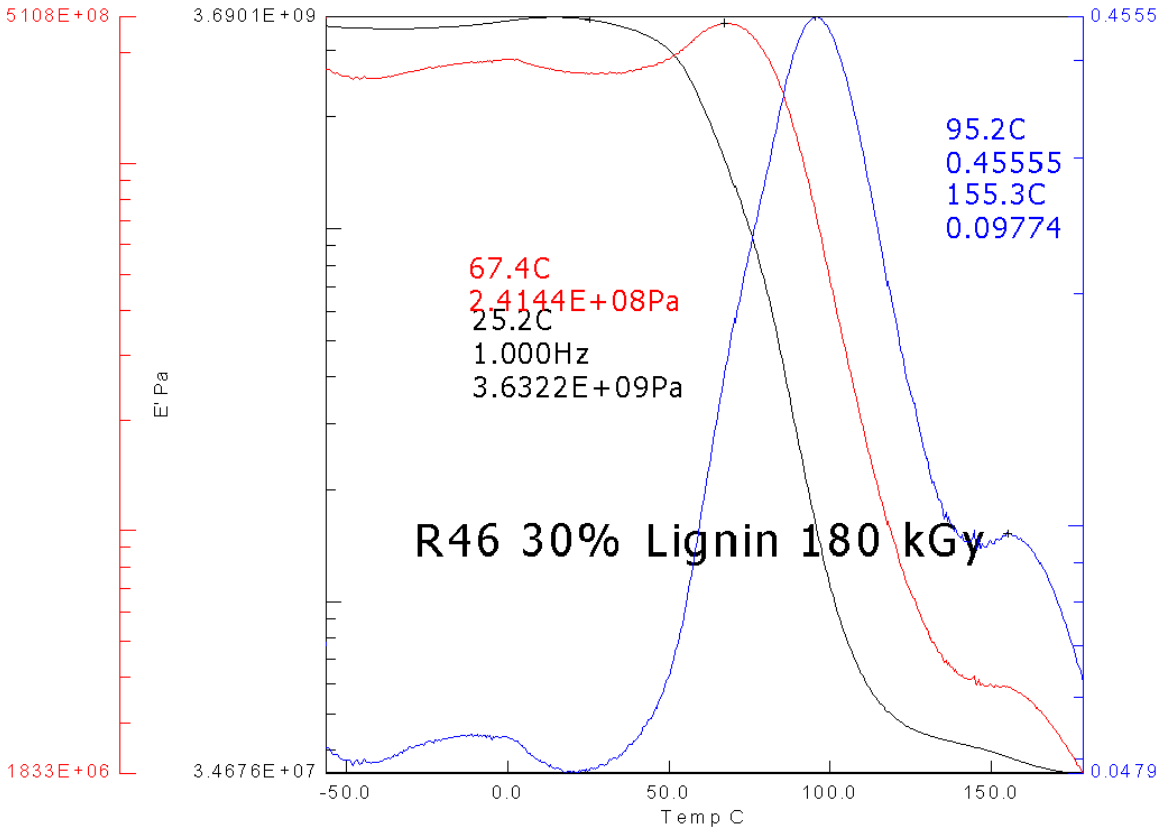

Figure B26: DMA output R46 30% Lignin Cured at 180 kGy

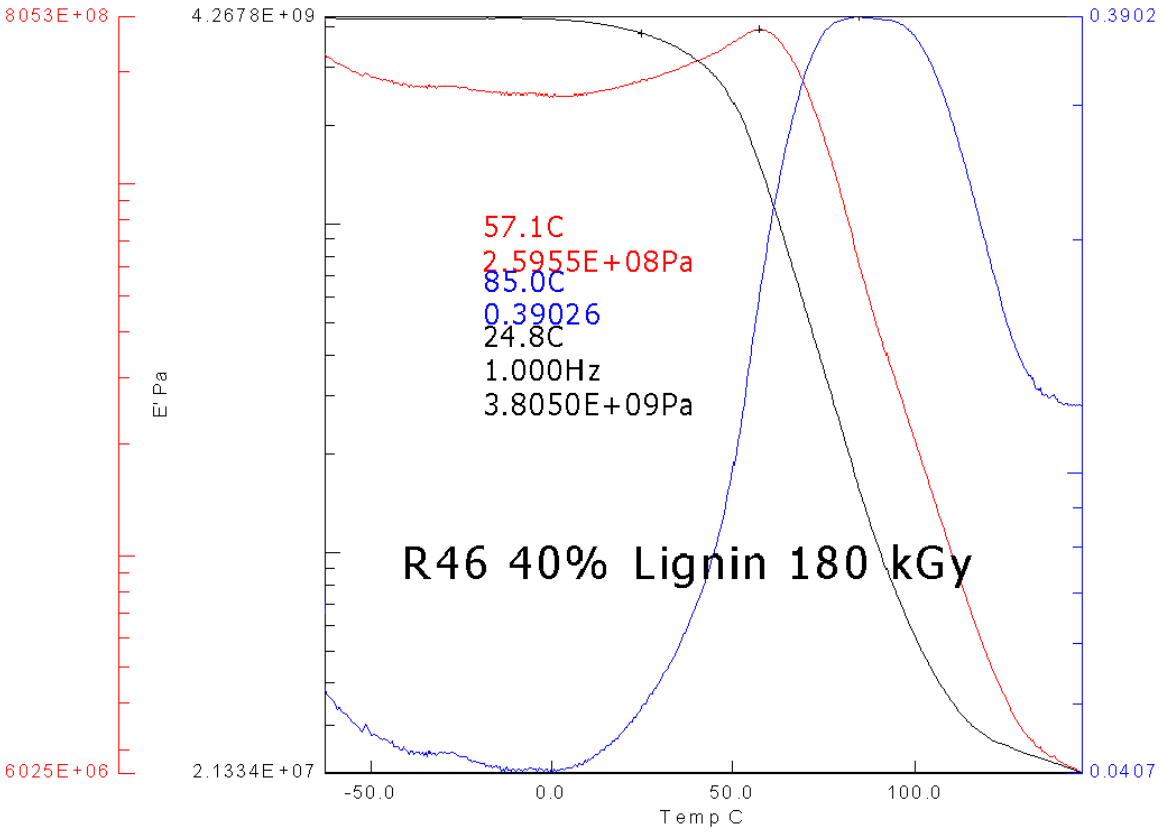

Figure B27: DMA output R46 40% Lignin Cured at 180 kGy

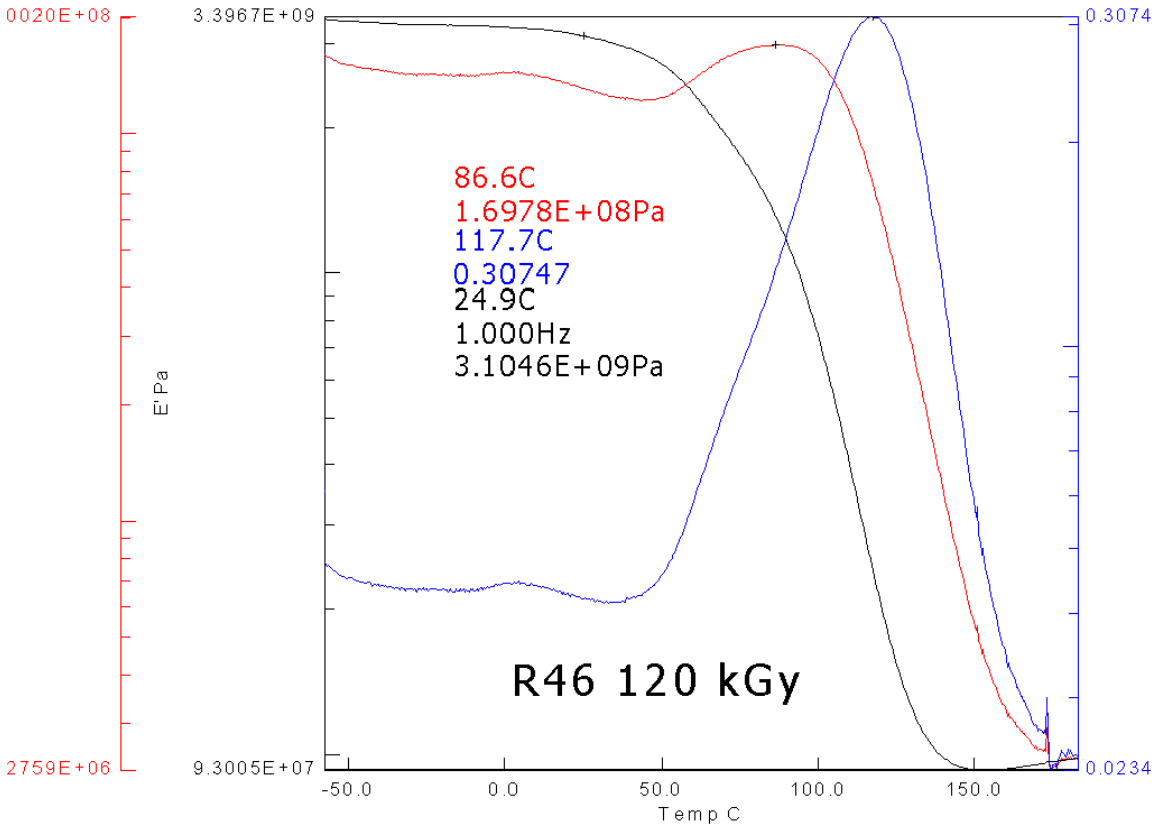

Figure B28: DMA output R46 Cured at 120 kGy

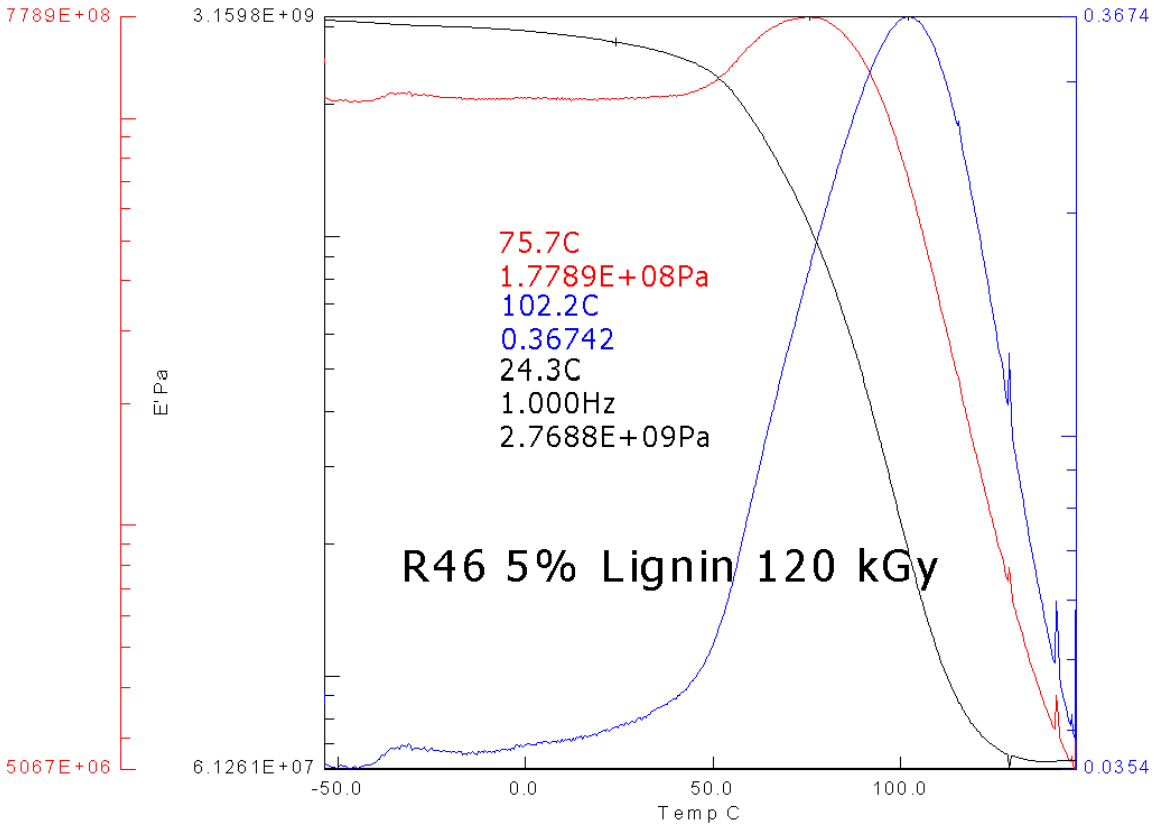

Figure B29: DMA output R46 5% Lignin Cured at 120 kGy

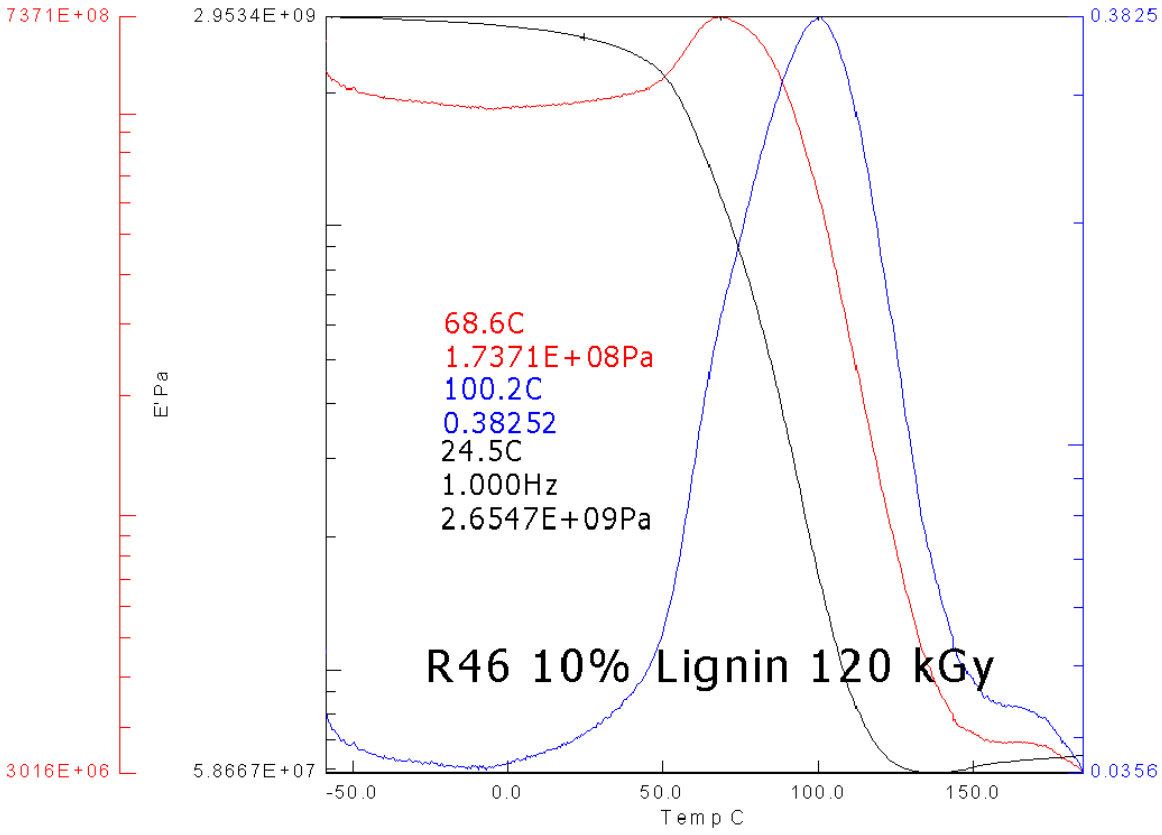

Figure B30: DMA output R46 10% Lignin Cured at 120 kGy

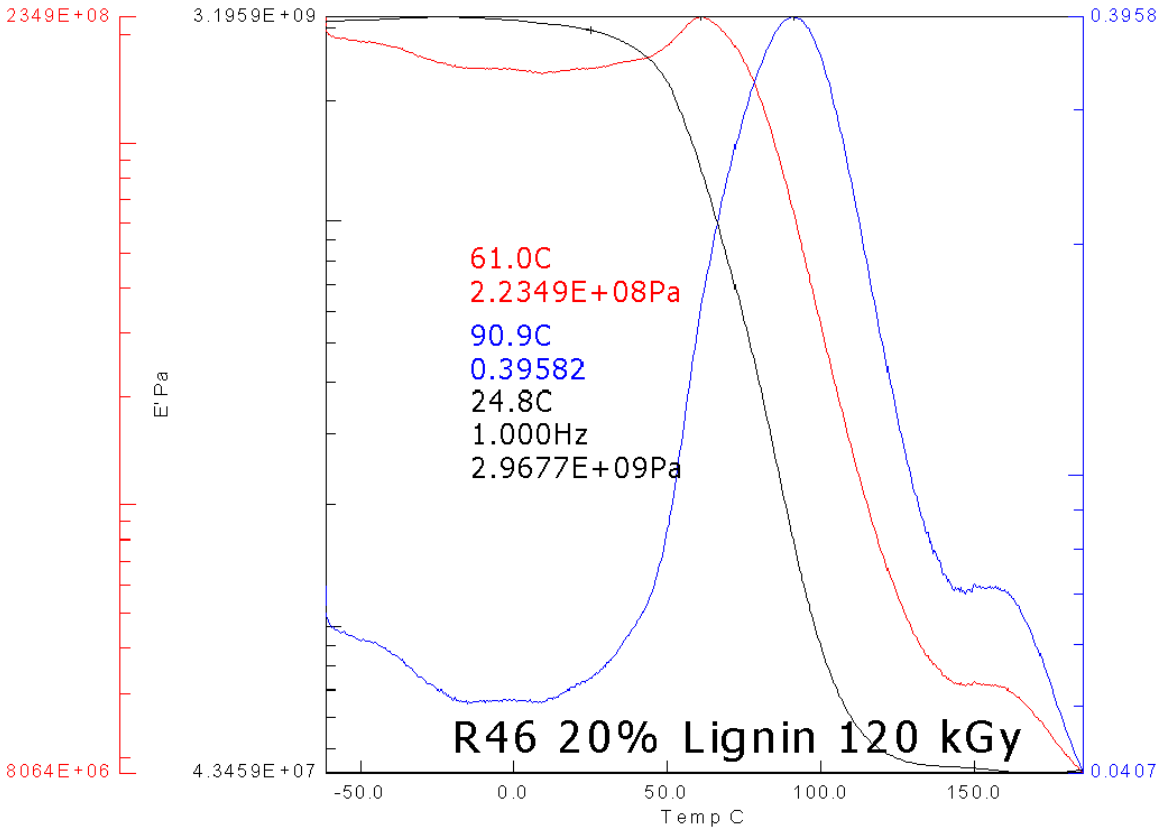

Figure B31: DMA output R46 20% Lignin Cured at 120 kGy

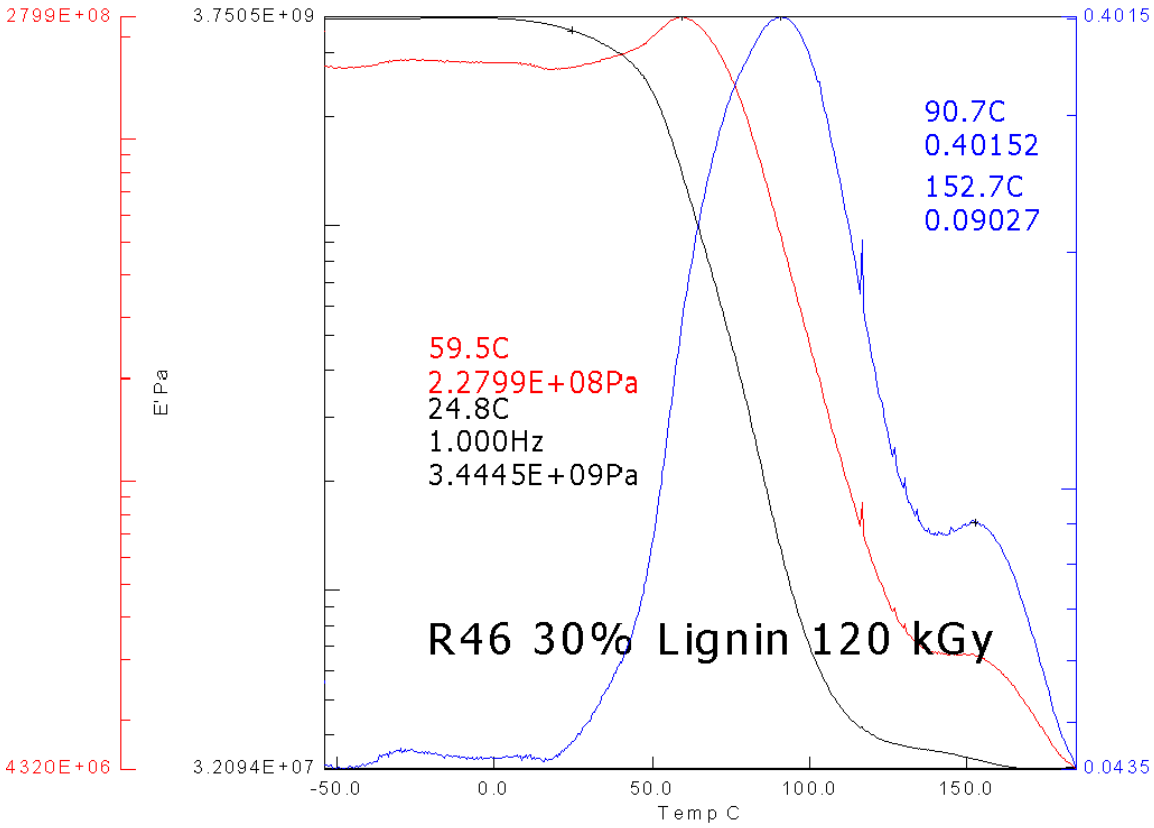

Figure B32: DMA output R46 30% Lignin Cured at 120 kGy

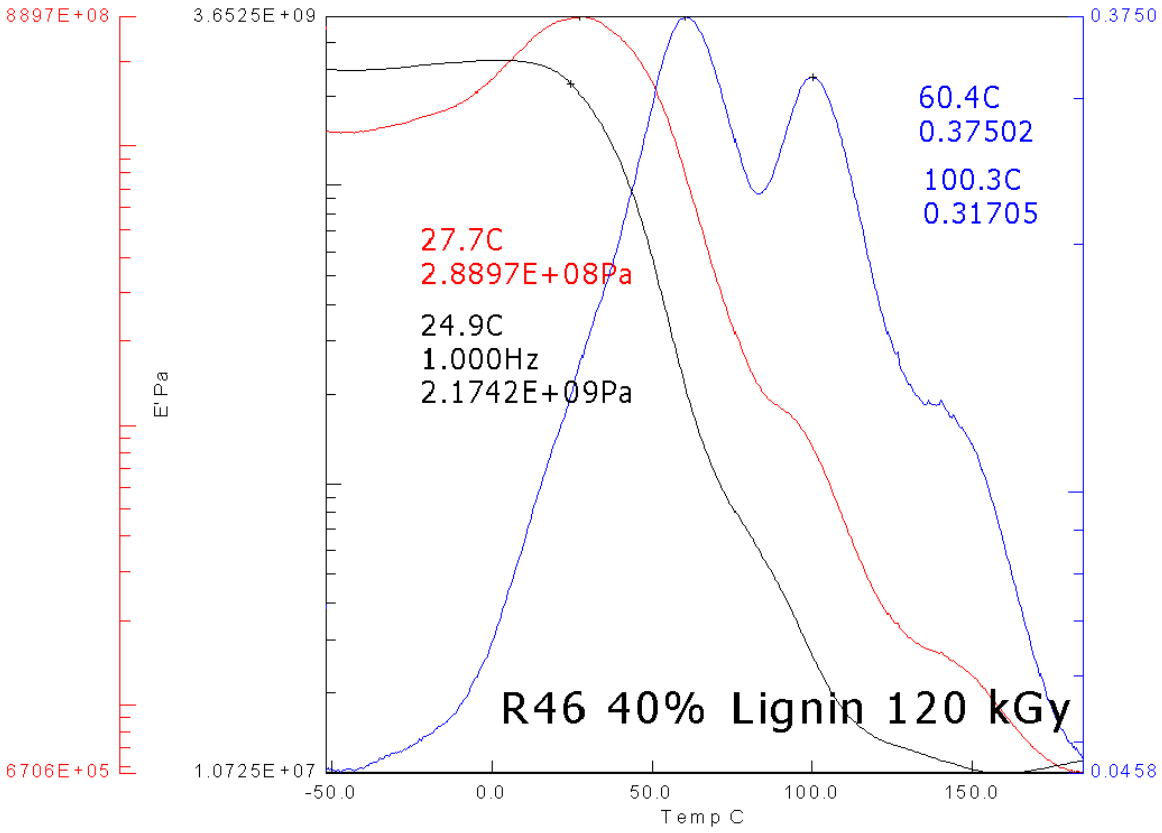

Figure B33: DMA output R46 40% Lignin Cured at 120 kGy

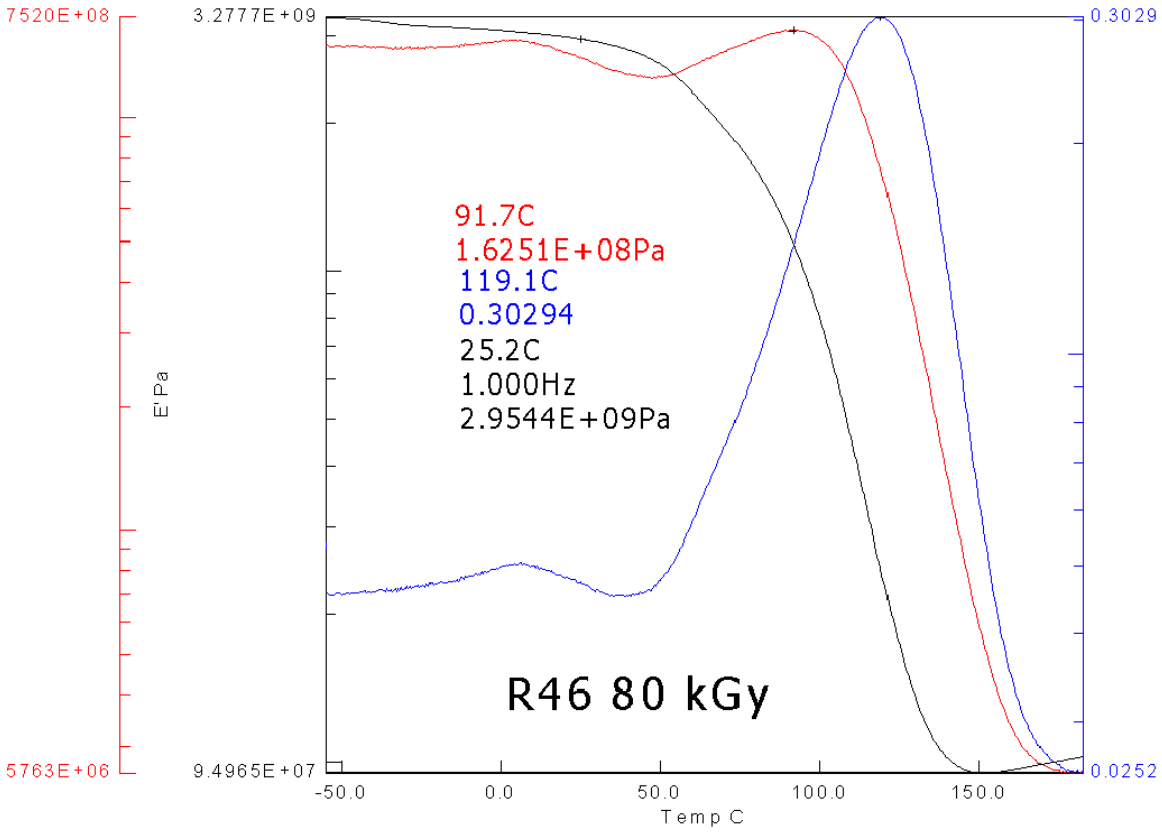

Figure B34: DMA output R46 0% Lignin Cured at 80 kGy

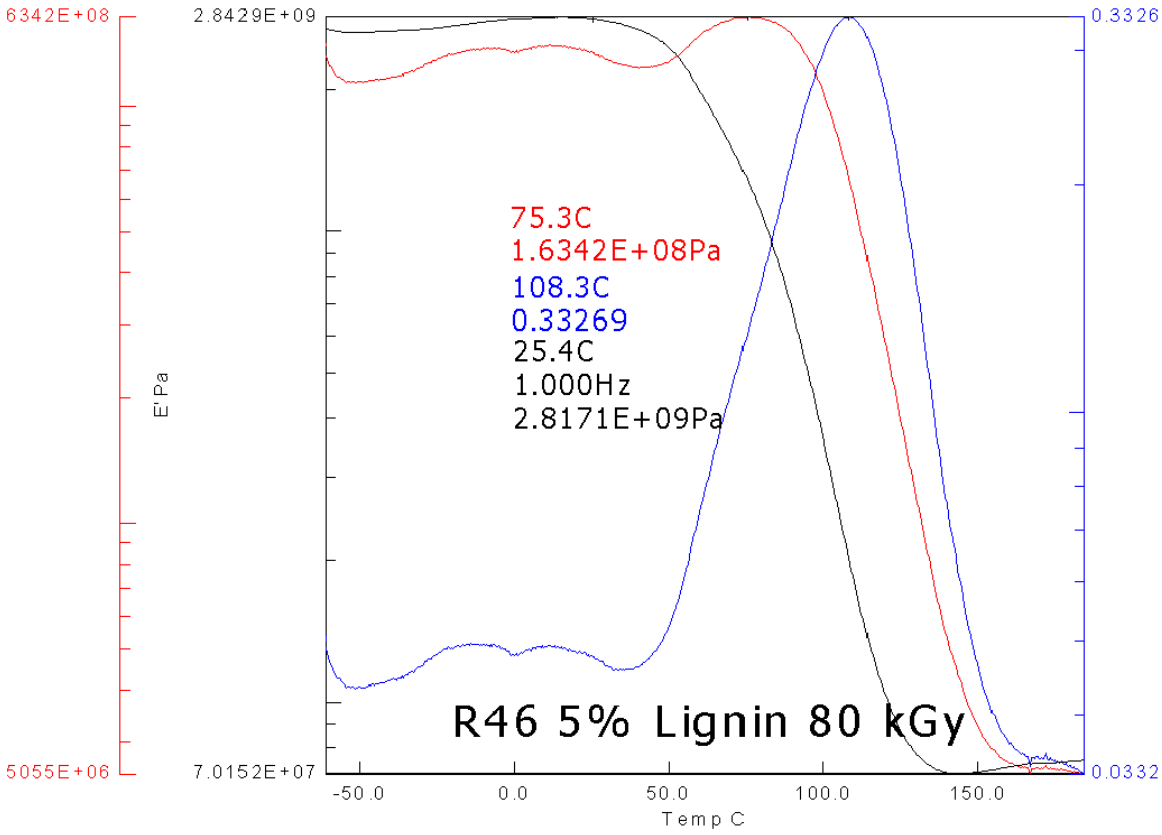

Figure B35: DMA output R46 5% Lignin Cured at 80 kGy

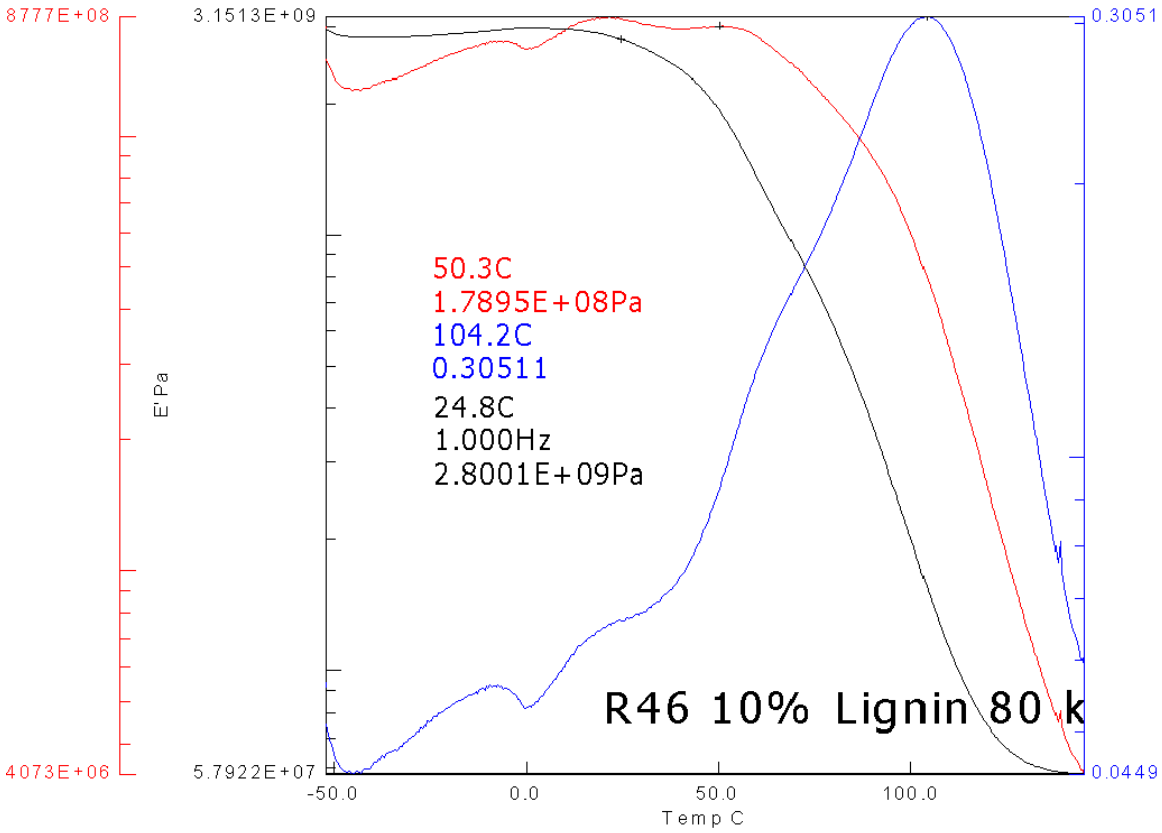

Figure B36: DMA output R46 10% Lignin Cured at 80 kGy

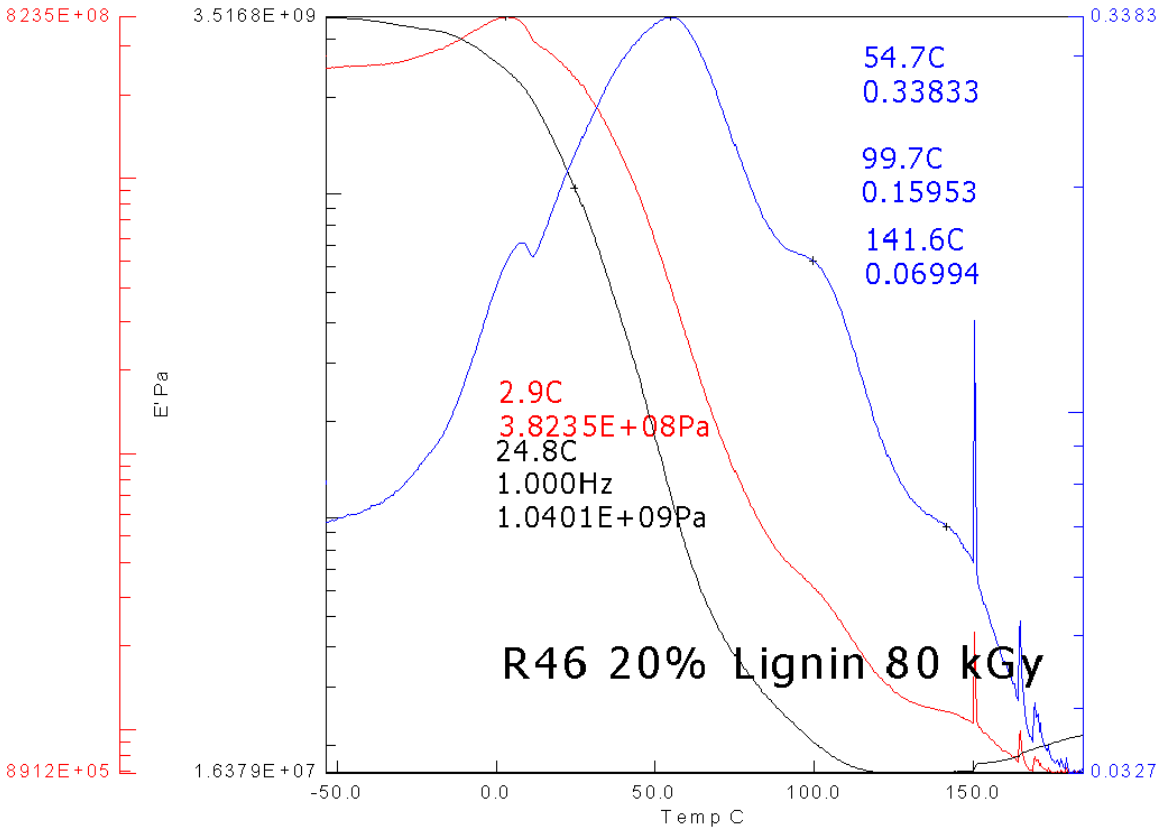

Figure B37: DMA output R46 20% Lignin Cured at 80 kGy

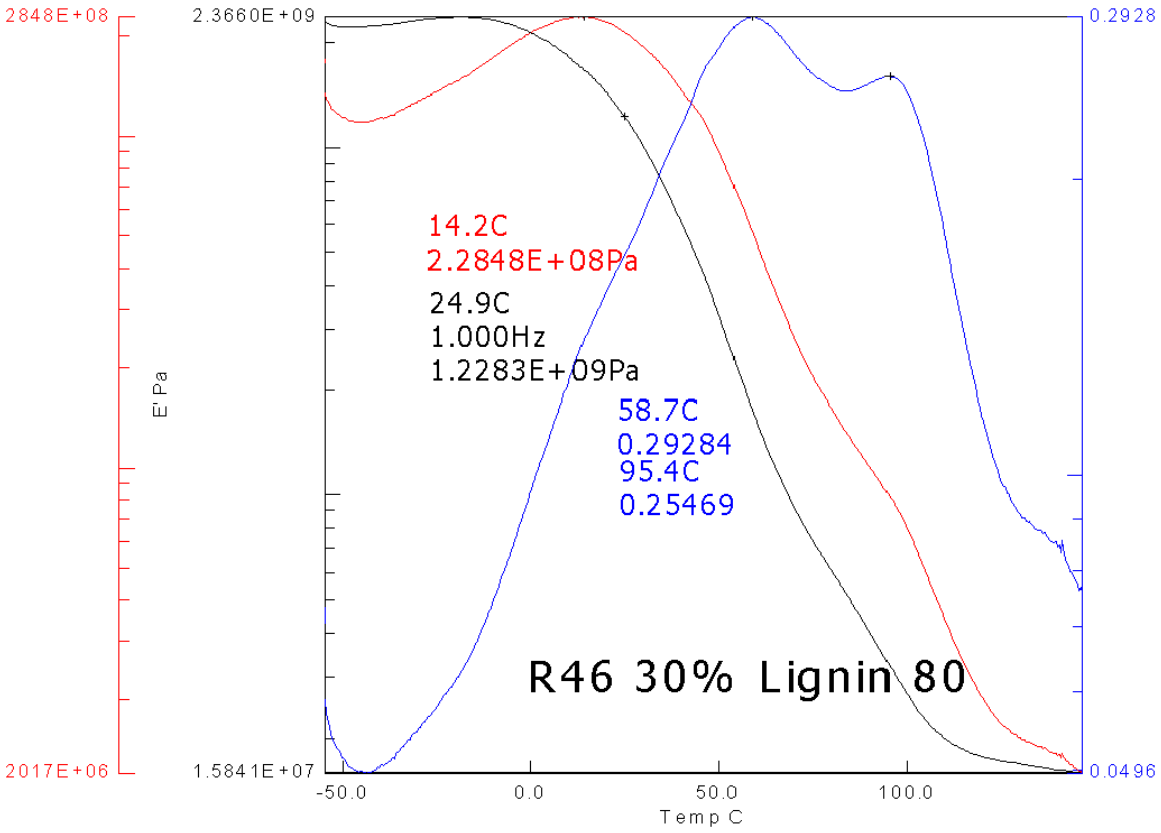

Figure B38: DMA output R46 30% Lignin Cured at 80 kGy

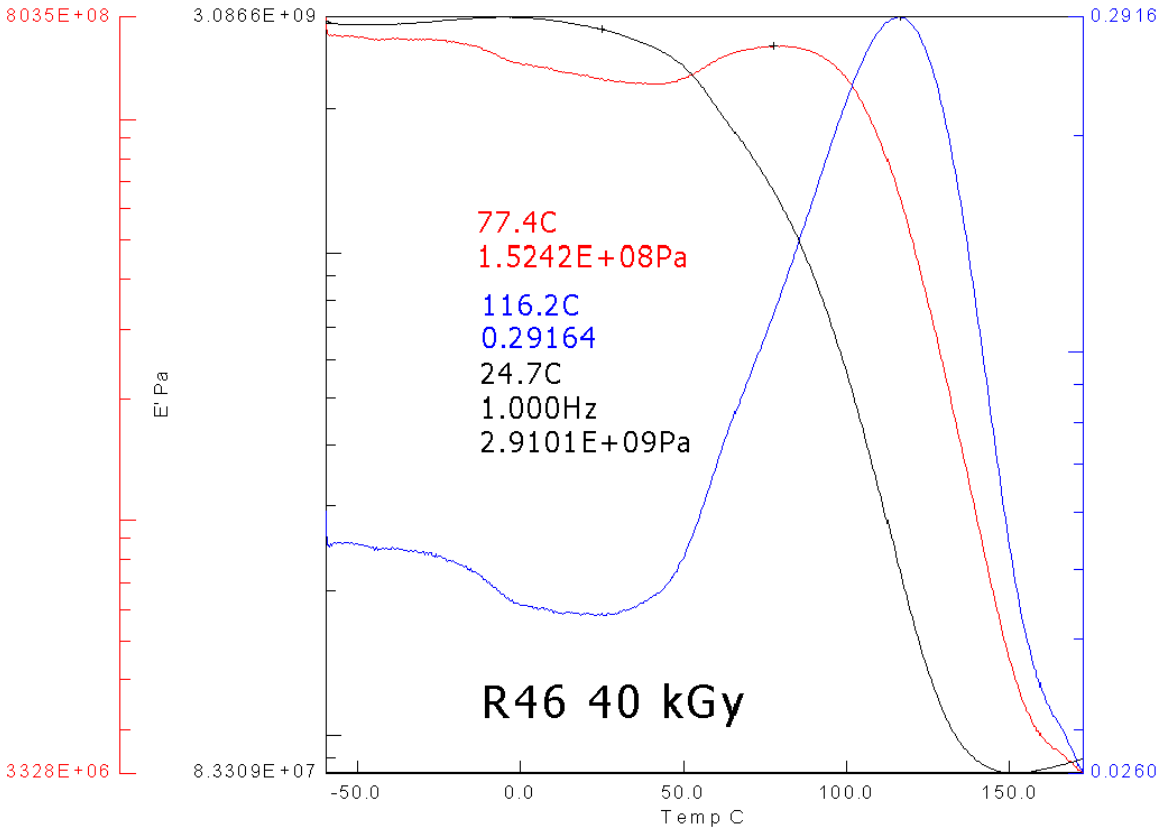

Figure B39: DMA output R46 0% Lignin Cured at 40 kGy

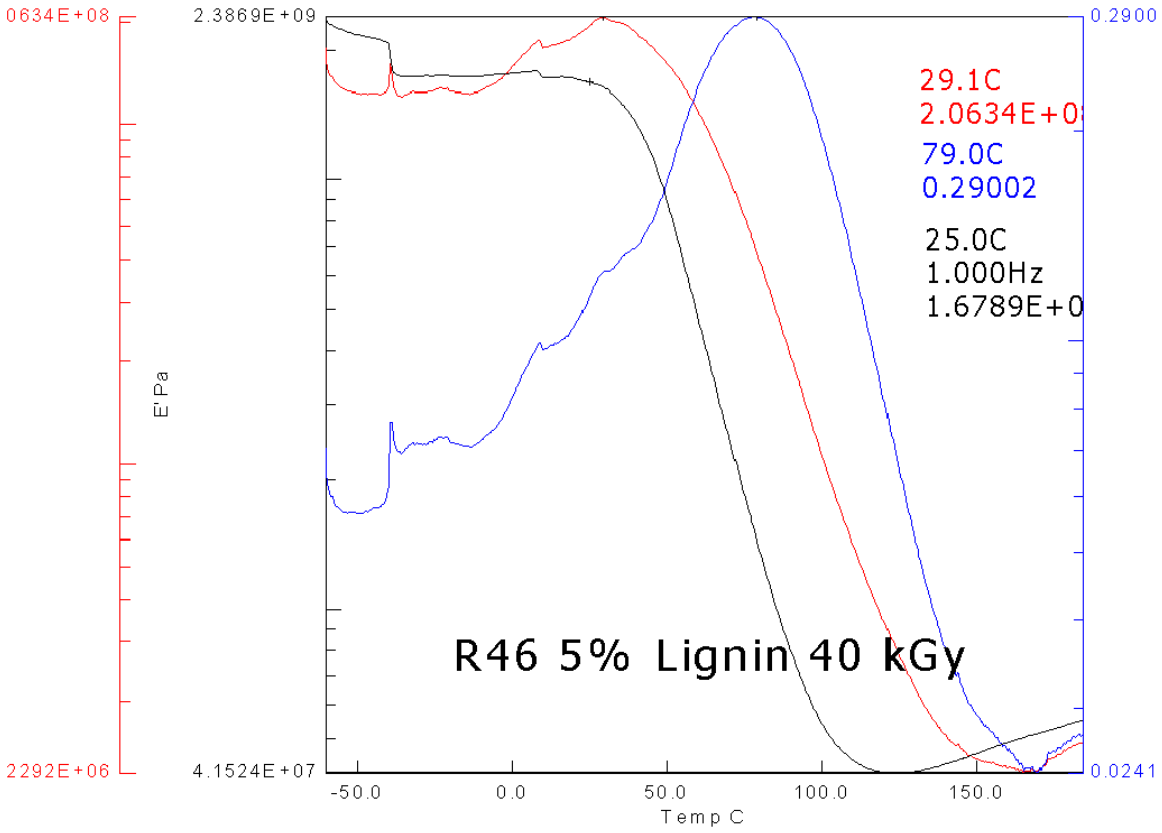

Figure B40: DMA output R46 5% Lignin Cured at 40 kGy

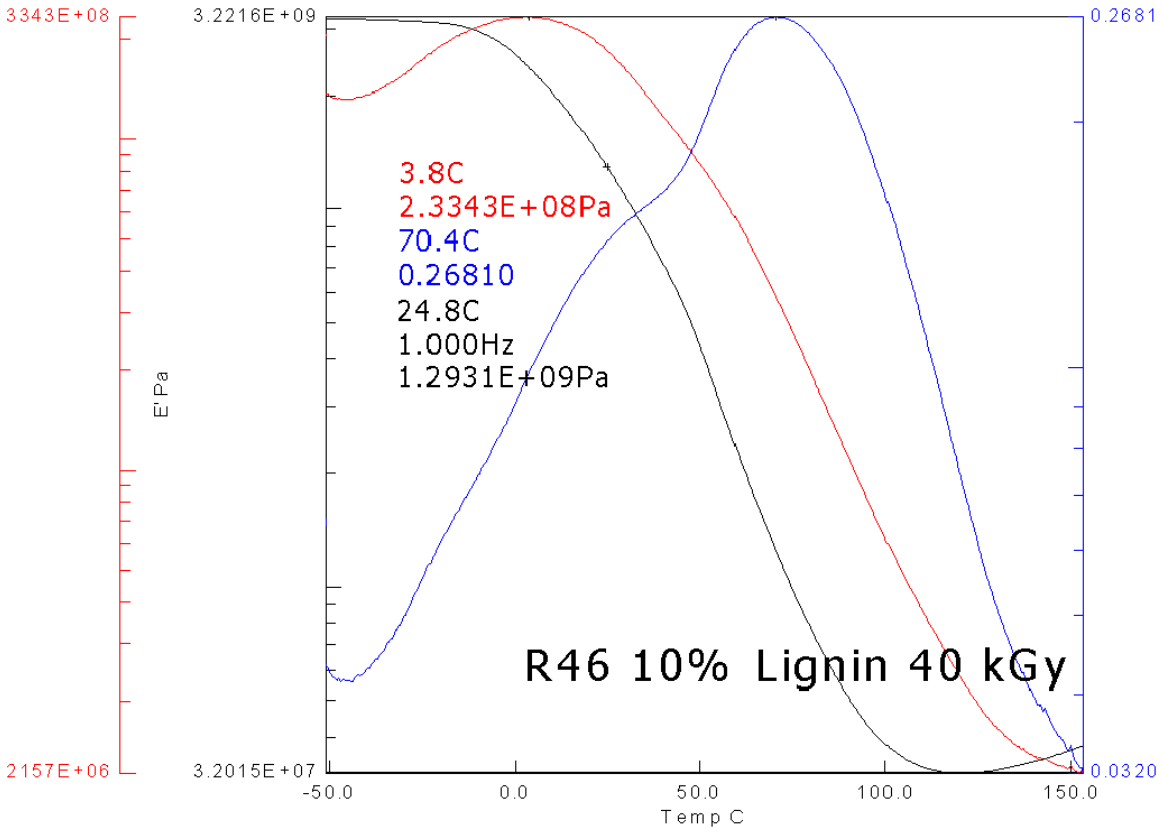

Figure B41: DMA output R46 10% Lignin Cured at 40 kGy

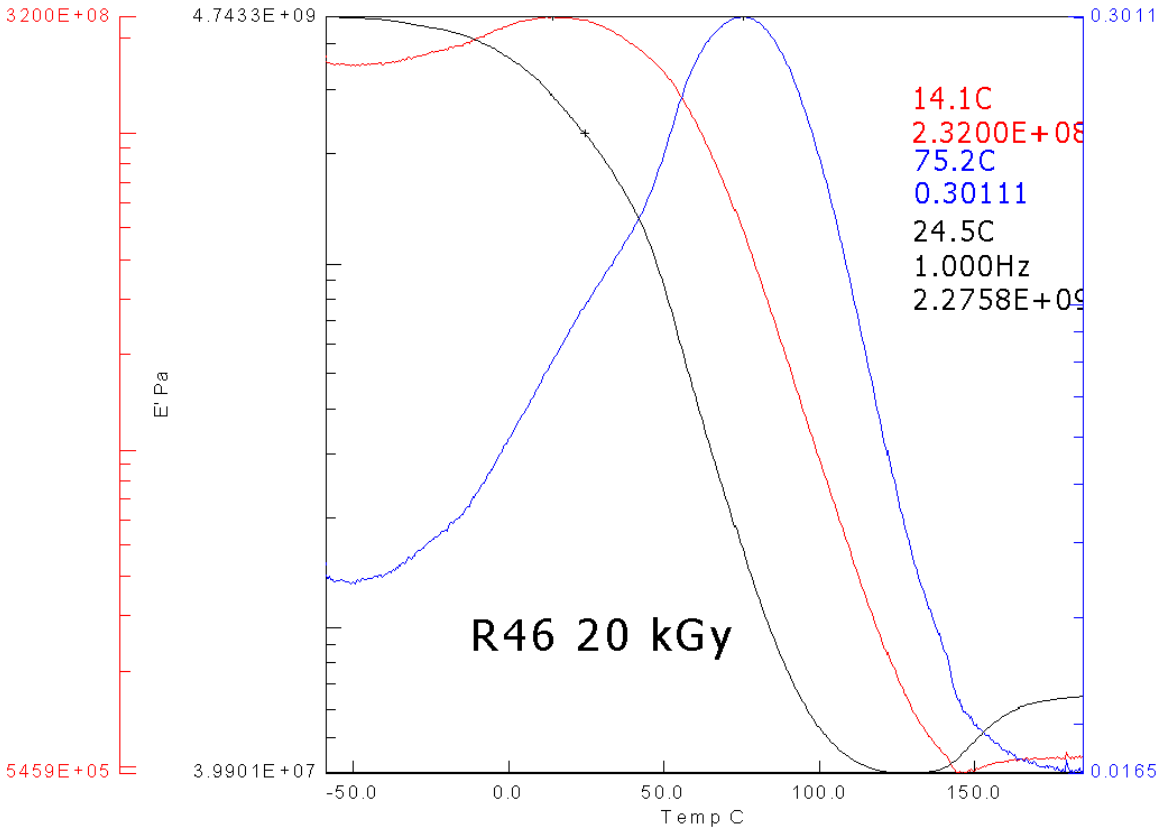

Figure B42: DMA output R46 0% Lignin Cured at 20 kGy

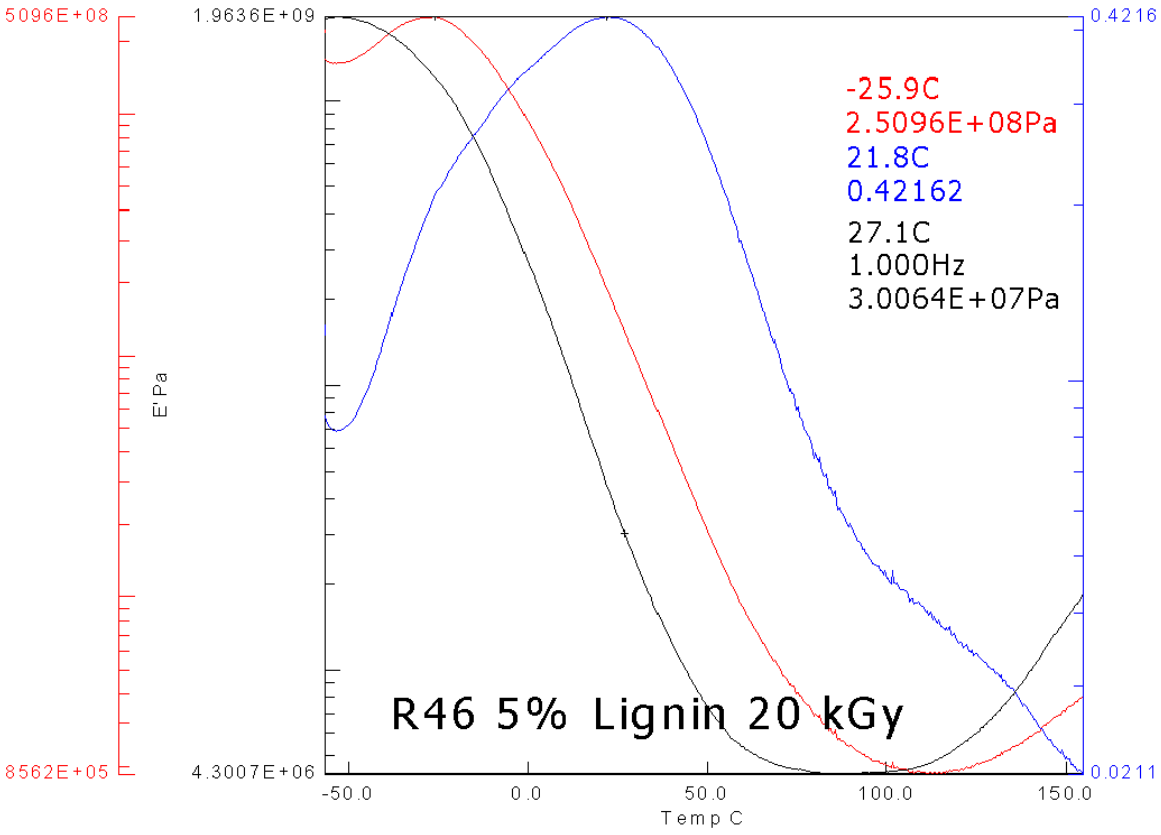

Figure B43: DMA output R46 5% Lignin Cured at 20 kGy

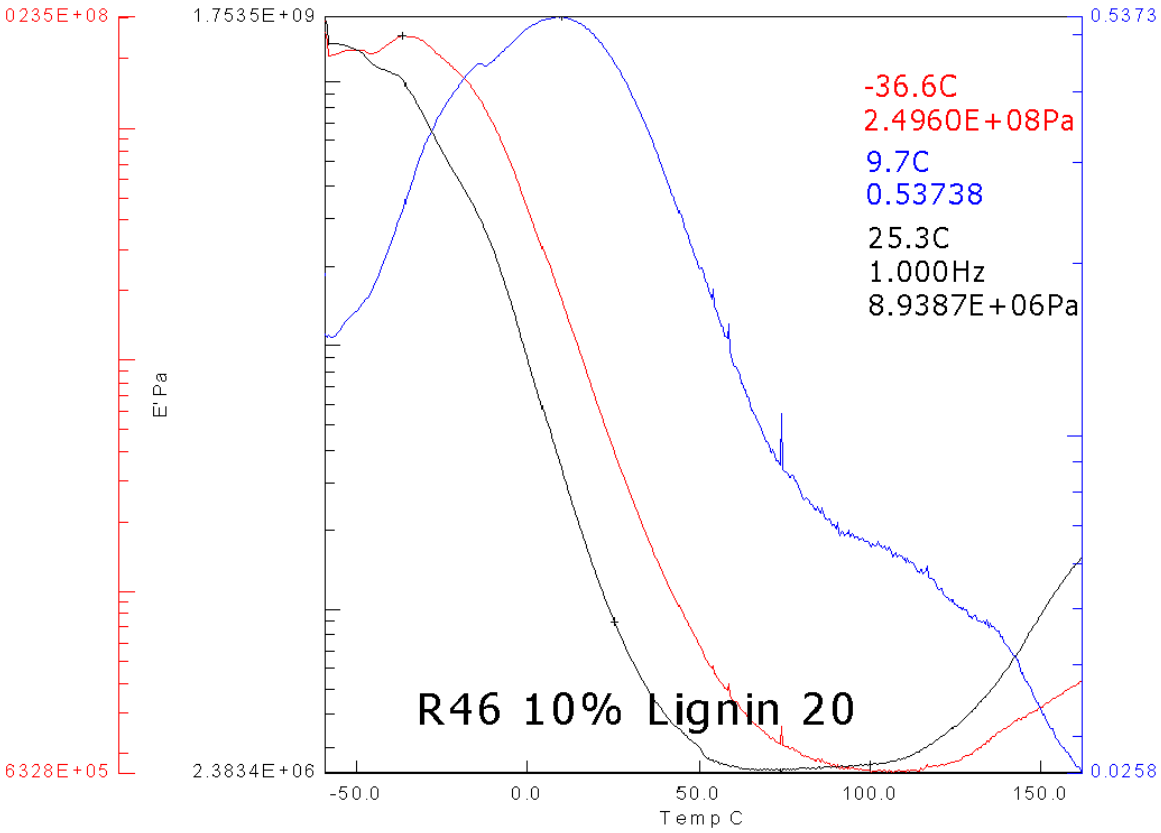

Figure B44: DMA output R46 10% Lignin Cured at 20 kGy

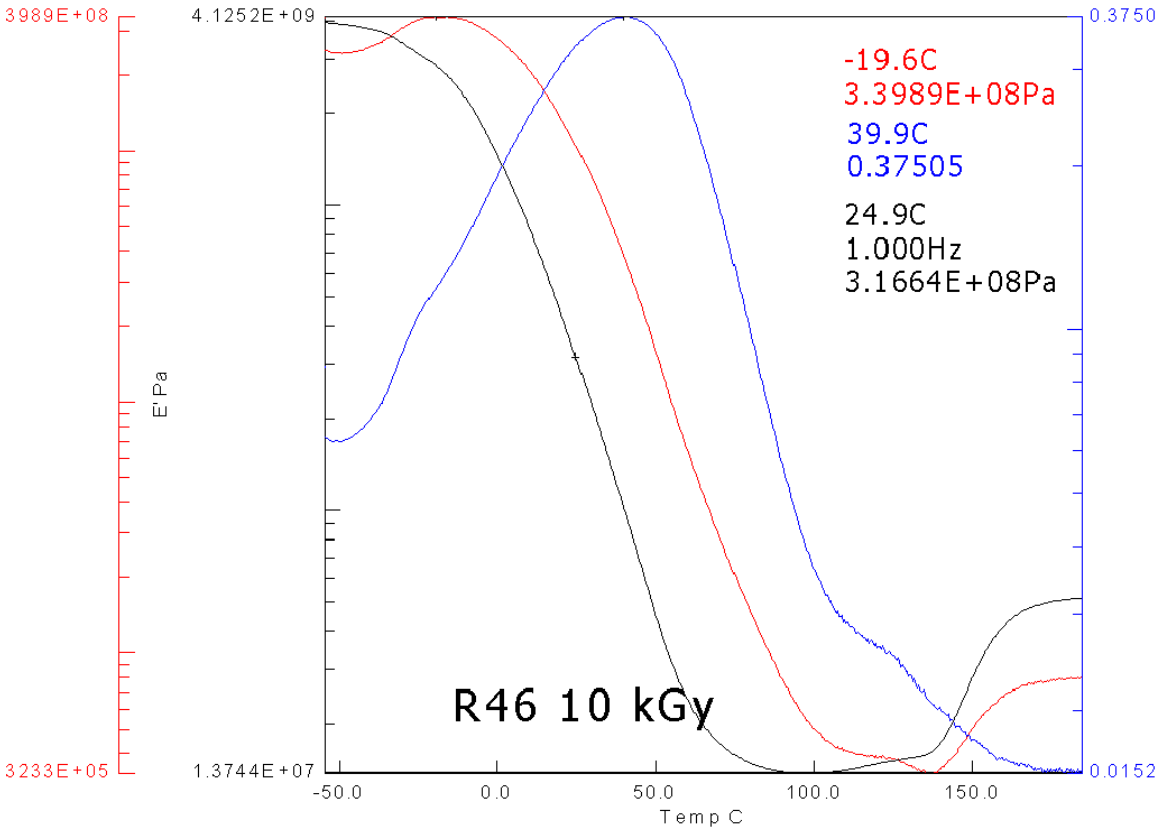

Figure B45: DMA output R46 0% Lignin Cured at 10 kGy

Vitae

I was born the youngest of five. My father worked as a mechanical engineer for thirty years at TVA, on cooling systems for power plants. One of my favorite memories is when I was very young (I think about eight) when TVA offered a tour of Watts Bar nuclear plant to employee families. I was fascinated. I asked a million questions. I stood at the top of the baffling in a cooling tower, in the very center, hearing the sound of air and echo.

My father ran a farm in his spare time (or maybe mostly in his boy's spare time). My mother reared five great kids. I worked for my father, feeding cows and chickens, raising corn and selling it in the neighborhood, stretching barb-wire fences. Dad paid us ten cents times our age per hour. I spent it on summer camps and bubble gum. I learned quickly to work hard, though this never really applied to my studies. I showed strong aptitude for math and science all the way up through high school. Unfortunately, this afforded me the opportunity to succeed academically without ever truly having to study. I remember two times I really had to study before college. The first time was in 3rd grade, with long division. I went into the hall closet at home with a flashlight and read through each step till I got it. The second time was the concept of a variable in algebra. I think I did the same thing. What was taking place was far from the development of quality study habits. Eventually, I ran out of useful science classes, getting A's in chemistry, biology, physics etc. My senior year I went on to take statics at a local community college. It was also easy for me. I knew where my abilities lay, and I knew what I wanted to do.

My freshman year at UT was a breeze. Honestly it felt like high school. Chemistry must have been the attempted 'weed out' course, but not for me. I chose chemical engineering from the other disciplines because it paid the most. I think Dad also said he would have done that if he could do it again. Much of my motivation for school was financial. I had

watched my parents with good jobs struggle to raise five kids. I thought maybe a family might be something I'd want, and I didn't want to shut myself out of that opportunity by getting a degree in say, english. To me school was an investment, and I was going to go in for all I could with it. Unfortunately I had lost my work ethic.

My sophomore year was when the wheels fell off. Frankly I'm not quite sure what my problem was. It seemed like I simply couldn't get it right off, and this caused me to despair rather than working harder. I knew I was failing, and this made me not want to go to class. I was very depressed. The class that broke me was thermodynamics. I couldn't apply appropriately enough the equations, manipulate the differentials, consider the physical parameters involved, and solve the problem. Not at first at least, and the first look seemed to be all I would show. I did not tell my parents I was failing until two semethers had passed. I lost scholarships, and my parents' financial support. This was very wise of them. I took a year off, auditing a class to stay in the UT system while working in a warehouse counting boxes fifty hours a week. I had to get my work ethic back. After a year off, I felt prepared to return to school. I remember people asking me sort of nonchalantly, "What are you doing this fall?" To this I would reply that I was returning to school *as I had planned*. They'd reply, "ohh… good for you". I wanted to yell at them that that had been my plan all along. I hadn't shown up on school. I still had the ability to succeed; I just needed to learn to apply myself again.

I returned to school and failed thermo again. Apparently I needed something more. I knew enough about the Army to know it could teach me two valuable lessons: I'm no different because I'm smarter than most, and I need to prepare and work hard in order to be successful. I enlisted that spring in the reserves. I returned to school after basic training in the summer, entered ROTC, and got a B+ in thermo. I proceeded to get a solid 3.5 average every semether thereafter, graduated in spring 2004, and recieved a commission as an officer in the National Guard in the summer.

I was victorious, however, because my GPA was destroyed by two years of failure, I was unable to find a job. Graduate school offered something amazing to me: school which was not only free, but for which I would be paid. Frankly it reminded me of the Army. I can't remember how many times I have wondered, "*they're* paying *me* for this?" Working at Tennessee Forest Products Center was a great experience. I thoroughly enjoyed the topic of my research, because it was something which had never been done before. The facilities at Forest Products, wood lab, wet chemistry lab and spectroscopy lab provided me with a superb workshop to develop my ideas for solving the essential problems of my research. Frankly I have been like a kid in a candy store for two years. I am already reminded of myself as a kid touring Watts Bar nuclear plant, but I know much more interesting things are to come. I have accepted a job as a Shift Technical Advisor at Y12 National Defense Complex, and look forward to a career as both an engineer and a soldier in service of my country.

I am eternally grateful to my parents and the Army for providing me with the motivation and impetus to achieve all that I am capable of in life. I am further grateful to Dr. Collier and the staff of the Department of Chemical Engineering at UT Knoxville for putting up with me. I consider myself to have been a bright but difficult student.